



Feasibility and Environment & Social Assessment Studies of the Priority Generation Investment Project in Liberia

Solar Measurement Station – Tier 2 automatic weather station final measurement report after 24 months of measurements



Funded by



ARTELIA / June 2023 / 8211050

VERSION	DESCRIPTION	ESTABLISHED BY	CONTROLLED BY	APPROVED BY	DATE
0	Final report	CSPServices	A.PORET	S. ST-PIERRE	30/06/2023
ARTELIA 6 rue de Lorraine – 38130 ECHIROLLES – FRANCE – TEL : 04.76.33.40.00					

CONTENTS

CONTENTS	3
Table	4
Figure	5
1 SUMMARY	10
2 SITE DESCRIPTION	11
2.1 Location	11
2.2 Surroundings and shading profile	12
2.3 Shadings visible in the measurement data	13
3 AUTOMATIC WEATHER STATION CONFIGURATION AND LAYOUT	14
3.1 Measurement equipment	14
3.2 Station Layout	15
3.3 Data MEASUREMENT, TRANSMISSION AND QUALITY CONTROL	16
4 STATION INSTALLATION, MAINTENANCE AND OPERATION	18
4.1 INSTALLATION, Maintenance and Operation TIMELINE	18
4.2 NOTABLE EVENTS DURING STATION OPERATION	21
5 INSTALLATION CHECKLIST	22
6 LOCAL MAINTENANCE PROCEDURES	24
7 MEASUREMENT DATA AND RESULTS	25
7.1 Measurement data upon installation	25
7.2 Measurement results for the reported measurement period	29
7.2.1 Monthly summaries	29
7.2.2 Solar irradiance	30
7.2.3 Temperature and relative humidity	32
7.2.4 Precipitation	33
7.2.5 Wind speed and direction	34
7.3 PV soiling measurement system (Soiling rate)	36
Solar Measurement Station – Tier 2 automatic weather station final measurement report after 24 months of measurements	
FEASIBILITY AND ENVIRONMENT & SOCIAL ASSESSMENT STUDIES OF THE PRIORITY GENERATION INVESTMENT PROJECT IN LIBERIA	

7.3.1	Measurement methodology	36
7.3.2	Measurement equipment	36
7.3.3	Measured values	37
7.3.4	Cleaning cycles	37
7.3.5	Data acquisition and processing	37
7.3.6	Data analysis	38
7.3.7	Comparison of measurement methodology with IEC 61724-1	41
7.3.8	Soiling measurement results	42
7.3.9	Average monthly and yearly soiling rates	42
7.3.10	Daily cleanliness and soiling rates	43
7.4	corrosion sampler (Corrosion rate)	50
8	DATA QUALITY CONTROL AND MEASUREMENT UNCERTAINTY	59
8.1	Clear sky index	59
8.2	Data quality assessment	60
8.3	Irradiance data comparison	61
8.4	Measurement uncertainty	62
8.5	Uncertainty of Long-Term GHI and DNI	63
9	PHOTOGRAPHIC DOCUMENTATION	64
9.1	Installation (June 2021)	64
9.2	Maintenance visit (January 2022)	73
9.3	Maintenance visit (August 2022)	78
9.4	Maintenance visit (January 2023)	83
9.5	Station handover (June 2023)	89
10	CALIBRATION PROCEDURES AND CERTIFICATES	90
10.1	Calibration of sensors upon station installation	90
10.1.1	RSI Solar Sensor (CSPS.MS.19.201.0005)	91
10.1.2	RSI Solar Sensor (CSPS.MS.21.203.0009)	93
10.1.3	CMP10 pyranometer	95
10.1.4	#40C anemometer	99
10.1.5	#200M Wind vane	101
10.1.6	CS106 (PTB100) barometer	102
10.2	Sensor calibration for the second year of measurements	103

TABLE

Solar Measurement Station – Tier 2 automatic weather station final measurement report after 24 months of measurements
FEASIBILITY AND ENVIRONMENT & SOCIAL ASSESSMENT STUDIES OF THE PRIORITY GENERATION INVESTMENT PROJECT IN LIBERIA

Table 1 – Site and installation information.....	9
Table 2 – Location information	11
Table 3 – Measurement equipment.....	14
Table 4 – Installation and maintenance activities	18
Table 5 – Notable events during operation	21
Table 6 – Installation checklist.....	22
Table 7 – Sensor cleaning schedule	24
Table 8 – Number of sensor cleaning visits per month for the reported measurement period ..	24
Table 9 – Measurement results, monthly average values	29
Table 10 – Soiling rate analysis methodology	41
Table 11 – Average monthly and yearly soiling rates	42
Table 12 – Daily soiling rates	44
Table 13 – Sensor calibration upon installation of the station.....	90

FIGURE

Figure 1 - Mount Coffee site in Liberia. The site is located on the Saint Paul River around 30 km north-east of Monrovia.....	10
Figure 2 - Location at the Mount Coffee site	11
Figure 3 - Location at the Mount Coffee site, the station is visible on recent images on Google Earth. The 10x10m fence with the station inside and the access road are visible at the center of the image	12
Figure 4 - Horizon line from the perspective of the pyranometer and sun path throughout the year.....	12
Figure 5 - Shading occurrences for sun elevations >5°	13
Figure 6 - Shading analysis of the measurement data	13
Figure 7 - Tier2 automatic weather station layout: Irradiance sensors, PV soiling rate measurement system, PV panels for power supply	15
Figure 8 - Tier2 automatic weather station layout: wind mast and wind sensors details.....	15
Figure 9 - Tier2 automatic weather station layout: foundation detail.....	16
Figure 10 - Communication status of LTE router for data transmission.....	17
Figure 11 – Measurement data quality control software	17
Figure 12 - Irradiance measurement. GHI, DNI and DHI	25
Figure 13 - Temperature and Humidity measurements.....	25
Figure 14 - Barometric air pressure measurement.....	26
Figure 15 - Precipitation measurement	26
Figure 16 - Wind speed measurement	27
Figure 17 - Wind direction measurement.....	27
Figure 18 - PV soiling measurements	28
Figure 19 - Sensor cleaning recordings. 2021-06-14, first cleaning of irradiance sensors and PV-S reference module	28
Figure 20: Monthly irradiation sums	30
Figure 21: Frequency distribution of hourly irradiance averages	30
Figure 22: GHI irradiance intensity.....	31
Figure 23: DNI irradiance intensity.....	31
Figure 24: Daily temperature and relative humidity averages.....	32
Figure 25: Frequency distribution of temperature and relative humidity	32
Figure 26: Daily sums of precipitation	33
Figure 27: Daily averages of wind speed	34
Figure 28: Frequency distribution of wind speeds	34
Figure 29: Wind direction distribution	35

Figure 30: Wind gust direction distribution	35
Figure 31: PV-soiling system with the clean reference panel (modA) and the measurement panel (modB). The measurement panel is kept clean by regular cleaning by the local maintenance staff whereas the measurement panel is allowed to accumulate soiling over time	36
Figure 32: Reference panel soiling assessment procedure	38
Figure 33: Example for increase of modB panel soiling accumulation; green curve: soiling ratio in 1-hour resolution	39
Figure 34: Time-of-day dependence of instantaneous SR measurements Source: (Gostein, Caron, & Littman, Measuring Soiling Losses at Utility-scale PV Power Plants, 2014)	40
Figure 35: Cleanliness of the measurement panel modB with measured rain (blue) and cleaning (black vertical lines) of modB	43
Figure 36: daily, monthly and yearly average soiling rates	43
Figure 37: Clear-sky index for the GHI (1min resolution).....	59
Figure 38: Multiplot overview of the data quality assessment (1min resolution).....	60
Figure 39: DNI calculated from GHI (CMP10) and DHI (RSI) in comparison with the DNI measured by the RSI (top), GHI calculated from DNI and DHI from the RSI sensor in comparison with the GHI measured by the CMP10 pyranometer (bottom)	61
Figure 40 - Achievable uncertainty for long-term average GHI and DNI data in relation to the availability of ground measurement data for site-adaptation (source: https://solargis.com/docs/methodology/site-adaptation).....	63
Figure 41 - Fence and foundation	64
Figure 42 - Station and wind mast foundations	64
Figure 43 - Wind mast preparations.....	64
Figure 44 - Wind mast foundations, ground cable fixed to ground bolt, protective tube for wind mast cables.....	64
Figure 45 - Water holes in foundations to prevent flooding (1).....	65
Figure 46 - Water holes in foundations to prevent flooding (2).....	65
Figure 47 - Wind direction sensor north mark aligned with mounting cantilever and north direction.....	65
Figure 48 - Wind sensors installed on wind mast.....	65
Figure 49 - Wind mast erected; wind direction sensor cantilever orientated to North	66
Figure 50 - Mounting of weather station structure.....	66
Figure 51 - CMP10 pyranometer serial number	66
Figure 52 - CMP10 pyranometer levelling	66
Figure 53 - Sensor levelling of the RSI (1)	67
Figure 54 - Sensor levelling of the RSI (2)	67
Figure 55 - Serial number of RSI.....	67
Figure 56 - Installed RSI.....	67
Figure 57 - RSI motor serial number.....	68
Figure 58 - Rain sensor and corrosion sampler	68
Figure 59 - Rain sensor mounting bar levelling	68
Figure 60 - Rain sensor serial number	68
Figure 61 - T/RH sensor and modem antenna	68
Figure 62 - T/RH sensor serial number	68
Figure 63 - Control box interior; top: datalogger; bottom: fuses and 12V circuit distribution, relays, RSI motor controller.....	69
Figure 64 - Modem with SIM card.....	69
Figure 65 - Assembly of PV-S structure + modules	69
Figure 66 - PV-S support structure with 9° tilt angle towards South	69
Figure 67 - PV-S modules connections.....	69

Figure 68 - PV-S system reference panel A (clean panel).....	69
Figure 69 - PV modules cleaning.	70
Figure 70 - 12V, 60Ah battery	70
Figure 71 - Wind mast with rain sensor and corrosion sampler	70
Figure 72 - Main mounting structure with solar sensors, T/RH sensor and PV panels for soiling measurement and power supply.	71
Figure 73 - Solar sensors and PV panels on mounting structure	72
Figure 74 - Site with completed station installation as seen from south-west. Picture taken from 6.49767°N, -10.65176°E.....	72
Figure 75: Maintenance staff on site.....	73
Figure 76: Wind mast top section with sensors and camera	73
Figure 77: Wind mast with foundations and guying ropes	73
Figure 78: RSI sensor	74
Figure 79: RSI sensor levelling	74
Figure 80: CMP10 pyranometer	74
Figure 81: CMP10 pyranometer levelling	74
Figure 82: Rain sensor cleaning	74
Figure 83: Rain sensor levelling	74
Figure 84: Rain sensor top view after cleaning	75
Figure 85: Corrosion sampler.....	75
Figure 86: T/RH sensor and modem antenna on the station mounting structure	75
Figure 87: Control box interior; top: datalogger; bottom: fuses and 12V circuit distribution, relays, RSI motor controller and modem	75
Figure 88: Battery box interior.....	75
Figure 89: Station structure with PV modules.....	75
Figure 90: PV supply and soiling modules after cleaning.....	76
Figure 91: PV-S support structure with 9° tilt angle towards South	76
Figure 92: PV modules cleaning	76
Figure 93: Irradiation sensors cleaning	76
Figure 94: Site with complete station as seen from south	77
Figure 95: Site with complete station as seen from east	77
Figure 96: Security camera view (the temporarily installed reference sensor can be seen right next to the permanently installed sensor on top of the weather station).....	78
Figure 97: Wind mast top section with sensors and camera.....	78
Figure 98: Wind mast with foundations and guying ropes	78
Figure 99: RSI sensor	79
Figure 100: RSI sensor levelling.....	79
Figure 101: CMP10 pyranometer	79
Figure 102: CMP10 pyranometer levelling.....	79
Figure 103: Rain sensor cleaning.....	79
Figure 104: Rain sensor levelling.....	79
Figure 105: Rain sensor top view after cleaning	80
Figure 106: Corrosion sampler before dismantling the plates	80
Figure 107: T/RH sensor and modem antenna on the station mounting structure	80
Figure 108: Control box interior; top: datalogger; bottom: fuses and 12V circuit distribution, relays, RSI motor controller and modem.....	80
Figure 109: Battery box interior.....	80
Figure 110: Corrosion samples dismantled and safely stored in individual plastic bags for shipping to the lab for analysis.....	80
Figure 111: Old RSI PU, after change.....	81

Figure 112: PV-S support structure with 9° tilt angle towards south.....	81
Figure 113: Site with completed station as seen from south	81
Figure 114: Site with completed station as seen from east	81
Figure 115: Station as seen from north (after removal of the reference sensor on 2022-08-23)	82
Figure 116: Station as seen from north-east (after removal of the reference sensor on 2022-08-23).....	82
Figure 117: Maintenance staff on site.....	83
<i>Figure 118: Wind mast with foundations and guying ropes</i>	<i>83</i>
<i>Figure 119: RSI sensor</i>	<i>84</i>
<i>Figure 120: RSI sensor levelling.....</i>	<i>84</i>
<i>Figure 121: CMP10 pyranometer</i>	<i>84</i>
<i>Figure 122: CMP10 pyranometer levelling.....</i>	<i>84</i>
Figure 123: Rain sensor cleaning.....	85
Figure 124: Rain sensor levelling.....	85
Figure 125: Rain sensor top view after cleaning	85
Figure 126: Toolbox	85
Figure 127: T/RH sensor and modem antenna on the station mounting structure	86
Figure 128: Control box interior; top: datalogger; bottom: fuses and 12V circuit distribution, relays, RSI motor controller and modem.....	86
Figure 129: Battery box interior.....	86
Figure 130: Station structure with PV modules.....	86
Figure 131: PV supply and soiling modules after cleaning	87
Figure 132: PV-S support structure with 9° tilt angle towards South	87
Figure 133: PV modules cleaning	87
Figure 134: Irradiation sensors cleaning	87
Figure 135: Site with completed station as seen from east	88
Figure 136: Site with completed station as seen from west	88
Figure 117: Station handover visit – view from south.....	89
Figure 118: Station handover visit	89
<i>Figure 137: Reference pyranometer installation.....</i>	<i>103</i>
<i>Figure 138: Comparison of GHI from permanently installed and reference pyranometers (CMP10)</i>	<i>104</i>
<i>Figure 139: Travelling standard reference pyranometer calibration certificate from World Radiation Center in Davos.</i>	<i>104</i>

Table 1 – Site and installation information

Site and Installation Information	
Client:	West African Power Pool
Site:	Mount Coffee hydro power plant, Liberia
Coordinates:	6.4978°N, -10.6517°E, altitude: 20 m
Station Type:	Tier2 automatic weather station
Date of commissioning:	2021-06-11
Reported measurement period	2021-06-12 - 2023-06-11
Responsible Staff	
Date: 2023-06-12	<p>Installation on site: Timothy Chollom, Bezaleel + Turnkey Contractors, Inc.</p> <p>Remote commissioning: Roman Affolter, CSP Services</p> <p>Data monitoring and reporting: Anne Forstinger, CSP Services Roman Affolter, CSP Services</p> <p>Station maintenance on site: Bezaleel + Turnkey Contractors, Inc. on-site staff</p>

1 SUMMARY

In the framework of the project “Feasibility and Environment & Social Assessment Studies of The Priority Generation Investment Project in Liberia”, 24 months of meteorological measurement data were collected at the Mount Coffee hydro power plant facility. This report summarizes the whole 24-month period for the measurements at the site between June 2021 and June 2023. It includes the description of the site and the installed measurement equipment, the installation and maintenance activities and a summary of the measurement results.

The purpose of this measurement campaign was to collect two years of ground measurement data for the planned utility scale photovoltaic (PV) power plant at the described location. Measurement parameters were primarily global horizontal irradiance (GHI), direct normal irradiance (DNI) and diffuse horizontal irradiance (DHI). Further, temperature and relative humidity, barometric pressure, rain, wind speed and direction as well as the soiling rate on PV modules and the corrosion rate on different metal samples were measured. The GHI was measured with a CMP10 pyranometer, the DNI and DHI with a Rotating Shadowband Irradiometer (RSI).

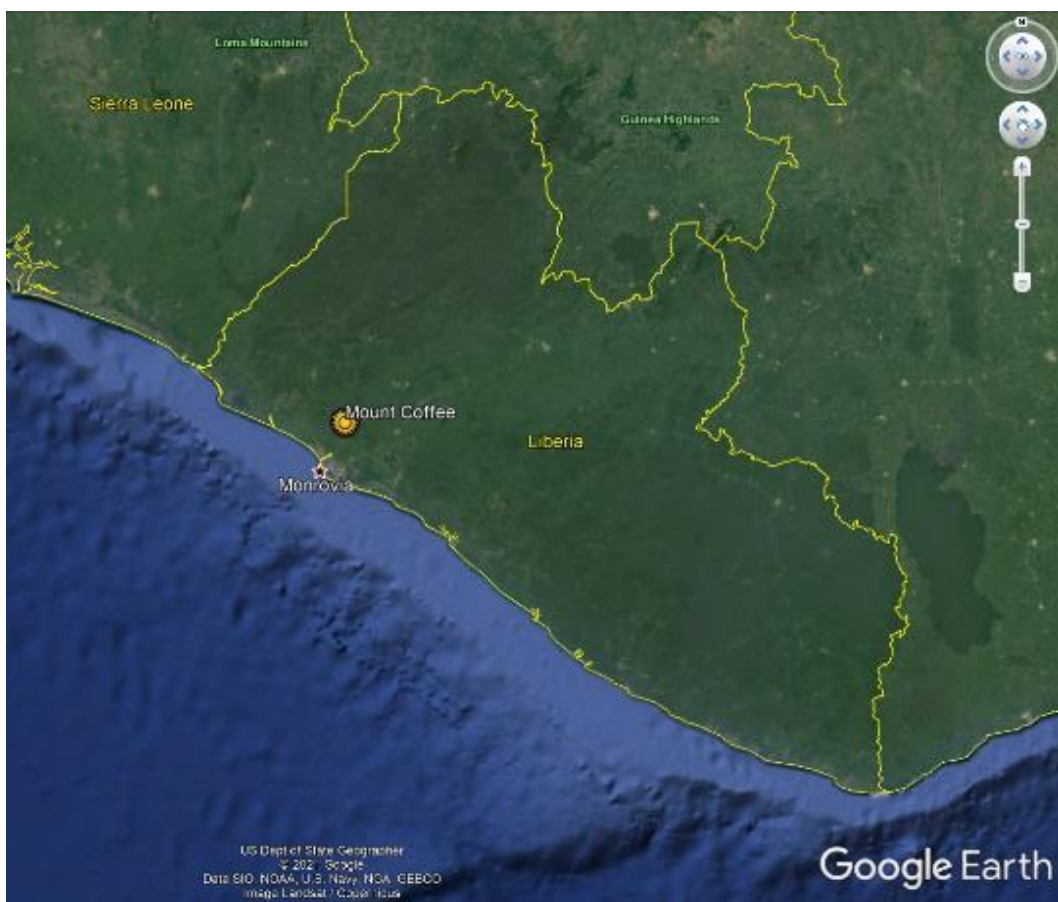


Figure 1 - Mount Coffee site in Liberia. The site is located on the Saint Paul River around 30 km north-east of Monrovia

Measurement data from the station were being transferred to CSPS in regular (hourly) intervals for data quality monitoring and control. Additionally, the data was available on a protected web server for near-real time data monitoring and download.

CSP Services applied daily data quality tests and provided quality-controlled final measurement data in monthly intervals. Local subcontracted staff was in charge of the maintenance and sensor cleaning of the solar irradiance sensors and the reference PV module for the soiling measurement. The responsible person was present during the installation of the station and was briefed on the maintenance and cleaning procedures.

The measurements were successfully concluded in June 2023 and the station was formally handed over to the local utility Liberia Electricity Corporation (LEC) by the end of June 2023.

2 SITE DESCRIPTION

2.1 LOCATION

Table 2 – Location information

Site:	Mount Coffee hydro power plant, Liberia
Coordinates:	6.4978°N, -10.6517°E, altitude: 20 m
Climate:	Tropical monsoon climate (Köppen-Geiger Am, (Kottek, Grieser, Beck, Rudolf, & Rubel, 2006))



Figure 2 - Location at the Mount Coffee site



Figure 3 - Location at the Mount Coffee site, the station is visible on recent images on Google Earth. The 10x10m fence with the station inside and the access road are visible at the center of the image

2.2 SURROUNDINGS AND SHADING PROFILE

The immediate surroundings are mainly flat with a dam of the hydropower facility to the east and south-east. After the installation of the automatic weather station, pictures of the horizon in all directions were taken from the location of the irradiance sensors and a panoramic view was generated from these pictures.

Figure 3 shows the panoramic picture with the horizon line and the sun path throughout the year.



Figure 4 - Horizon line from the perspective of the pyranometer and sun path throughout the year

Figure 4 shows the analysis of the horizon line and the expected shading occurrences on the irradiance data measurements. The analysis shows an almost free field of view for the sensors, no relevant obstructions at sun elevations higher than a few degrees above horizon exist, especially in east and west direction where the sun is near the horizon on sunrise and sunset. Only very little shading is expected for a very short period after sunrise from the dam in the east and for a very short period before sunset from the trees in the west of the measurement site.

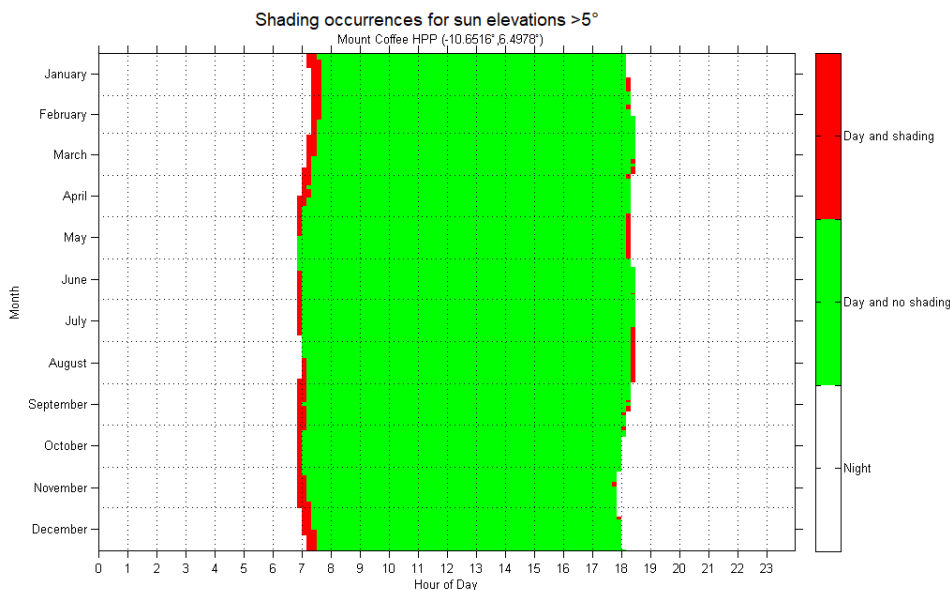


Figure 5 - Shading occurrences for sun elevations >5°

2.3 SHADINGS VISIBLE IN THE MEASUREMENT DATA

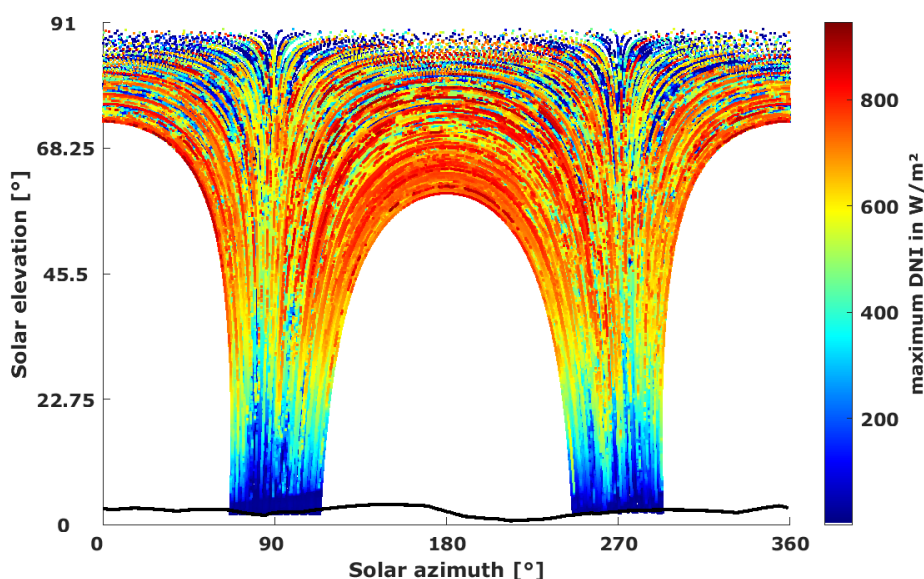


Figure 6 - Shading analysis of the measurement data

Figure 6 shows the measured DNI from the station for the reported period in an elevation-azimuth plot. Each of the plotted lines corresponds to a sun path on any given day. The maximum recorded DNI at each sun position is indicated by the colour of the pixel. Low solar elevation angles and solar azimuth centered around 180° (south) correspond to winter days (around December) on the northern hemisphere. High solar elevations and solar azimuth towards 0/360° (north) correspond to summer days (around June) on the northern hemisphere.

Shading of the irradiance sensor would have shown as white or blue regions in the plot where otherwise high DNI was to be expected. The analysis confirms the findings from the shading analysis performed after the installation of the station with only very little shading visible for a very short period after sunrise from the dam in the east.

3 AUTOMATIC WEATHER STATION CONFIGURATION AND LAYOUT

This section gives an overview of the installed equipment and sensors with respective serial numbers. Further, a layout drawing of the weather station as built is shown.

3.1 MEASUREMENT EQUIPMENT

Table 3 – Measurement equipment

Equipment and serial numbers		
Automatic weather station	CSP Services Tier2 automatic weather station	CSPS.MT.21.229
Main control box	CSP Services	CA.21.202.0004
Datalogger	Campbell CR1000X	18088
Modem	RUT240 Teltonika Networks	1110018427
Power supply	Autonomous power supply with PV panels and battery	-
RSI drive unit	CSP Services Twin RSI	CSPS.DR.20.201.0002

Measured parameter	Unit	Sensor type	Serial Number
GHI	W/m ²	Kipp&Zonen CMP10 pyranometer (installed 2m above ground)	210860
DHI, DNI	W/m ²	CSP Services Rotating Shadowband Irradiometer (installed 2m above ground)	Until 2022-08-19: CSPS.MS.19.201.0005 After 2022-08-19: CSPS.MS.21.203.0009
Temperature (T)	°C	Hygrovue5 temperature and relative humidity sensor with RAD06 radiation shield (installed 1.5m above ground)	E2596
Humidity (RH)	%		
Barometric pressure (BP)	hPa	Vaisala PTB110 (CS106)	S4750162
Precipitation (Rain)	mm	Campbell Scientific 52203 (installed 2m above ground)	TB 16367
Wind speed (WS)	m/s	NRG #40C Class 1 anemometer (installed 10m above ground)	17950-0334055
Wind direction (WD)	°N	NRG #200M wind vane (installed 10m above ground)	10070-00009014
Soiling rate	%	CSP Services PV soiling measurement system (installed 1.5m above ground)	-
Corrosion rate	%	Fraunhofer corrosion sampler with 12 standardized metal samples of aluminum, carbon steel, zinc and copper (three samples from each metal)	-

The RSI sensor head was replaced against a recently calibrated one upon the maintenance visit on 2022-08-19. The previously installed RSI sensor head had shown some higher than usual deviations when compared with the CMP10 pyranometer (see chapter 0 for further details).

Further information on the listed sensors and measurement systems can be found in the station specification documentation. For calibration certificates of sensors see chapter 9.

3.2 STATION LAYOUT

The layout of the Tier2 AWS is shown in the figures below. The main components are the mounting structure with the irradiance sensors and the wind mast with additional sensors. The autonomous power supply system is integrated in the station (2x 30W PV panel and 1x 60 Ah battery).

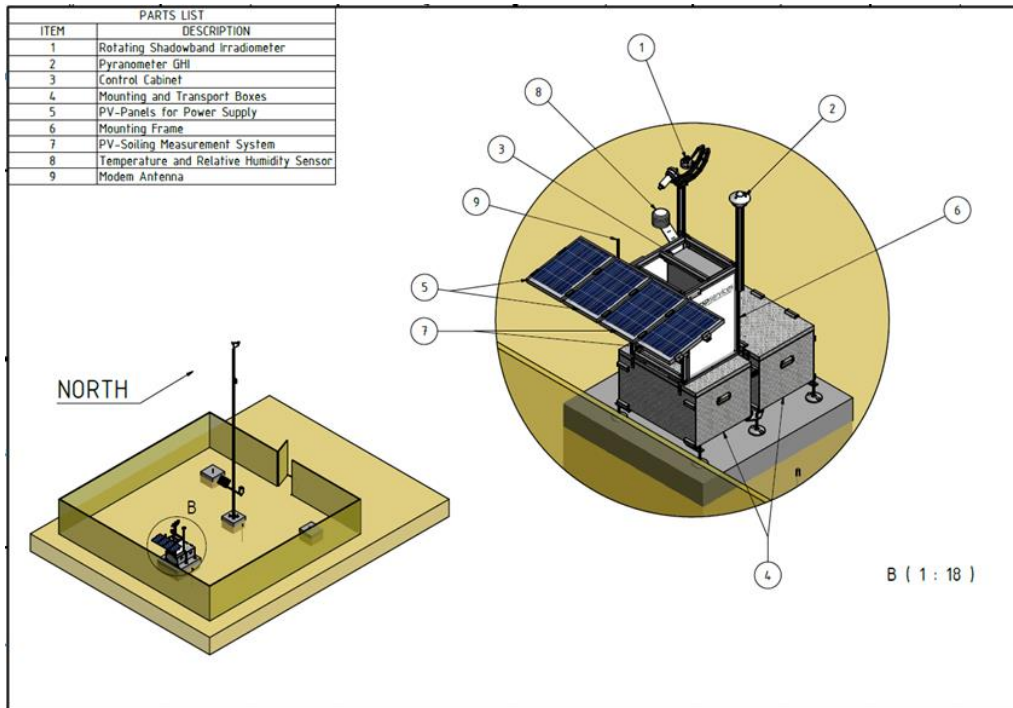


Figure 7 - Tier2 automatic weather station layout: Irradiance sensors, PV soiling rate measurement system, PV panels for power supply

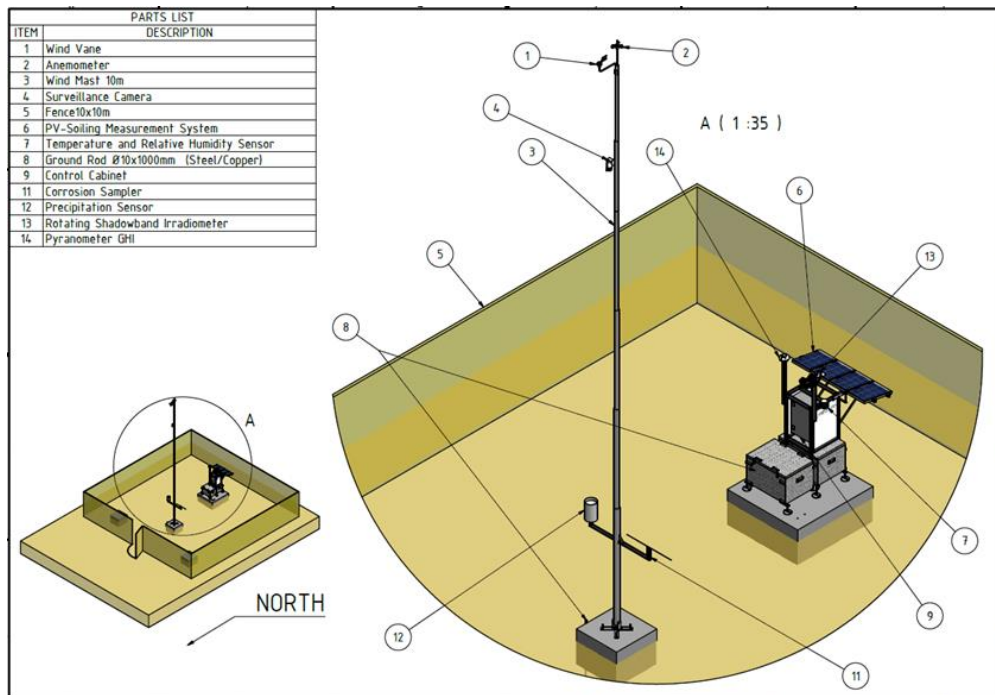


Figure 8 - Tier2 automatic weather station layout: wind mast and wind sensors details

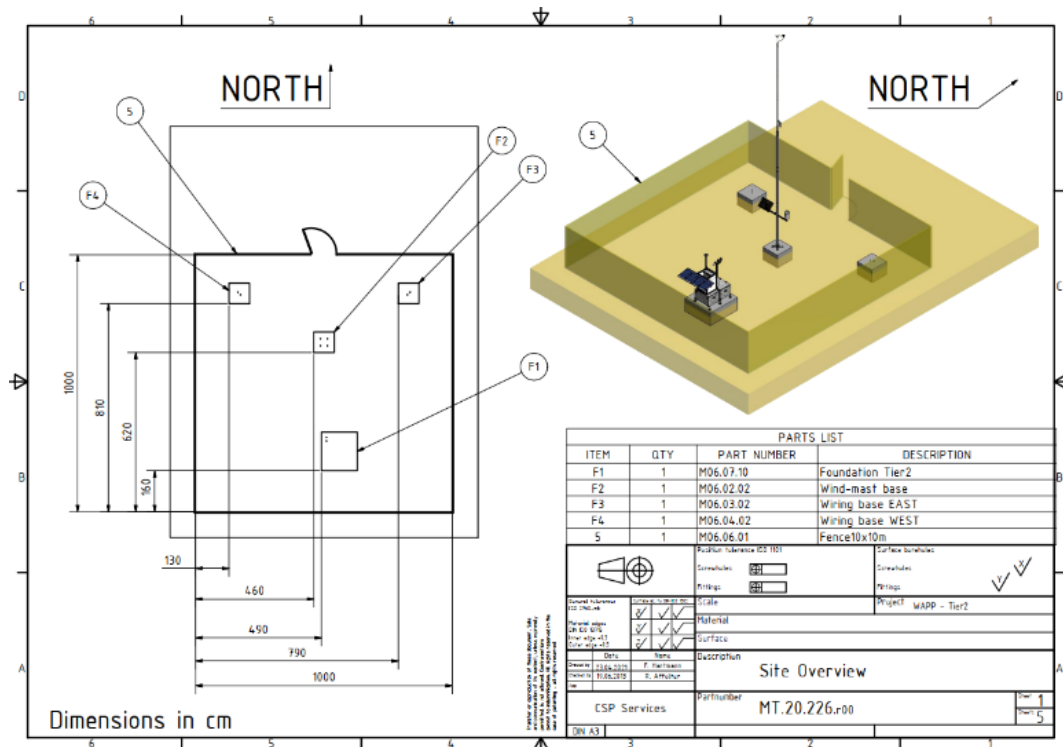


Figure 9 - Tier2 automatic weather station layout: foundation detail

The wind mast is anchored to the wind mast foundations and guying rope foundations. The station itself stands freely on its concrete foundation.

The dimensions and distances are shown in the foundation drawings in the figure above. The height of the fence is 2m plus the barbed wire on top. The distance of the PV-Soiling system to the fence is approximately 1.5m.

3.3 DATA MEASUREMENT, TRANSMISSION AND QUALITY CONTROL

The sensor signals are scanned with a frequency of 1 Hz and stored in 1-minute and 10-minute average data tables in the datalogger's internal memory. The measurements are taken in 1 second resolution (1 Hz) and stored in 1 minute average tables together with the max, min and StDev values.

The measurement data is sent to the CSPS servers in near-real time through a 4G LTE router with a SIM card from a local operator (Orange Liberia).

The measurement data is sent in parallel to the CSPS data processing server and the web server for client access for data monitoring and download (see section 7). It is stored in the internal memory of the datalogger for more than 3 months. In case of prolonged network issues, the data can be retrieved after the network issues have been resolved or manually on site via direct USB access to the datalogger if necessary.

Together with the measurement data, pictures from the surveillance camera are transmitted to the CSPS server in regular intervals (usually one picture every 10 minutes, depending on network availability, data usage and battery charging status).

The communication status of the LTE router and the settings of the mobile configuration (Auto APN) is shown in Figure 8. The data usage depends mainly on the amount of transmitted pictures and videos from the camera and is expected to be less than 1 GB/months during normal operation (Figure 8 shows the usage including the tests performed during the installation).

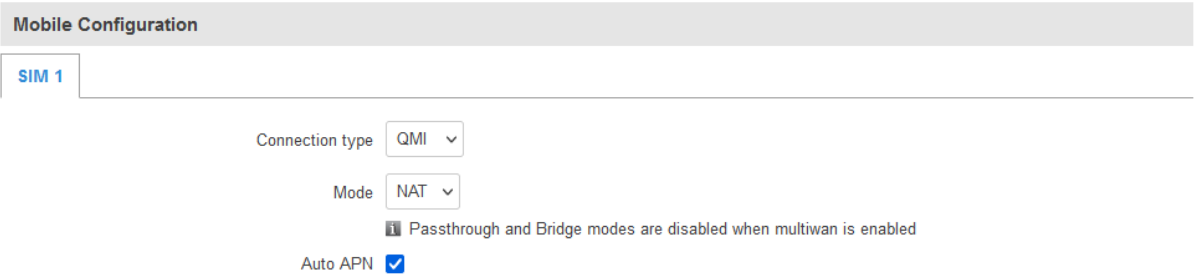
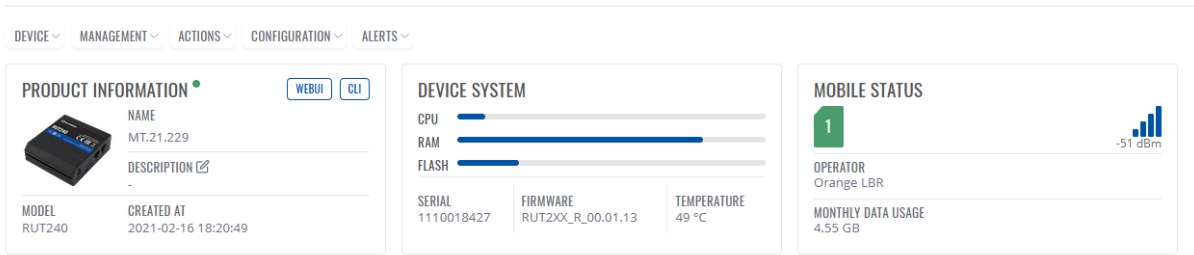


Figure 10 - Communication status of LTE router for data transmission

For the data quality control procedures, CSPS performs the following tasks for data QA/QC:

- Daily data retrieval via mobile phone network
- Check of correct operation of the equipment, coordination of local maintenance staff
- Data analysis including data quality screening and reporting according to international standards
- Correction of apparently erroneous values and gap filling (where possible and reasonable)
- Supervision of maintenance frequency, correct sensor cleaning, analysis of sensor soiling

For the surveillance of the measurement station, a surveillance camera is installed which sends pictures to a server in regular intervals. This server is operated by CSPS.

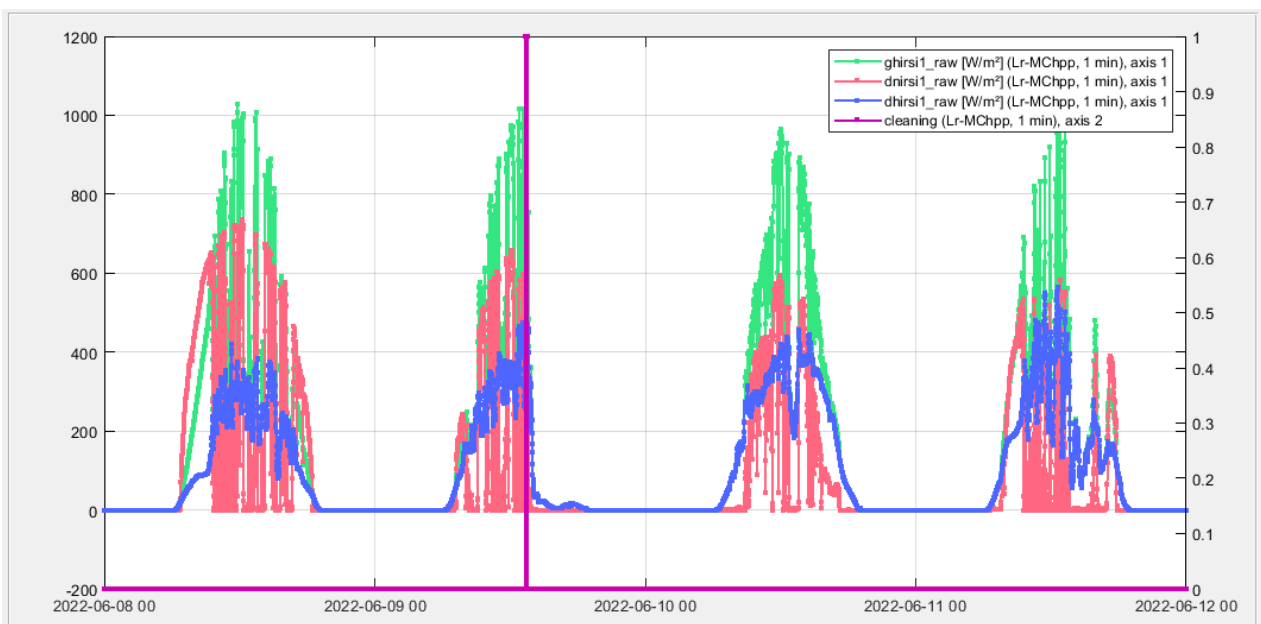


Figure 11 – Measurement data quality control software

4 STATION INSTALLATION, MAINTENANCE AND OPERATION

The station installation and commissioning were completed on 2021-06-11 and the measurement campaign started on 2021-06-12. Before the installation, the site was prepared with a fence and foundations for the stable and secure installation of the automatic weather station for the period of the measurement campaign.





This chapter describes the installation timeline and the completed tasks until the commissioning as well as the maintenance activities for the reported period. A checklist for the installation completion and functionality of the equipment is given in chapter 5.



A complete photographic documentation of the installation and maintenance activities are given in chapter 9.



4.1 INSTALLATION, MAINTENANCE AND OPERATION TIMELINE

Table 4 – Installation and maintenance activities

Completion date	Task	Picture
2021-05-14	Determination of the station location and the north direction. Perimeter marked and correct location and orientation verified.	
2021-05-17 – 2021-05-26	Levelling of the ground and installation of the fence.	
2021-05-31 – 2021-06-04	Positioning of the cement blocks and casting of the foundations.	

<p>2021-06-06</p>	<p>Installation of the mounting structure and measurement control box</p> <p>Installation of the PV module soiling measurement system (PV-S):</p> <ul style="list-style-type: none"> • PV panel mounting structure installed • PV thin-film panels mounted on structure, orientation towards south • PV panel temperature sensors installed on panel backsides 	
<p>2021-06-07</p>	<p>Installation and connection of the irradiance and other meteorological sensors</p>	
<p>2021-06-08 – 2021-06-09</p>	<p>Verification of the PV panel structure levelling and inclination. Connection of the PV-S soiling measurement system and the power supply panels.</p>	
<p>2021-06-10 – 2021-06-11</p>	<ul style="list-style-type: none"> • Functionality checks (local engineers with remote support from CSPS staff) • Commissioning of the station (remotely by CSPS staff) • Operator training 	

2021-06-12	Start of measurement campaign	
2022-01-17	<p>Scheduled maintenance visit after approx. six months of measurements:</p> <ul style="list-style-type: none"> • Foundations and surrounding fence checked for integrity • All parts and sensors of the station examined for damage, dust or condensed humidity, current status recorded and equipment cleaned where necessary • Vertical alignment of wind mast checked, wind mast anchorage and wind mast guying ropes checked for stability, secure fixation in the ground and tightness • Irradiance sensor levelling checked. Irradiance sensors checked for proper operation and functionality; sensors cleaned • Power supply system checked for correct operation. Fuses, electrical components and wiring checked • Datalogger program correct operation verified, measured quantities of all sensors checked for proper operation and correct values • Rain sensor, barometric pressure sensor, temperature and humidity sensor inspected and correct operation verified • Procedures for local maintenance and sensor cleaning discussed with the on-site maintenance team. Availability of spare parts and cleaning equipment verified 	
2022-08-19	<p>Scheduled maintenance visit after approx. twelve months of measurements:</p> <ul style="list-style-type: none"> • Standard maintenance tasks (as above for the visit after approx. six months of measurements) • Installation of GHI reference sensor for GHI signal comparison. Dismounting of GHI reference sensor (2022-08-24) • Dismounting of corrosion samples (exposure time of corrosion samples is specified to be at least twelve months by the manufacturer) 	

2023-01-19	<p>Scheduled maintenance visit after approx. 18 months of measurements:</p> <ul style="list-style-type: none"> • Standard maintenance tasks (as above for the visit after approx. six months of measurements) 	
2023-06-11	Conclusion of measurement campaign	
2023-06-28	Handover of measurement equipment to local utility	

4.2 NOTABLE EVENTS DURING STATION OPERATION

The functionality of the equipment was good throughout the reported measurement period. Table 5 gives an overview on all notable events during the reported measurement period.

Table 5 – *Notable events during operation*

Date	Event
2021-06-10	Installation and commissioning
2021-06-12	Start of measurement campaign
2022-01-17	Scheduled maintenance visit after approximately 6 months of operation
2022-08-19	Scheduled maintenance visit after approximately 12 months of operation, sensor comparison with reference sensor (GHI). Dismounting of corrosion sampler. Replacement of RSI PU sensor head.
2023-01-19	Scheduled maintenance visit after approximately 18 months of operation
2023-06-11	Conclusion of measurement campaign
2023-06-28	Handover of measurement equipment to local utility

5 INSTALLATION CHECKLIST

Table 6 – Installation checklist

Component	Work item	Checked/ approved		Comments
		yes	no	
Foundations, fence	Foundations correctly prepared	X		
	Threaded bolts correctly prepared	X		
	Fence correctly prepared	X		
	Door can be locked	X		
Support structure with Control box	Sensor mounts extended	X		
	PV mounting bar adjusted	X		
	Horizontally leveled	X		
	Grounding cable connected	X		
	All bolts tightened	X		
Wiring, cables	Visual examination	X		
	Fuses ok	X		
	All sensors connected	X		Data connection to CSPS server established
	All cables orderly fixed	X		
RSI	Fixed to MDI Stand	X		
	PU Unit with Licor installed	X		
	Shadow band installed	X		
	Horizontal leveling	X		
	Licor Sensors Clean	X		
	Cable connected to RSI and Box	X		
	RSI operative	X		
Pyranometer	Pyranometer installed	X		
	Horizontal leveling	X		
Barometric Pressure Sensor	Sensor installed and cabled	X		
	Pressure exchange vent	X		Inside control cabinet
	Visual examination, operability	X		
Precipitation Sensor	Sensor installed and leveled	X		
	Visual examination, operability	X		

T_{amb} / RH	Irradiation shield fixed to MDI stand	X	
	Sensor probe with filter cap inserted	X	
	Cable connected to Control Box	X	
Wind tower, wind speed and direction sensors	Tower extended	X	Extended to length of 10 m
	Guy wires safely attached and tense	X	
	Grounding cable connected	X	To metal rod driven into ground
	Wind sensors installed	X	
	North Orientation of WD sensor	X	
	Cable fixed to sensors, tower and box	X	
	Operability of sensors	X	
PV soiling measurement system	Mounting structure installed and fixed to concrete foundations guying ropes fixed	X	
	Mounting structure leveled and aligned to south	X	
	PV panels installed	X	Top of panels horizontally levelled
	Inclination angle adjusted	X	9 degrees from horizontal
	Module temp. sensors installed	X	
	Shunt box connected to AWS	X	
	Operability of system	X	
	Panels cleaned	X	
Modem	SIM card inserted	X	
	APN, username, password of SIM	X	Correctly configured (Auto APN, see section 3.3)
	Server connection	X	Connection to server confirmed
Datalogger	Operation system installed	X	Version: CR1000X Std.05.00
	Datalogger configuration saved	X	
	IP visible in logger configuration	X	IP: dynamic
	Correct sensor constants in program	X	Compared against photographs of installed sensors
	Correct coordinates in program	X	Obtained from GPS
	Datalogger program installed	X	Program name: Lr-MChpp_2021-06-10_str.CR1X Subroutines: Subroutines-Tier2_2021-02-21.CR1X
	Program set to "Run always"	X	
	Datalogger clock correct	X	Local standard time, no daylight saving time: UTC +0

6 LOCAL MAINTENANCE PROCEDURES

Regular on-site maintenance and sensor cleaning was performed by a locally contracted on-site maintenance team (OMT). The maintenance and sensor cleaning procedures were defined prior to the installation of the station and a manual with the defined procedures was provided to the OMT. Additionally, an operator training was held during the commissioning phase of the station. The irradiance sensors and the PV panels for the PV-S soiling measurement system were cleaned according to the table below.

(The measurement of the soiling rate with the PV-S soiling measurement system is based on the comparison of a clean reference module (Module A) to a measurement module (Module B) which is allowed to accumulate soiling on its surface. Module A is therefore cleaned upon each visit by the OMT and Module B is cleaned once per month to restart the soiling measurement cycle.)

Table 7 – Sensor cleaning schedule

Sensors	Cleaning		Comments
	2 x per week	1 x per month	
RSI Licor sensors	x		First and fourth day of each week
GHI pyranometer	x		First and fourth day of each week
Clean module (Module A)	x		First and fourth day of each week
Dirty module (Module B)		x	First day of each month

Scheduled maintenance visits for extended system maintenance were performed approximately every six months for the duration of the measurement campaign (see Table 5 for exact dates when the visits were performed).

The table below shows the number of sensor cleaning visits that were recorded for the the reported measurement period for each month.

Table 8 – Number of sensor cleaning visits per month for the reported measurement period

Month	Number of maintenance visits by local staff	Month	Number of maintenance visits by local staff
Jun 2021	5		
Jul 2021	8	Jul 2022	8
Aug 2021	9	Aug 2022	9
Sep 2021	9	Sep 2022	9
Oct 2021	8	Oct 2022	8
Nov 2021	8	Nov 2022	8
Dec 2021	9	Dec 2022	6
Jan 2022	9	Jan 2023	8
Feb 2022	8	Feb 2023	7
Mar 2022	9	Mar 2023	9
Apr 2022	7	Apr 2023	8
May 2022	9	May 2023	9
Jun 2022	9	Jun 2023	3
Total		199	

7 MEASUREMENT DATA AND RESULTS

7.1 MEASUREMENT DATA UPON INSTALLATION

The measurement data can be accessed on a protected web server for near-real time data monitoring and download. Additionally, CSPS will provide monthly data reports with the final quality-controlled measurement data. The graphs below show exemplary data shortly after the installation.

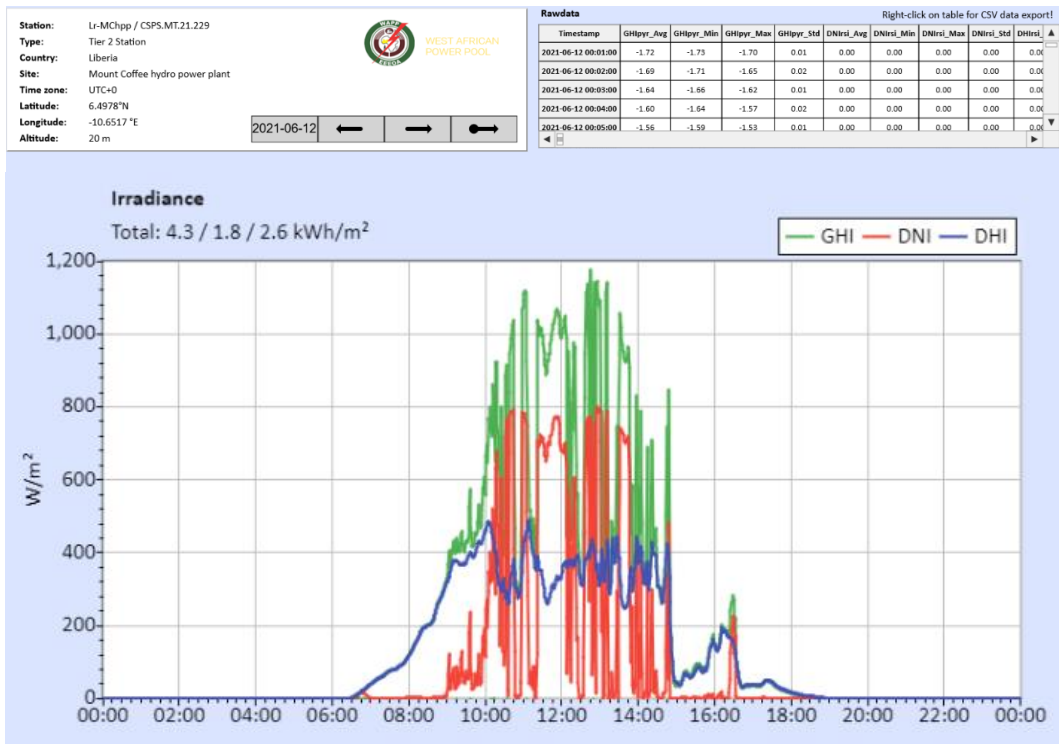


Figure 12 - Irradiance measurement. GHI, DNI and DHI

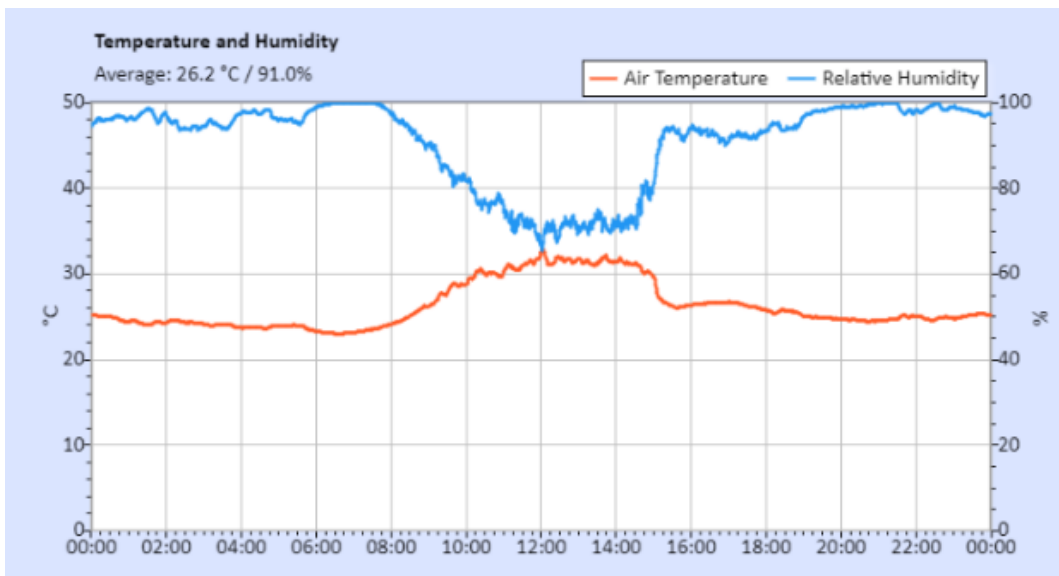


Figure 13 - Temperature and Humidity measurements

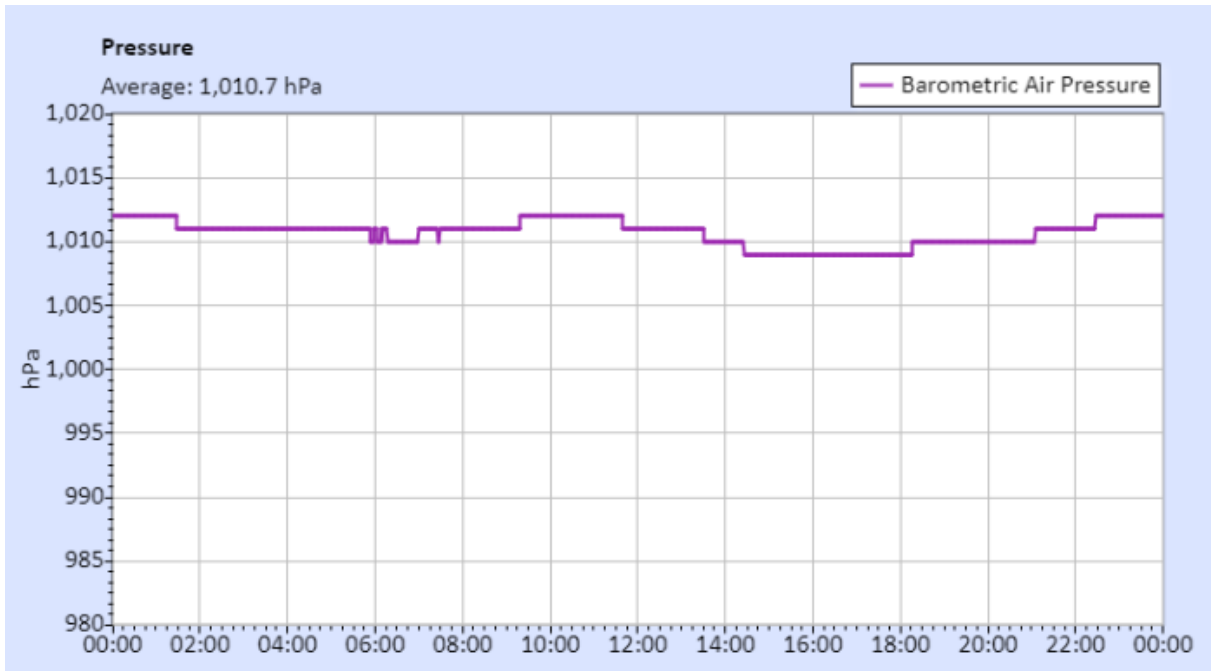


Figure 14 - Barometric air pressure measurement

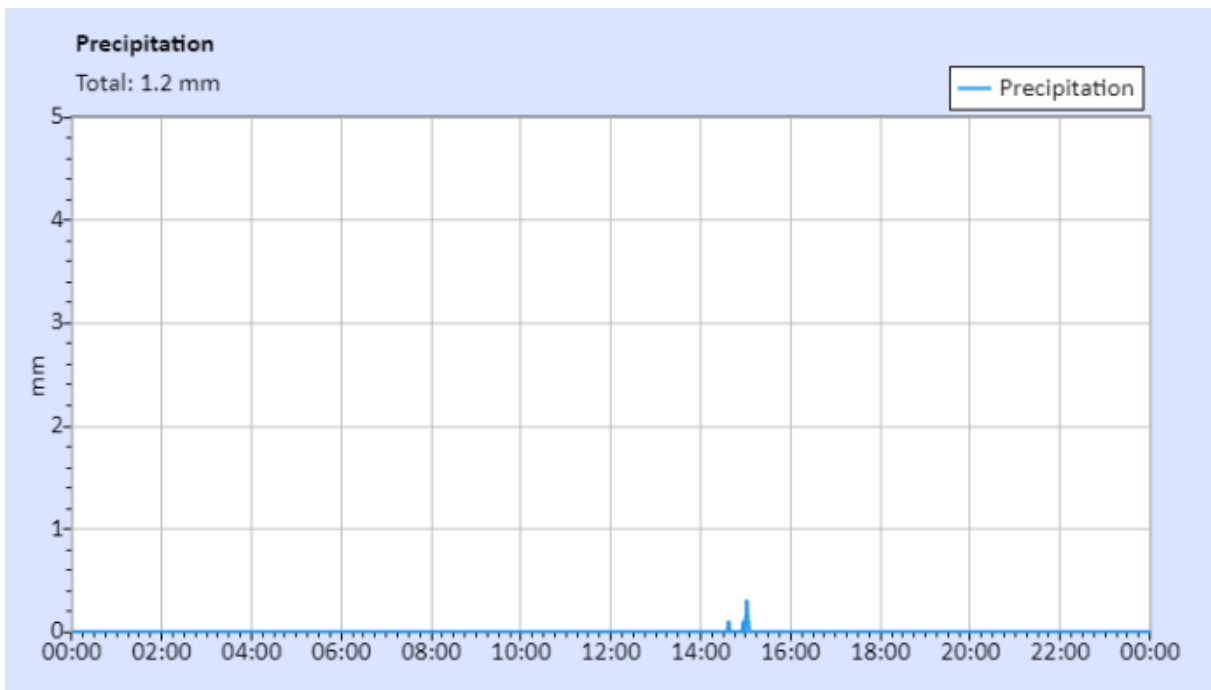


Figure 15 - Precipitation measurement

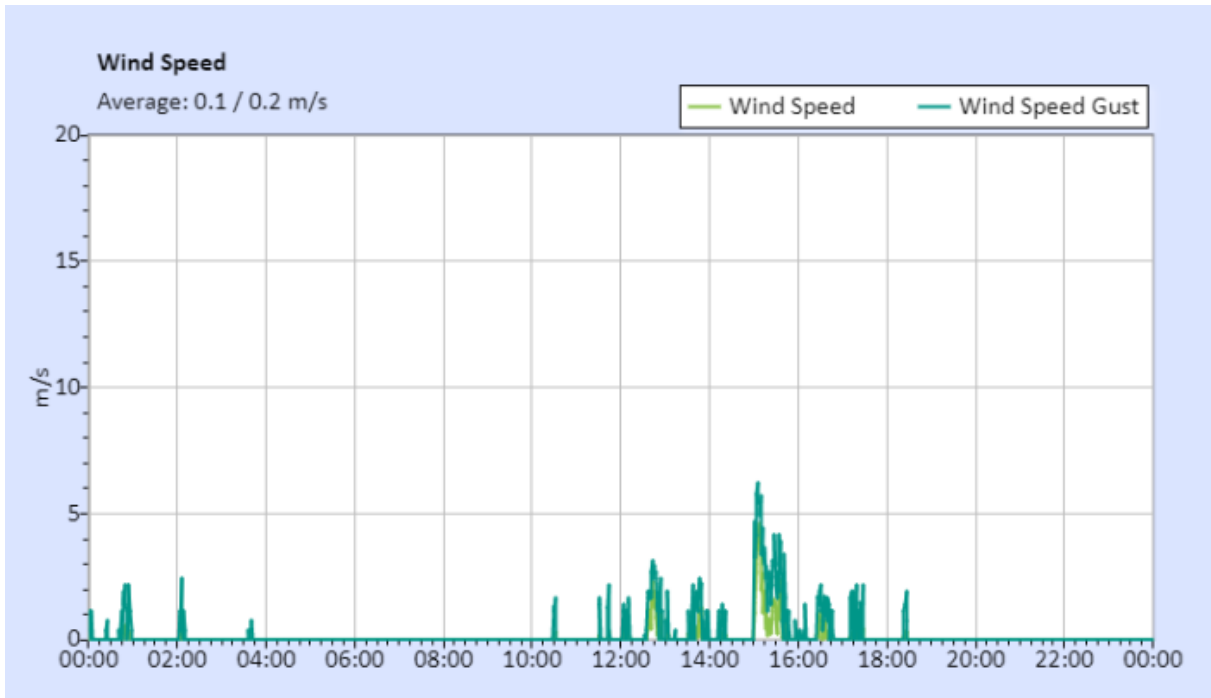


Figure 16 - Wind speed measurement

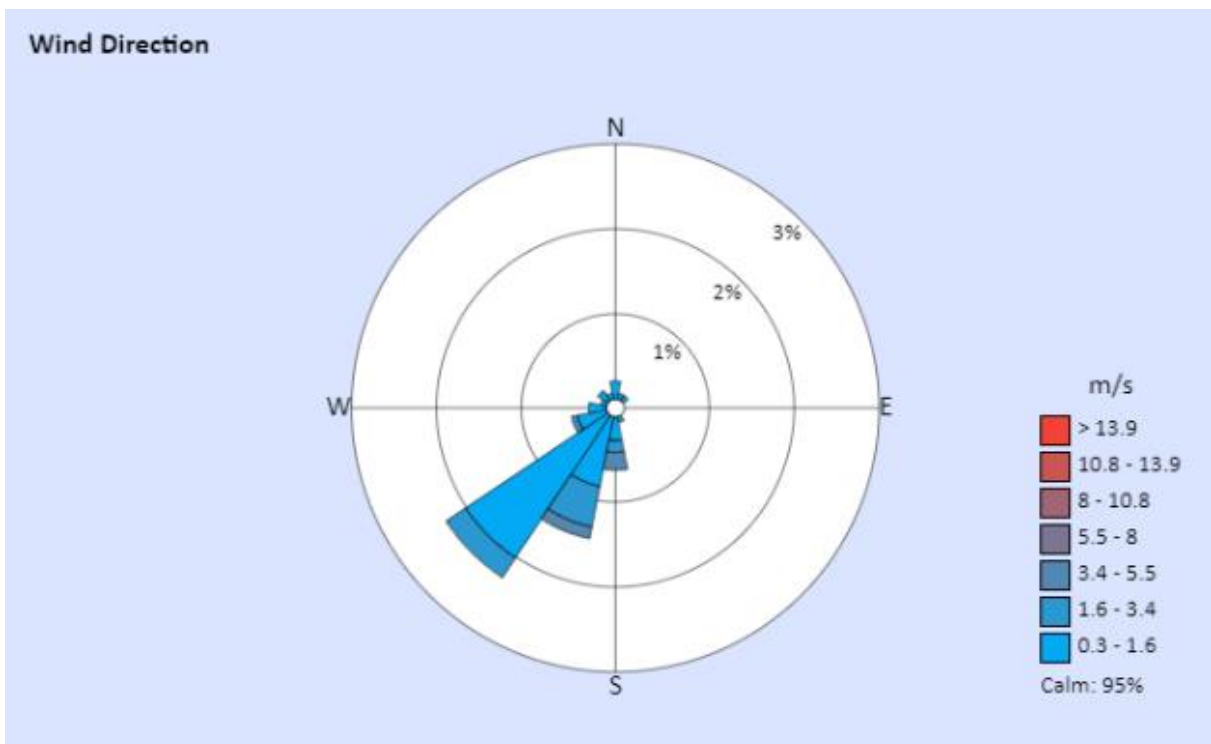


Figure 17 - Wind direction measurement

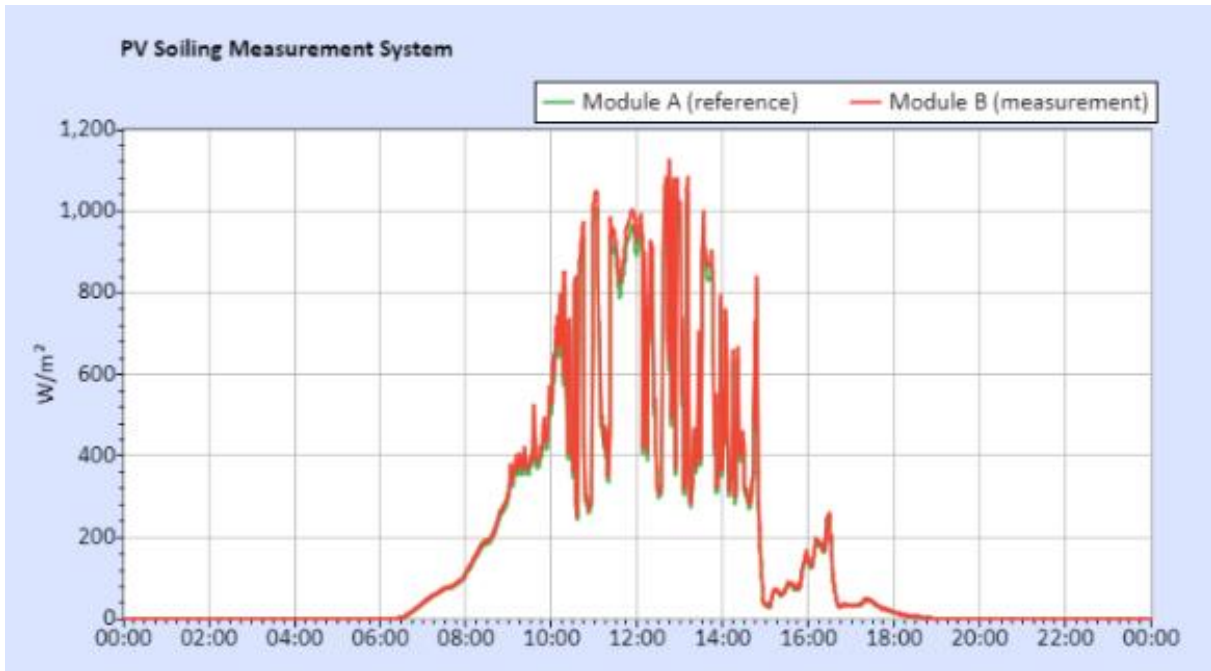


Figure 18 - PV soiling measurements

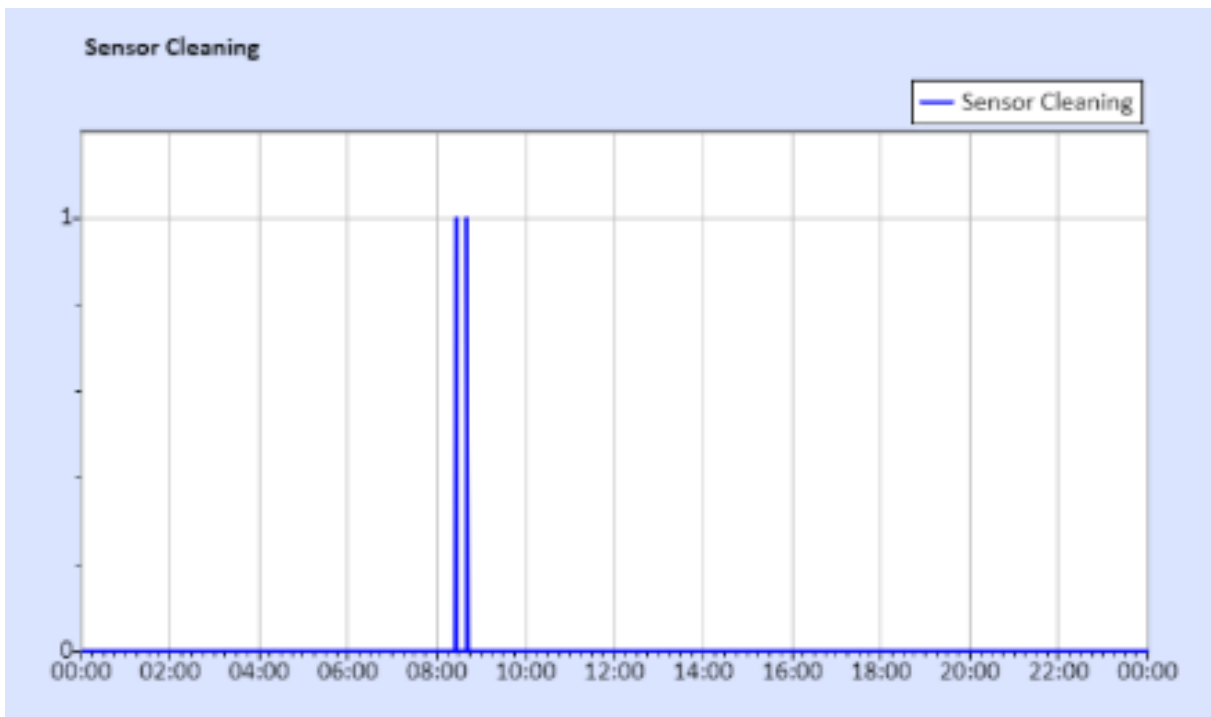


Figure 19 - Sensor cleaning recordings. 2021-06-14, first cleaning of irradiance sensors and PV-S reference module

7.2 MEASUREMENT RESULTS FOR THE REPORTED MEASUREMENT PERIOD

7.2.1 Monthly summaries

Table 9 summarizes the irradiance sum per month and the complete year as well as the average and sum of the other measured meteorological parameters. The results are shown for the reported measurement period, the first and the last months are usually partial months for which the data availability adds up to 100%.

Table 9 – Measurement results, monthly average values

Month	Sum irradiance [kWh/m ²]			Avg. temp. [°C]	Avg. wind speed [m/s]	Avg. pressure [hPa]	Avg. humidity [%]	Sum rain [mm]	Data availability
	GHI	DNI	DHI						
Jun-21	76	31	51	25.6	0.1	1012	93	225	63.3%
Jul-21	100	29	75	25.0	0.1	1013	93	616	100%
Aug-21	117	39	83	25.2	0.2	1012	91	331	100%
Sep-21	137	60	86	25.7	0.2	1011	90	256	100%
Oct-21	146	78	81	26.5	0.2	1010	88	92	100%
Nov-21	149	100	71	26.9	0.2	1009	85	0	100%
Dec-21	144	87	75	27.3	0.1	1009	84	0	100%
Jan-22	148	92	75	27.1	0.2	1009	81	10	100%
Feb-22	141	72	80	27.4	0.5	1009	79	56	100%
Mar-22	168	74	100	27.3	0.6	1008	79	69	100%
Apr-22	152	65	92	26.9	0.5	1009	81	170	100%
May-22	137	54	87	26.7	0.3	1011	85	117	100%
Jun-22	121	48	79	25.7	0.3	1011	86	228	100%
Jul-22	103	34	73	24.9	0.3	1013	86	218	100%
Aug-22	89	14	76	24.6	0.3	1012	89	540	100%
Sep-22	105	36	78	25.1	0.3	1012	89	667	100%
Oct-22	138	65	88	25.9	0.2	1011	87	288	100%
Nov-22	136	78	80	26.1	0.2	1010	85	133	100%
Dec-22	149	110	72	26.5	0.2	1010	82	9	100%
Jan-23	163	120	75	26.7	0.3	1010	80	11	100%
Feb-23	144	76	83	27.3	0.5	1009	78	4	100%
Mar-23	164	90	90	27.1	0.6	1009	80	110	100%
Apr-23	159	77	95	27.3	0.4	1009	82	181	100%
May-23	155	80	92	27.5	0.4	1011	84	129	100%
Jun-23	42	14	30	26.4	0.3	1012	87	105	36.7%
Jun-21 - Jun-22	1665	806	985	26.4	0.3	1010	86	1962	100%
Jun-22 - Jun-23	1617	819	981	26.2	0.3	1010	84	2604	100%
Total	3283	1625	1966	26.3	0.3	1010	85	4566	100%

For a description of the installed measurement equipment, please refer to section 3.1. The results are further detailed in the following section.

7.2.2 Solar irradiance

Figure 20 shows the measured monthly irradiance sums in a bar chart. The results are shown for the reported measurement period, the first and the last months are usually partial months.

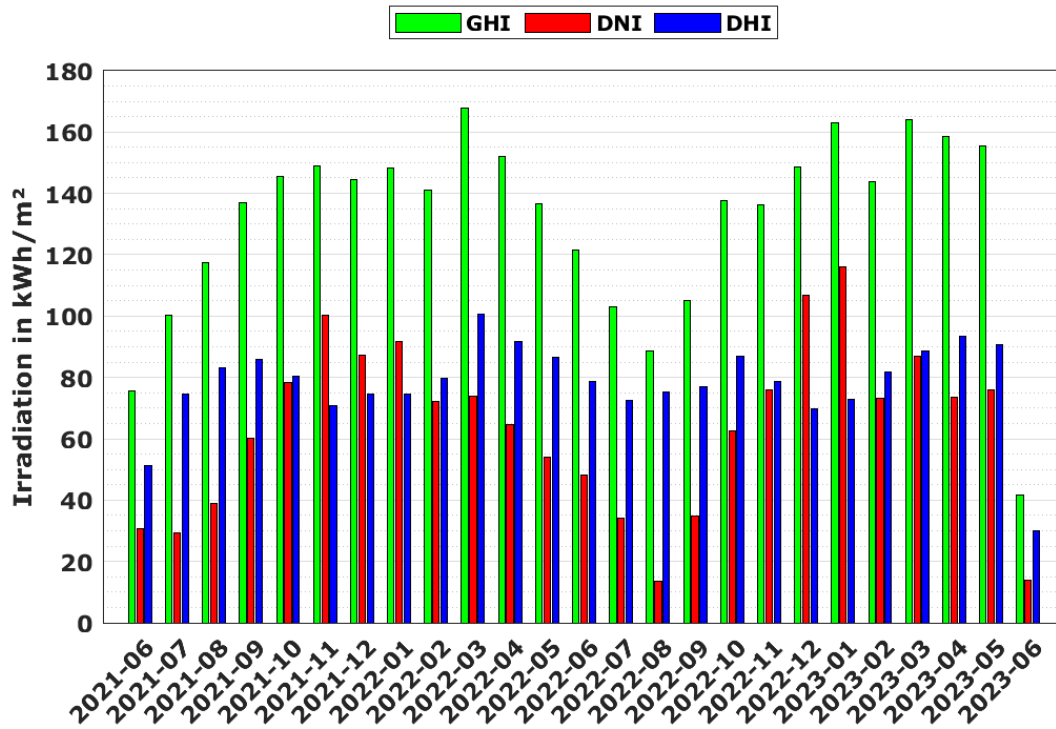


Figure 20: Monthly irradiance sums

Figure 21 shows the frequency distribution of the irradiance for the reported measurement period.

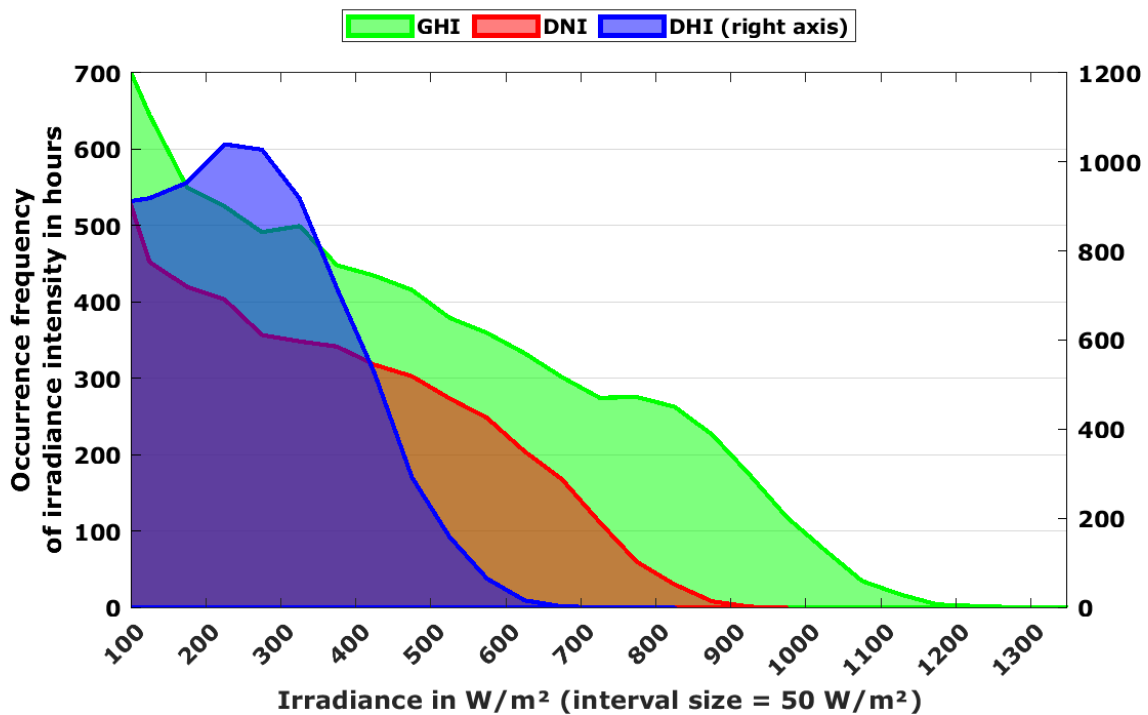


Figure 21: Frequency distribution of hourly irradiance averages

Figure 22 shows the irradiance intensity for GHI over the reported measurement period. The irradiation intensity and the length of the days vary with the seasons. Cloudy periods with low GHI values are visible as blue vertical stripes and occur mostly during the rainy season.

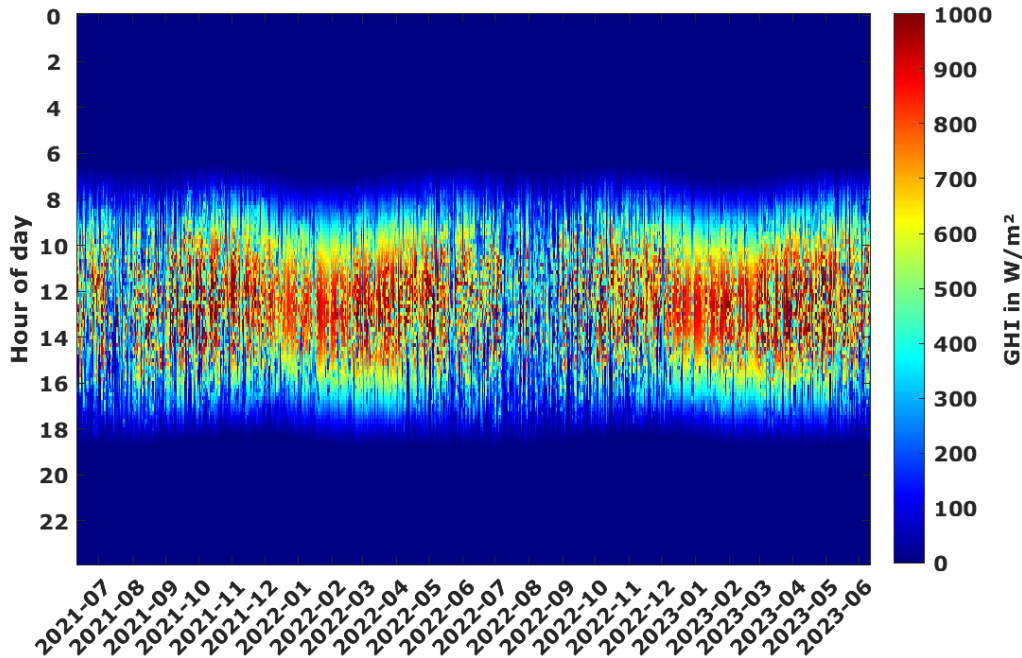


Figure 22: GHI irradiance intensity

Figure 23 shows the irradiance intensity for DNI over the reported measurement period. The irradiation intensity and the length of the days vary with the seasons. Cloudy periods with low DNI values are visible as blue vertical stripes and occur mostly during the rainy season.

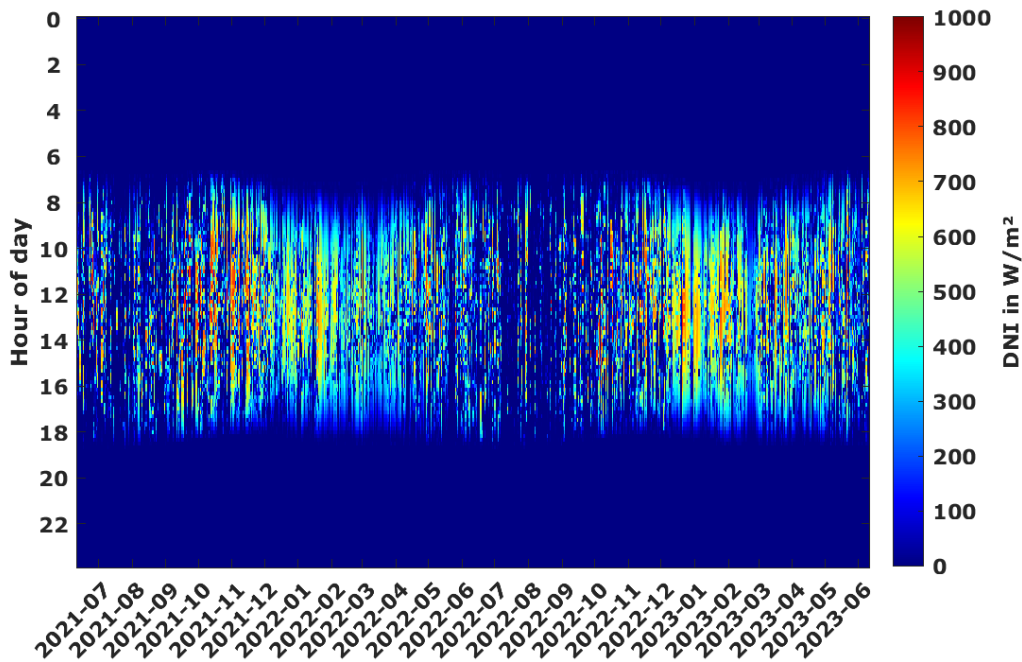


Figure 23: DNI irradiance intensity

7.2.3 Temperature and relative humidity

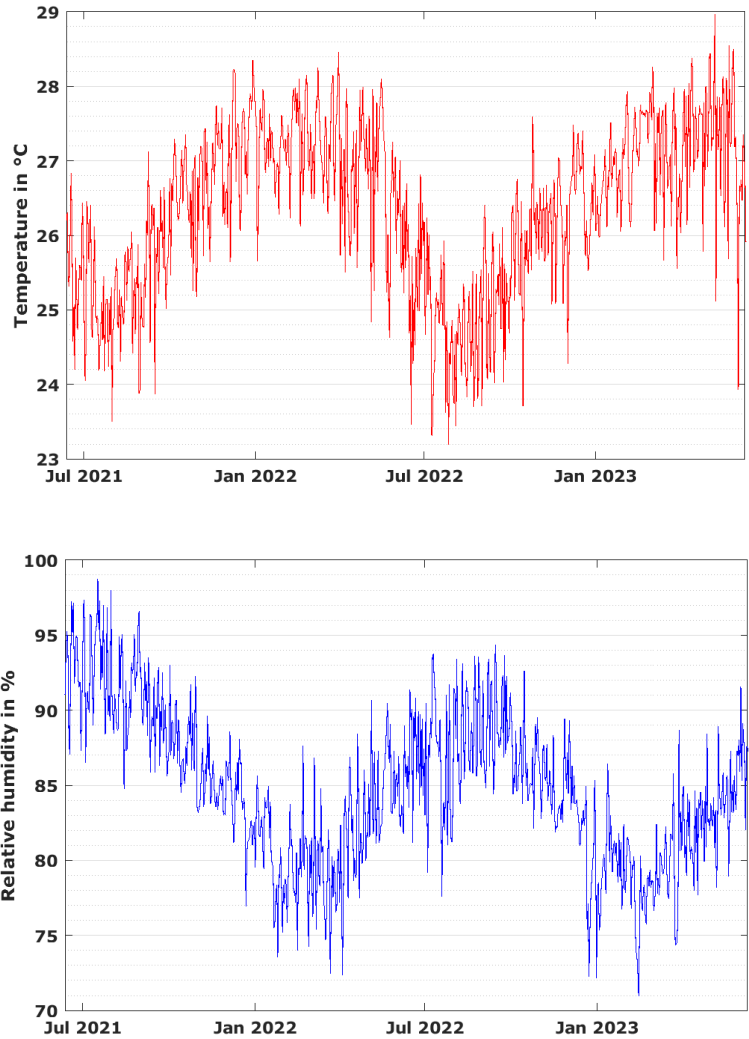


Figure 24: Daily temperature and relative humidity averages

Figure 24 shows daily averages of temperature and relative humidity over the reported measurement period. The variability over the seasons is visible in the graphics with usually higher humidity values during the rainy season. Figure 25 shows the frequency distribution of temperature and relative humidity.

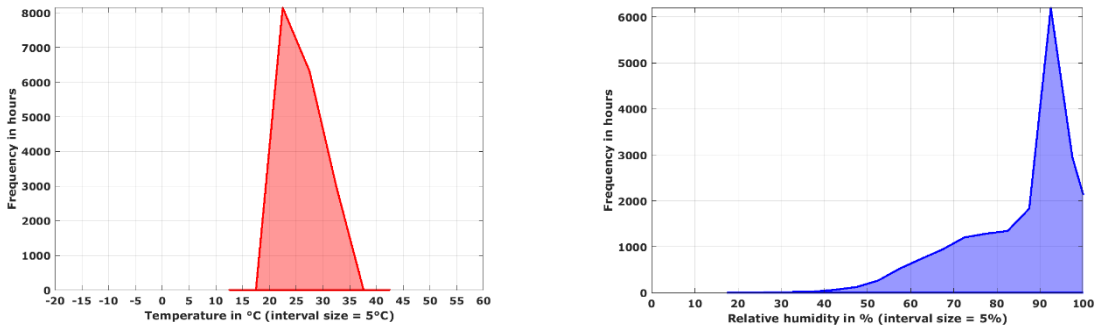


Figure 25: Frequency distribution of temperature and relative humidity

7.2.4 Precipitation

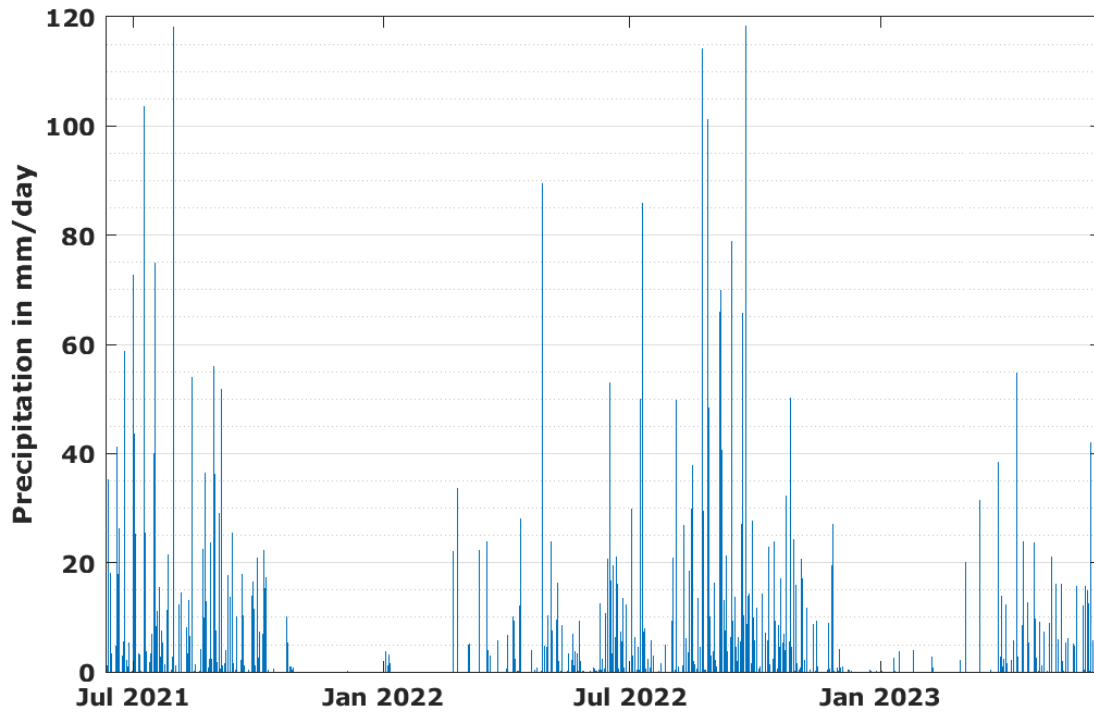


Figure 26: Daily sums of precipitation

Figure 26 shows the daily sums of precipitation. Again, a seasonal variability was observed with a dry period with little precipitation from November to March and period with frequent precipitation observed between April and October.

7.2.5 Wind speed and direction

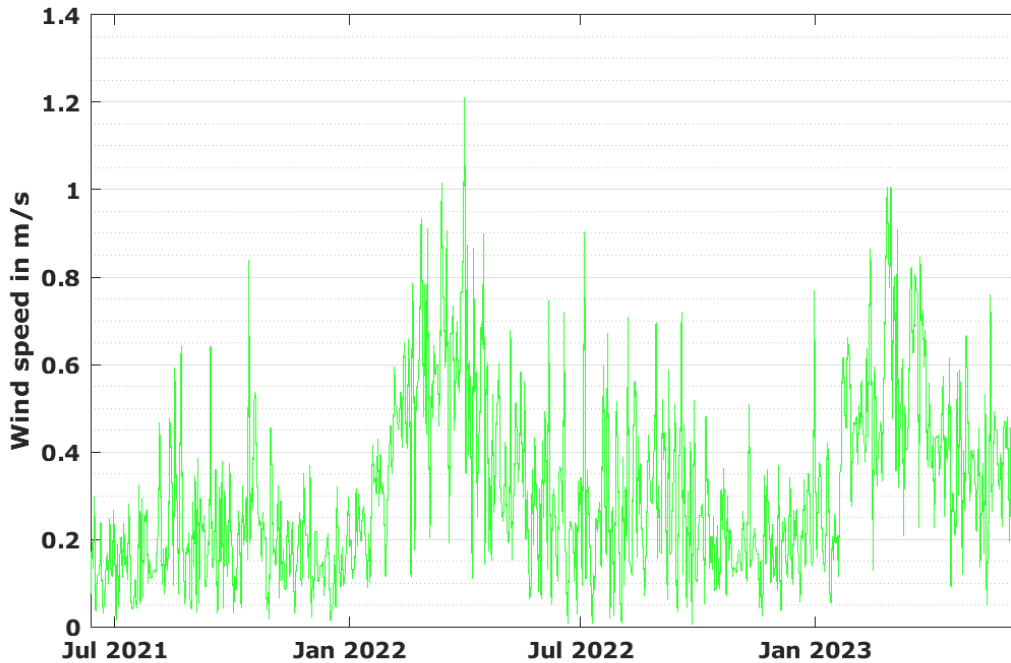


Figure 27: Daily averages of wind speed

Figure 27 shows the daily averages of wind speed. They are continuously low and only a small seasonal dependency was observed. The frequency distribution, shown in Figure 28, emphasizes that low wind speeds and wind gusts are common. High wind speeds of more than 6 m/s were barely recorded.

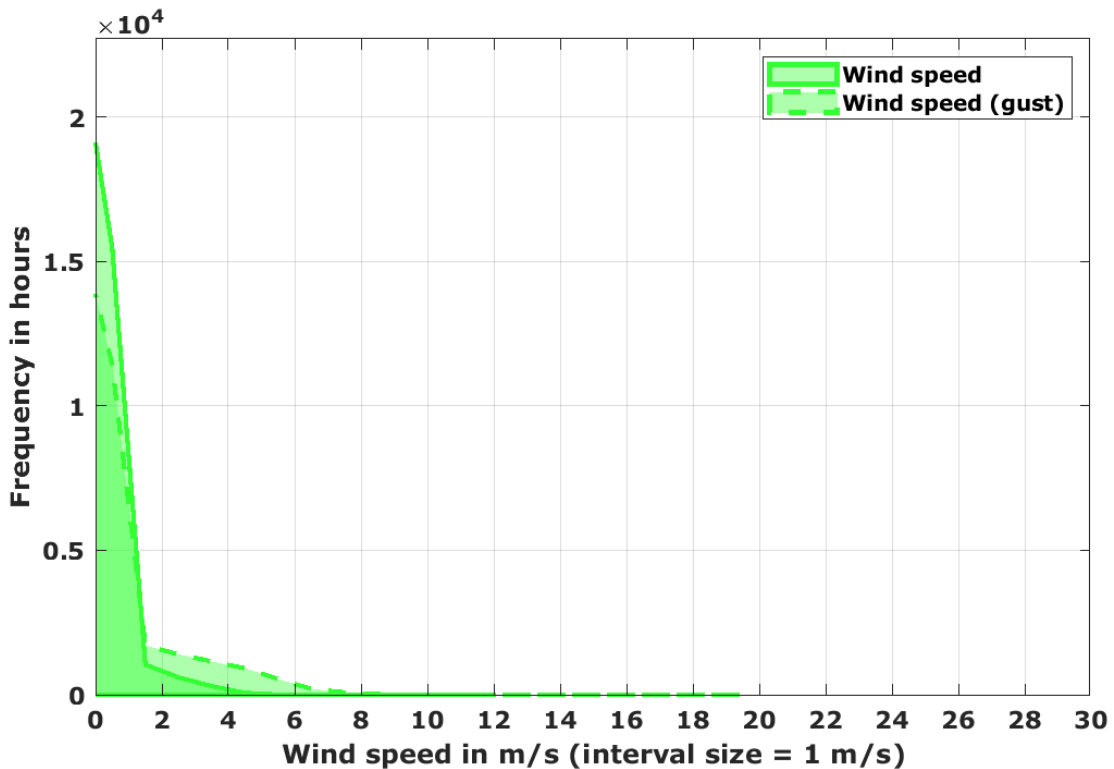


Figure 28: Frequency distribution of wind speeds

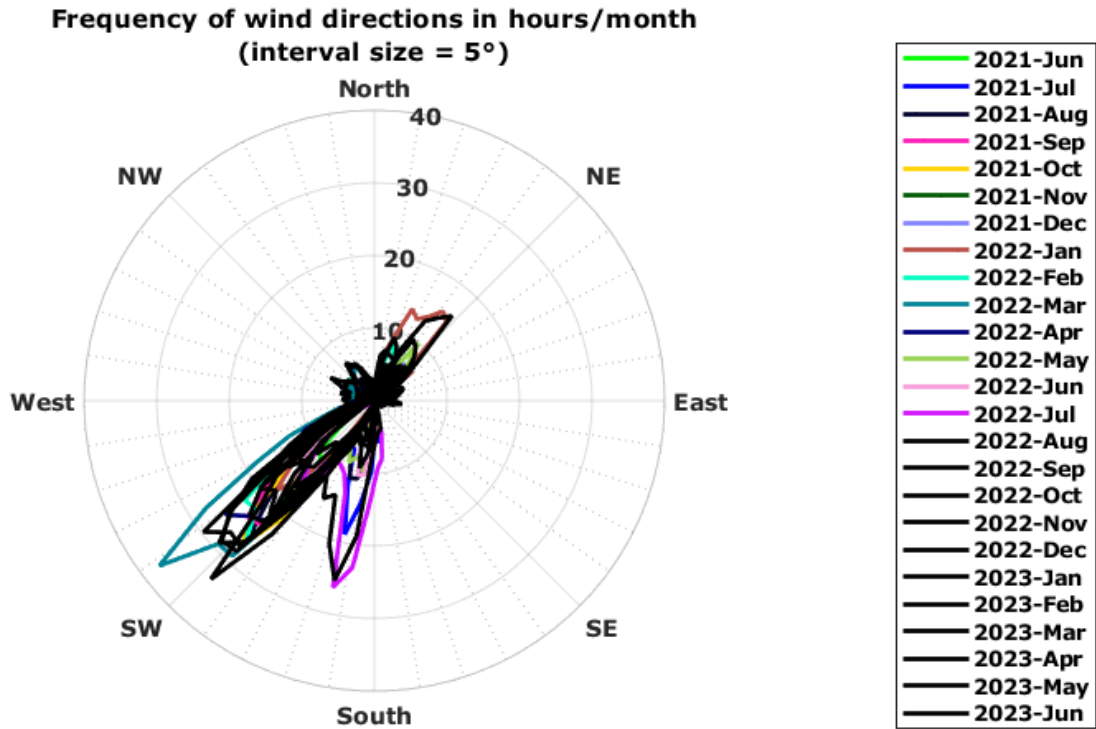


Figure 29: Wind direction distribution

Figure 29 shows the frequency distribution of wind direction. Different seasonal wind directions are visible but most of the year the most common with direction was from south-southwest.

Figure 30 shows that the few recorded strong wind gusts were from the north-northeast mostly.

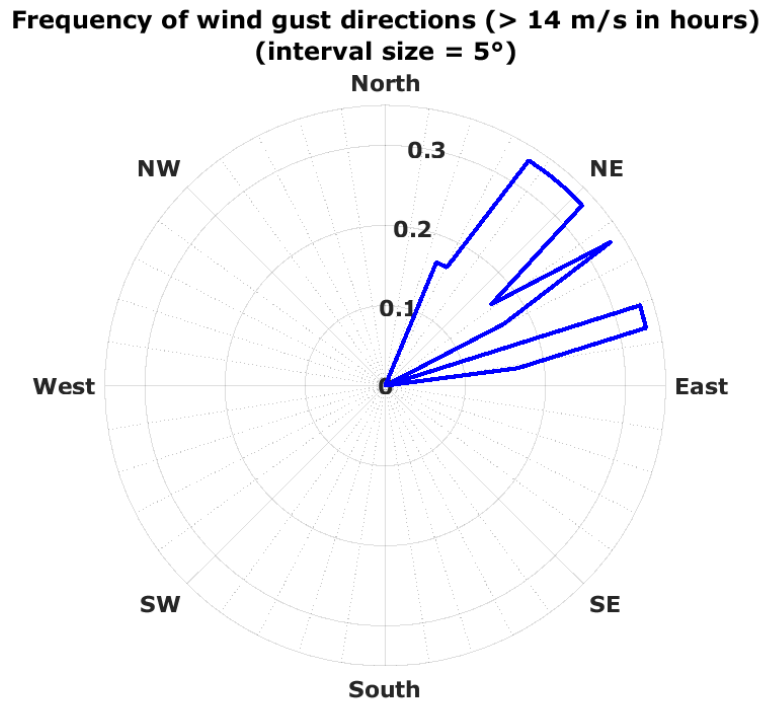


Figure 30: Wind gust direction distribution

7.3 PV SOILING MEASUREMENT SYSTEM (SOILING RATE)

7.3.1 Measurement methodology

The measurement methodology applied for the PV soiling measurement system largely follows the methodology presented by (Zorilla-Casanova, et al., 2016), (Gostein, Caron, & Littman, Measuring Soiling Losses at Utility-scale PV Power Plants, 2014) and (Gostein, Littman, Caron, & Dunn, 2013) with a few simplifications and modifications. The method is based on the idea to compare a clean surface (reference value) with a surface which accumulates soiling over intervals of roughly one month. From the comparison to the clean reference, the impact of the accumulated soiling can be assessed.

7.3.2 Measurement equipment

The PV-soiling system consists of two PV panels (Phaesun Sun Plus 30 S monocrystalline solar panel, 30 W) mounted next to each other in a south-orientated tilted plane (see Figure 31). The tilt angle is chosen according to globalsolaratlas.info (“Optimum tilt of PV modules”). The panels are regular, commercially available panels from the manufacturer and have not been calibrated by a laboratory to identify individual short-circuit current under reference conditions. This is further explained in this chapter.

Please note that the installed modules are not calibrated reference cells or similar, i.e., the purpose is to measure the soiling rate (by comparing the changing signal of the two panels to each other) and not to measure the irradiance. The measured values should only be used for the purpose of the assessment of the soiling rate.



Figure 31: PV-soiling system with the clean reference panel (modA) and the measurement panel (modB). The measurement panel is kept clean by regular cleaning by the local maintenance staff whereas the measurement panel is allowed to accumulate soiling over time

7.3.3 Measured values

From both panels, the short-circuit current and the panel backside temperature is measured. The short-circuit current of the modules is used to calculate the temperature-corrected incident irradiance for each of the modules individually.

The incident irradiation on module A, further called “modA”, is the reference value and the panel is kept clean by regular cleaning. Module B, further called “modB”, is allowed to accumulate soiling over intervals of roughly one month (see Figure 31).

To calculate the present soiling ratio at each timestamp, the dirty-to-clean ratio of the simultaneously measured irradiance from both panels and the cleanliness of modB is calculated.

The change of the cleanliness of modB over time (e.g. from one day to the next) is defined as the soiling rate (for the referenced time interval). It can be expressed as an average value for a specified time period, e.g. average daily soiling rate in one calendar month.

7.3.4 Cleaning cycles

As explained above, a clean PV module (reference value) is compared with a soiled module. Naturally, this comparison is only accurate when the reference panel is nearly perfectly clean at all times. Cleaning cycles and the correct implementation of cleaning procedures are therefore very important. The first objective is to ensure an all-time clean reference value.

The second objective is to prevent any saturation effect of the soiling measurement on the surface of modB and to keep the soiling non-uniformity in a range where it does not significantly reduce the accuracy of the soiling measurement with the chosen method.

The scheduled cleaning cycles for both panels were chosen to ensure a clean surface of the reference panel modA and the cleaning of the soiled surface of modB before saturation effects occur, also considering efficiency and feasibility in the field.

- (Gostein, Caron, & Littman, Measuring Soiling Losses at Utility-scale PV Power Plants, 2014) suggest that the reference module should be cleaned at least once per week, more often in regions with higher soiling effect. For the measurement campaign described in this report, the reference module modA was cleaned twice per week during the whole measurement period. To further approach an ideal all-time clean reference module, soiling correction was applied to the values measured with modA (see below for details). Upon the cleanings of modA, all other irradiance sensors on the automatic weather station except of modB were also cleaned.
- The soiled module modB is usually cleaned roughly in monthly intervals to avoid saturation effects in periods of high soiling rates (deviation from the linear soiling increase pattern).

7.3.5 Data acquisition and processing

The 1-Hz measurement values were logged by the data logger in one-minute and ten-minute average values and transmitted to the CSP Services data acquisition server. A specialized software tool for data analysis was used on the data acquisition server.

This tool automatically stores the data in an SQL database and offers data analysis and visualization functionality. The data analysis is further described in the following section.

7.3.6 Data analysis

The data analysis is carried out along the following scheme:

1. Application of soiling correction to the measured values from the reference module according to a method developed by (F. Wolfertstetter, 2013):

The soiling present at the time of cleaning can be detected by the sudden increase of the measurement signal upon cleaning, and the comparison with a reference value before and after the cleaning process. In this case (cleaning of modA), the sudden increase in signal can be analyzed and quantified from the 1-minute resolution data. It can be assumed that this change is solely attributable to the layer of soiling that has accumulated on modA since its last cleaning, because no other parameters are changing.

This unwanted soiling effect on modA was removed for cases of strong modA soiling. This was achieved by linearly interpolating backwards toward the last cleaning event, i.e. after cleaning the soiling is zero and linearly builds up towards the next cleaning event. In case of dust outbreaks, rain or other events that do not allow assumption of linear soiling accumulation, these events are singled out and the linear interpolation is not applied.

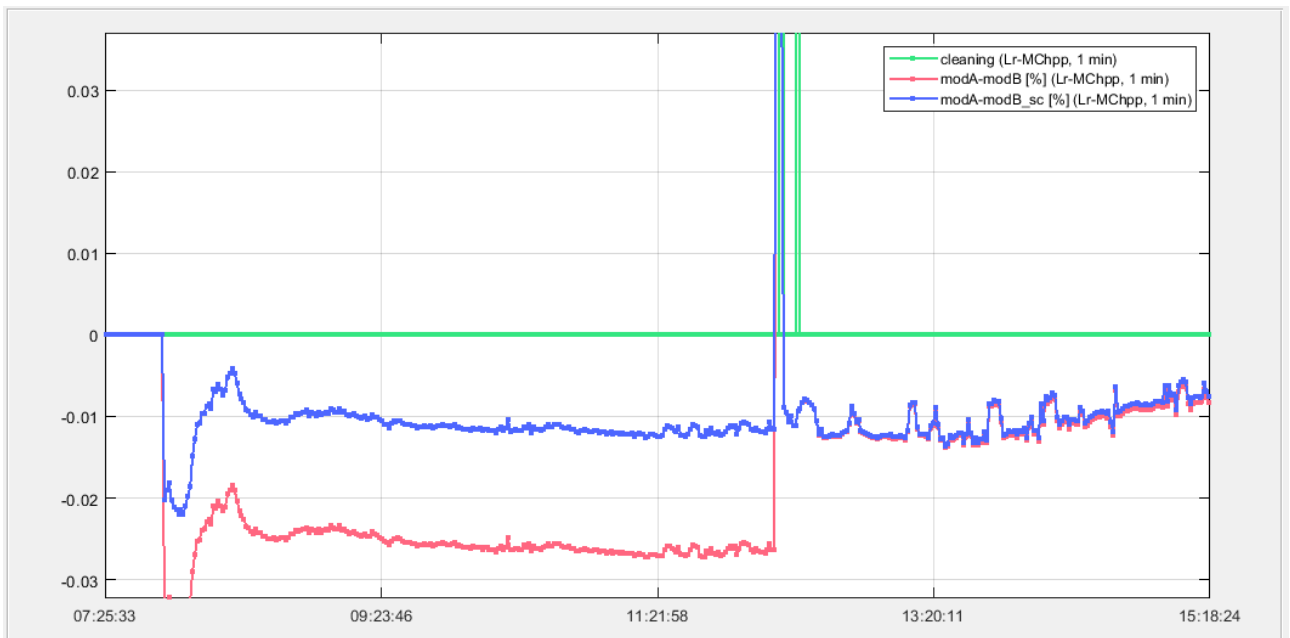


Figure 32: Reference panel soiling assessment procedure

Figure 32 illustrates this procedure with an example. It shows the difference in signal between modA and modB vs. the local time of day (example from 2022-02-14). The blue line includes the application of soiling correction to the modA values. The red line shows the uncorrected values. The discontinuity in the curve at the cleaning event (green bar) is visible for the uncorrected values. The increase in the modA values in this example was found to be 1.5 %. Therefore, a linearly increasing correction between 0.0 % and 1.5 % was applied to the modA values between this cleaning and the one before.

2. Division of the measurement period into intervals of nearly constant soiling rates:
 - a) Cleaning of modB: Each modB cleaning starts a new interval
 - b) Weather events: Occurrences of rain (self-cleaning effect), strong wind speed or wind gusts or high diffuse irradiance (representing days with a high aerosol load and potentially resulting high soiling deposition) might be used for dividing the data in sub-intervals (usually several days to weeks). A weather event is used as an indicator to set a new interpolation interval when these values reach or exceed certain thresholds which were identified as reasonable limits during the analysis.
3. Calculation of the daily soiling rate in each sub-interval: The average daily soiling rate corresponds to the average increase of the daily soiling ratio from one day to the next within the sub-interval. In most cases, a linear increase is a fine approximation, as Figure 33 shows. Periods with many rain events often results in no soiling rate because no soiling is accumulated between the rain events.

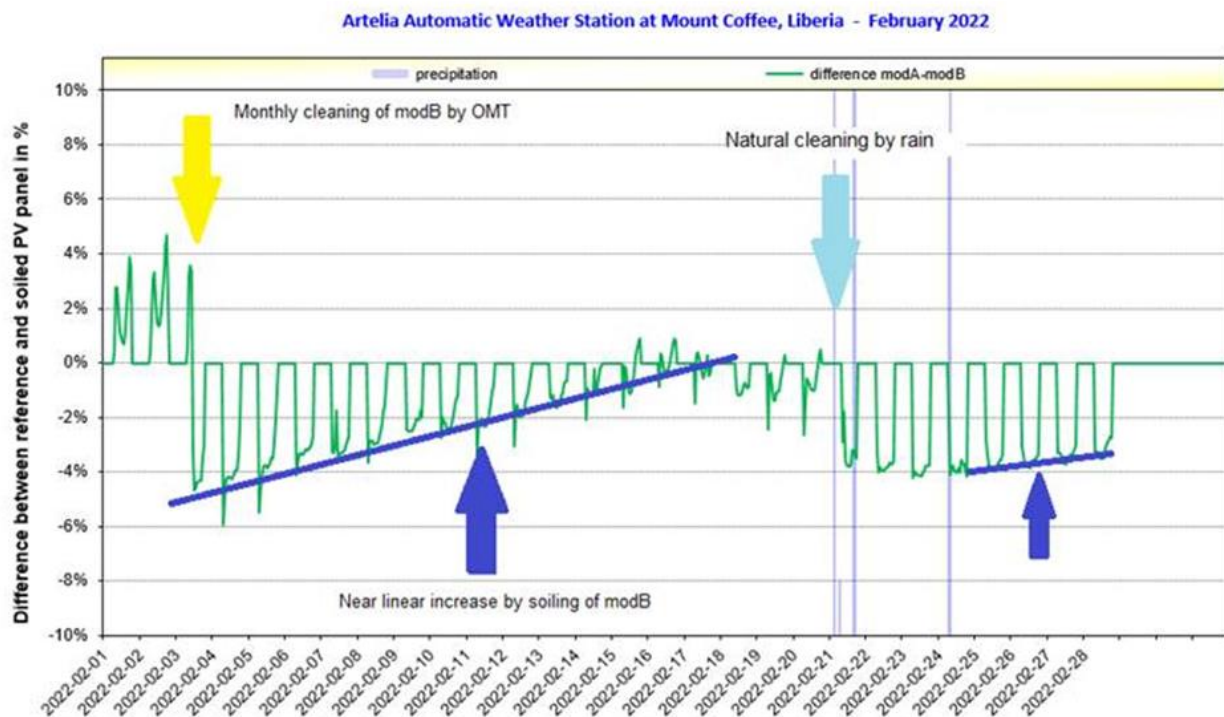


Figure 33: Example for increase of modB panel soiling accumulation; green curve: soiling ratio in 1-hour resolution

Another important characteristic of the chosen methodology is visible from Figure 33: After cleaning or sufficient amounts of rain, the difference between the readings of the two panels does not necessarily return to a value of 0 %, which could have been expected intuitively (because both panels are supposedly clean and in identical state). This is due to several contributing factors:

- The cleaning may not have been perfect. In field conditions (extreme heat, occasionally no demineralized water available, cleaning cloth not perfectly clean, operator failure to comply with the procedure etc.), perfect cleaning is often not achievable.
- The panels do not have individual calibration and sensitivity factors, instead the typical value from the manufacturer's datasheet is used. Therefore, the panels can have an offset on both directions (modA > modB or vice versa) even in perfectly clean state.
- The sensitivity of the panel to irradiation conditions other than standard test conditions may be individually different for each panel.
- Residual alignment errors between the panels.

However, it is not necessary that the panels have identical values after cleaning, or to use the offset factor between the panels upon installation as a calibration factor. This has two main reasons:

- the lack of an absolute reference is not relevant because in the chosen methodology, only relative values are compared. The absolute values measured by the panels is not of interest, only the relative difference between the soiled and clean panel is evaluated.
- Defining a new relative reference allows to exclude influences on the absolute measurement value such as imperfect cleanliness or the actual module state. For example, if a new interval is defined after a rain event which caused a partial cleaning, the reference for calculating the soiling rate in the following interval necessarily needs to take into account the actual state of the module at interval start. With this method, even small damages to the panel which influence the absolute value, but not the relative change of the soiling ratio from one day to the next due to soiling accumulation, do not influence the measurement. Hence, the method is more robust in field conditions.

The soiling rate was derived by introducing interpolation lines such as shown in Figure 33 allowing to consider periods of nearly constant soiling rates as well as periods with special weather events.

Please note: This short-circuit-measurement based soiling rate measurement provides information on the soiling-induced loss of available solar irradiance that arrives on the solar panels and is available there for conversion into electricity (“effective irradiance”). It is not equal to the soiling-induced loss of PV module power output, although the difference between the loss of incident irradiance and loss of power output is small for low soiling levels and uniform soiling distribution on the module surface. Therefore, to use the soiling rates presented in this report correctly, they must be applied as a diminishing influence to the effective irradiance that is used as an input of PV power plant performance models (Gostein, Littman, Caron, & Dunn, 2013).

As shown by (Gostein, Caron, & Littman, Measuring Soiling Losses at Utility-scale PV Power Plants, 2014), the instantaneously measured soiling rate (SR) of PV panels typically shows a dependence on the time of day. Further, there are some residual differences in azimuth and tilt alignment of the panels, resulting in slightly varying irradiance incidence angle on the two adjacent panels.

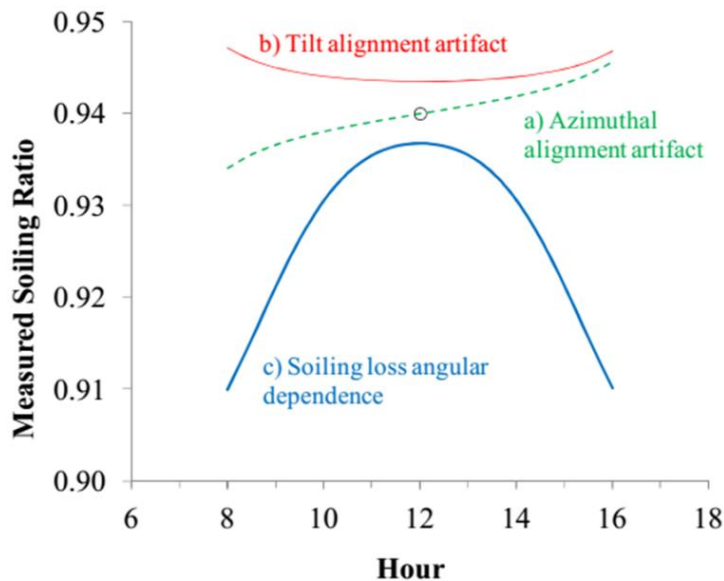


Figure 34: Time-of-day dependence of instantaneous SR measurements
 Source: (Gostein, Caron, & Littman, Measuring Soiling Losses at Utility-scale PV Power Plants, 2014)

The tilt alignment and azimuthal alignment have been done with great care upon installation, the installation frame upon which the panels rest was designed to ensure that both panels are as closely as possible to identical orientation. The residual error should therefore not be larger than presented as typical in the literature. The angular dependence of the soiling ratio has been addressed by fitting a linear trend line (Least-Square-Method) through the soiling ratio values to determine the soiling rates from the slope of the linear trend line.

7.3.7 Comparison of measurement methodology with IEC 61724-1

In March 2017, the International Standard IEC 61724-1 was published. This standard contains a section on soiling ratio measurement (section 7.3.4), in which two different procedures are defined. The second method defined in the standard is very similar to the method utilized in this measurement campaign.

Both methods are compared below:

Table 10 – Soiling rate analysis methodology

Item / Procedure	IEC 61724-1	Methodology used in this report
Calibration value for short-circuit current at designated reference condition	Manufacturer’s datasheet values	Manufacturer’s datasheet values
Calibration in the field	Derive modB short-circuit current calibration factor by comparing measured effective irradiance of modB to modA (both cleaned), this provides the I_{sc} calibration factor for modB	Calibration of modB short-circuit current to clean reference modA is done by using individual factors for each analysis interval
Measurement procedure	<ol style="list-style-type: none"> 1) Measure module temperatures and short-circuit currents 2) Calculate effective irradiance on modA using datasheet factor 3) Calculate expected modB short-circuit current using I_{sc} calibration factor of modB 4) Calculate soiling ratio by dividing measured modB short circuit current by the expected modB short-circuit current 	<ol style="list-style-type: none"> 1) Measure module temperatures and short-circuit currents 2) Calculate effective irradiance on modA and modB using datasheet I_{sc} factor 3) Calculate the soiling ratio from effective irradiances 4) Calculate cleanliness by referencing to soiling ratio at last cleaning

The methodology presented in this report slightly differs from the IEC standard. The methodology used in this field campaign is referencing the soiling ratio in each analysis interval instead of referencing to a static calibration factor. This takes into account that cleaning of modA/B in field conditions may not always yield perfect cleaning results that are identical to the first cleaning in the campaign. $SR(t_0)$ is an interval-specific calibration of the measurement, which is more adequate in a field measurement campaign than using a static calibration that is done right after equipment installation.

The compatibility of the methodology with IEC 61724-1 is generally given due to identical equipment requirements. The results should be transferable.

7.3.8 Soiling measurement results

The soiling rate measurement results are displayed in this chapter. The measurement data for the parameters modA and modB was submitted to the client together with the other measurement data from the station at the end of each month. These reports include the comparison between modA and modB for the PV-soiling measurement system. Also, graphical illustrations of these measurement parameters and their comparison were provided.

A summary of the calculated daily soiling rates is provided in Table 12.

7.3.9 Average monthly and yearly soiling rates

An overview of the average daily soiling rate over each calendar month and over the entire year is given in the table below.

Table 11 – Average monthly and yearly soiling rates

Month	Average soiling rate PV-soiling [%/day]	Month	Average soiling rate PV-soiling [%/day]
Jun-21	0.02	Jun-22	0.01
Jul-21	0.03	Jul-21	0.03
Aug-21	0.02	Aug-21	0.06
Sep-21	0.01	Sep-21	0.09
Oct-21	0.01	Oct-21	0.03
Nov-21	0.02	Nov-21	0.00
Dec-21	0.11	Dec-21	0.01
Jan-22	0.20	Jan-22	0.21
Feb-22	0.22	Feb-22	0.14
Mar-22	0.17	Mar-22	0.18
Apr-22	0.05	Apr-22	0.11
May-22	0.03	May-22	0.00
Jun-22	0.01	Jun-23	0.00
Total Jun-21 – Jun-22	0.07	Total Jun-22 – Jun-23	0.07

The observed soiling rates vary from season to season and are affected by natural cleaning of the PV modules by rain. For periods with little rainfall, higher soiling rates of up to 0.22 %/day on monthly averages were measured. For periods with higher amounts of rainfall, only very small soiling rates were measured.

7.3.10 Daily cleanliness and soiling rates

During periods with a significant soiling rate, the cleanliness of the PV-soiling system shows a characteristic saw tooth pattern. This indicates that the signal from the measurement panel is reduced more and more by the accumulation of dust on the surface. The signal reduction usually follows a near-linear reduction until the next cleaning event of the measurement module (naturally by rain or by the monthly cleaning by the local staff).

This is shown in Figure 35 by the grey columns for the average daily cleanliness (left scale). Rain events are displayed by a blue column. The amount of rain (in mm/day) is indicated by the height of the blue column and given on the right scale. Note that the soiling rate is measurable even though the cleanliness is not 1 after such an event.

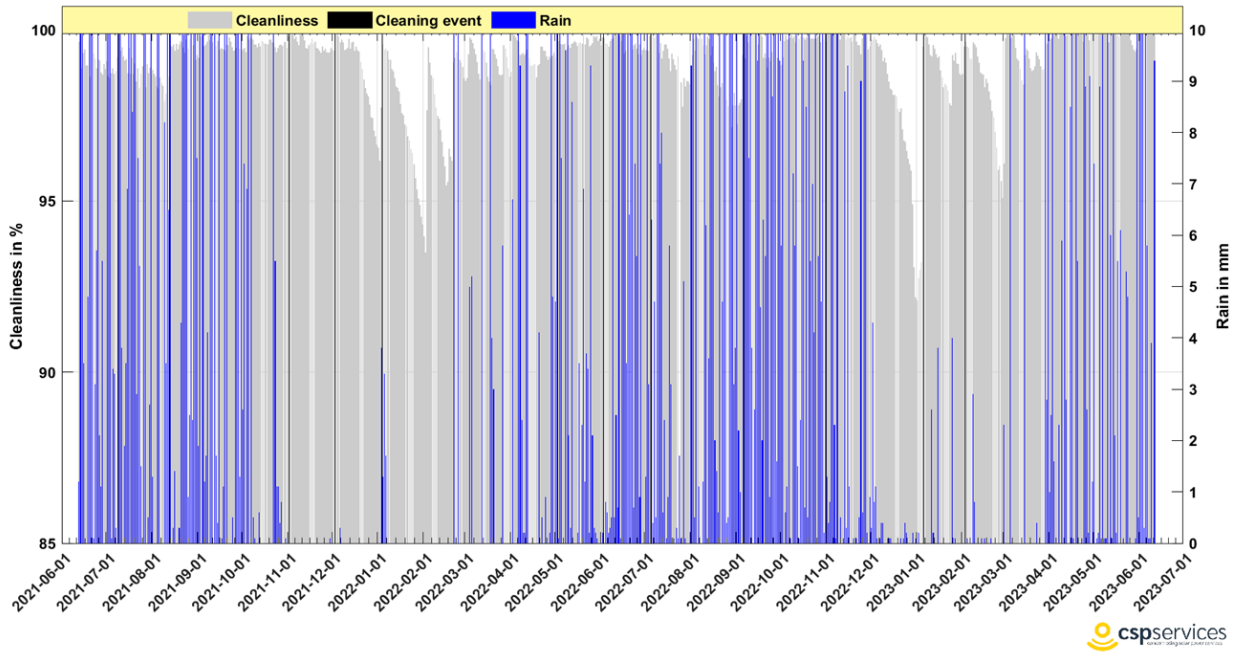


Figure 35: Cleanliness of the measurement panel modB with measured rain (blue) and cleaning (black vertical lines) of modB

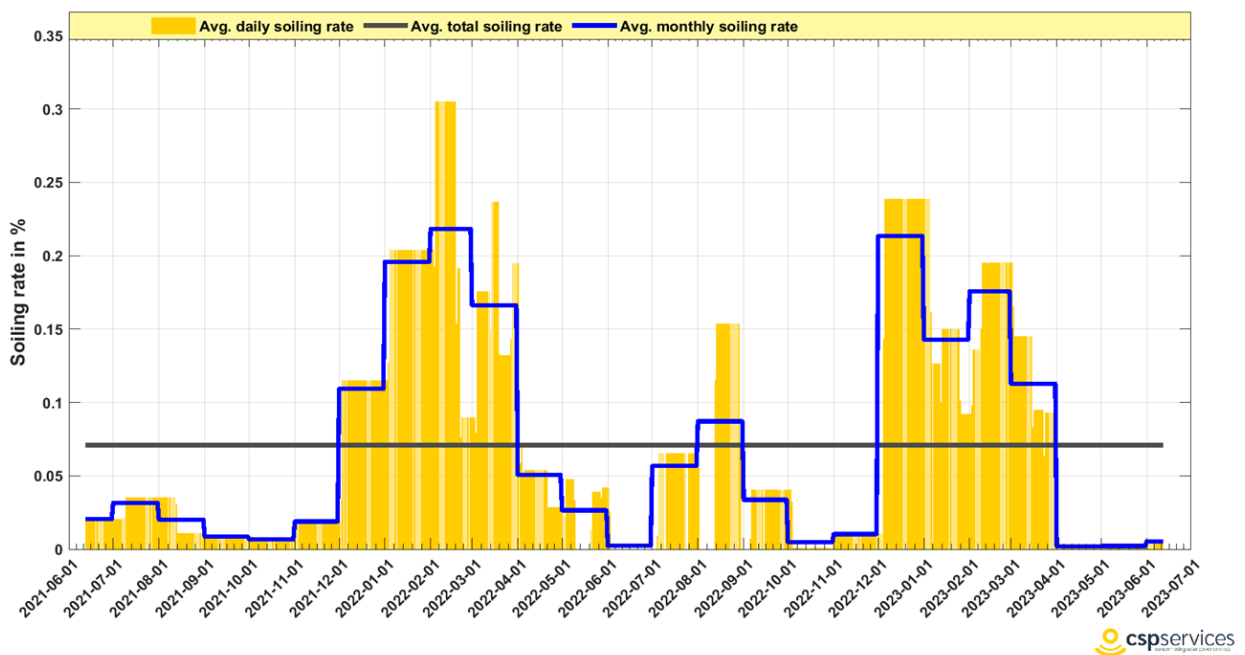


Figure 36: daily, monthly and yearly average soiling rates

Table 12 – Daily soiling rates

Date	PV Soiling Rate (%/day)	Date	PV Soiling Rate (%/day)
2021-06-12	0.02	2022-06-12	0.0
2021-06-13	0.02	2022-06-13	0.0
2021-06-14	0.02	2022-06-14	0.0
2021-06-15	0.02	2022-06-15	0.0
2021-06-16	0.02	2022-06-16	0.0
2021-06-17	0.02	2022-06-17	0.0
2021-06-18	0.02	2022-06-18	0.0
2021-06-19	0.02	2022-06-19	0.0
2021-06-20	0.02	2022-06-20	0.0
2021-06-21	0.02	2022-06-21	0.0
2021-06-22	0.02	2022-06-22	0.0
2021-06-23	0.02	2022-06-23	0.0
2021-06-24	0.02	2022-06-24	0.0
2021-06-25	0.02	2022-06-25	0.0
2021-06-26	0.02	2022-06-26	0.0
2021-06-27	0.02	2022-06-27	0.0
2021-06-28	0.02	2022-06-28	0.0
2021-06-29	0.02	2022-06-29	0.0
2021-06-30	0.02	2022-06-30	0.0
2021-07-01	0.02	2022-07-01	0.0
2021-07-02	0.02	2022-07-02	0.0
2021-07-03	0.02	2022-07-03	0.0
2021-07-04	0.02	2022-07-04	0.01
2021-07-05	0.02	2022-07-05	0.07
2021-07-06	0.02	2022-07-06	0.07
2021-07-07	0.02	2022-07-07	0.07
2021-07-08	0.02	2022-07-08	0.07
2021-07-09	0.04	2022-07-09	0.07
2021-07-10	0.04	2022-07-10	0.07
2021-07-11	0.04	2022-07-11	0.07
2021-07-12	0.04	2022-07-12	0.07
2021-07-13	0.04	2022-07-13	0.07
2021-07-14	0.04	2022-07-14	0.07
2021-07-15	0.04	2022-07-15	0.07
2021-07-16	0.04	2022-07-16	0.07
2021-07-17	0.04	2022-07-17	0.07
2021-07-18	0.04	2022-07-18	0.07
2021-07-19	0.04	2022-07-19	0.07
2021-07-20	0.04	2022-07-20	0.07
2021-07-21	0.04	2022-07-21	0.07
2021-07-22	0.04	2022-07-22	0.07
2021-07-23	0.04	2022-07-23	0.07
2021-07-24	0.04	2022-07-24	0.07
2021-07-25	0.04	2022-07-25	0.07
2021-07-26	0.04	2022-07-26	0.07
2021-07-27	0.04	2022-07-27	0.07
2021-07-28	0.04	2022-07-28	0.07
2021-07-29	0.04	2022-07-29	0.07
2021-07-30	0.04	2022-07-30	0.07
2021-07-31	0.04	2022-07-31	0.07
2021-08-01	0.04	2022-08-01	0.06
2021-08-02	0.04	2022-08-02	0.0
2021-08-03	0.04	2022-08-03	0.0
2021-08-04	0.04	2022-08-04	0.0
2021-08-05	0.04	2022-08-05	0.0
2021-08-06	0.04	2022-08-06	0.0
2021-08-07	0.04	2022-08-07	0.0
2021-08-08	0.04	2022-08-08	0.0
2021-08-09	0.04	2022-08-09	0.0
2021-08-10	0.04	2022-08-10	0.0
2021-08-11	0.04	2022-08-11	0.0
2021-08-12	0.03	2022-08-12	0.12

Date	PV Soiling Rate (%/day)	Date	PV Soiling Rate (%/day)
2021-08-13	0.01	2022-08-13	0.15
2021-08-14	0.01	2022-08-14	0.15
2021-08-15	0.01	2022-08-15	0.15
2021-08-16	0.01	2022-08-16	0.15
2021-08-17	0.01	2022-08-17	0.15
2021-08-18	0.01	2022-08-18	0.15
2021-08-19	0.01	2022-08-19	0.15
2021-08-20	0.01	2022-08-20	0.15
2021-08-21	0.01	2022-08-21	0.15
2021-08-22	0.01	2022-08-22	0.15
2021-08-23	0.01	2022-08-23	0.15
2021-08-24	0.01	2022-08-24	0.15
2021-08-25	0.01	2022-08-25	0.15
2021-08-26	0.01	2022-08-26	0.15
2021-08-27	0.01	2022-08-27	0.15
2021-08-28	0.01	2022-08-28	0.15
2021-08-29	0.01	2022-08-29	0.07
2021-08-30	0.01	2022-08-30	0.0
2021-08-31	0.01	2022-08-31	0.0
2021-09-01	0.01	2022-09-01	0.0
2021-09-02	0.01	2022-09-02	0.0
2021-09-03	0.01	2022-09-03	0.0
2021-09-04	0.01	2022-09-04	0.0
2021-09-05	0.01	2022-09-05	0.01
2021-09-06	0.01	2022-09-06	0.04
2021-09-07	0.01	2022-09-07	0.04
2021-09-08	0.01	2022-09-08	0.04
2021-09-09	0.01	2022-09-09	0.04
2021-09-10	0.01	2022-09-10	0.04
2021-09-11	0.01	2022-09-11	0.04
2021-09-12	0.01	2022-09-12	0.04
2021-09-13	0.01	2022-09-13	0.04
2021-09-14	0.01	2022-09-14	0.04
2021-09-15	0.01	2022-09-15	0.04
2021-09-16	0.01	2022-09-16	0.04
2021-09-17	0.01	2022-09-17	0.04
2021-09-18	0.01	2022-09-18	0.04
2021-09-19	0.01	2022-09-19	0.04
2021-09-20	0.01	2022-09-20	0.04
2021-09-21	0.01	2022-09-21	0.04
2021-09-22	0.01	2022-09-22	0.04
2021-09-23	0.01	2022-09-23	0.04
2021-09-24	0.01	2022-09-24	0.04
2021-09-25	0.01	2022-09-25	0.04
2021-09-26	0.01	2022-09-26	0.04
2021-09-27	0.01	2022-09-27	0.04
2021-09-28	0.01	2022-09-28	0.04
2021-09-29	0.01	2022-09-29	0.04
2021-09-30	0.01	2022-09-30	0.04
2021-10-01	0.01	2022-10-01	0.04
2021-10-02	0.01	2022-10-02	0.04
2021-10-03	0.01	2022-10-03	0.03
2021-10-04	0.01	2022-10-04	0.0
2021-10-05	0.01	2022-10-05	0.0
2021-10-06	0.01	2022-10-06	0.0
2021-10-07	0.01	2022-10-07	0.0
2021-10-08	0.01	2022-10-08	0.0
2021-10-09	0.01	2022-10-09	0.0
2021-10-10	0.01	2022-10-10	0.0
2021-10-11	0.01	2022-10-11	0.0
2021-10-12	0.01	2022-10-12	0.0
2021-10-13	0.01	2022-10-13	0.0
2021-10-14	0.01	2022-10-14	0.0
2021-10-15	0.01	2022-10-15	0.0

Date	PV Soiling Rate (%/day)	Date	PV Soiling Rate (%/day)
2021-10-16	0.01	2022-10-16	0.0
2021-10-17	0.01	2022-10-17	0.0
2021-10-18	0.01	2022-10-18	0.0
2021-10-19	0.01	2022-10-19	0.0
2021-10-20	0.01	2022-10-20	0.0
2021-10-21	0.01	2022-10-21	0.0
2021-10-22	0.01	2022-10-22	0.0
2021-10-23	0.01	2022-10-23	0.0
2021-10-24	0.01	2022-10-24	0.0
2021-10-25	0.01	2022-10-25	0.0
2021-10-26	0.01	2022-10-26	0.0
2021-10-27	0.01	2022-10-27	0.0
2021-10-28	0.01	2022-10-28	0.0
2021-10-29	0.01	2022-10-29	0.0
2021-10-30	0.01	2022-10-30	0.0
2021-10-31	0.01	2022-10-31	0.0
2021-11-01	0.01	2022-11-01	0.01
2021-11-02	0.02	2022-11-02	0.01
2021-11-03	0.02	2022-11-03	0.01
2021-11-04	0.02	2022-11-04	0.01
2021-11-05	0.02	2022-11-05	0.01
2021-11-06	0.02	2022-11-06	0.01
2021-11-07	0.02	2022-11-07	0.01
2021-11-08	0.02	2022-11-08	0.01
2021-11-09	0.02	2022-11-09	0.01
2021-11-10	0.02	2022-11-10	0.01
2021-11-11	0.02	2022-11-11	0.01
2021-11-12	0.02	2022-11-12	0.01
2021-11-13	0.02	2022-11-13	0.01
2021-11-14	0.02	2022-11-14	0.01
2021-11-15	0.02	2022-11-15	0.01
2021-11-16	0.02	2022-11-16	0.01
2021-11-17	0.02	2022-11-17	0.01
2021-11-18	0.02	2022-11-18	0.01
2021-11-19	0.02	2022-11-19	0.01
2021-11-20	0.02	2022-11-20	0.01
2021-11-21	0.02	2022-11-21	0.01
2021-11-22	0.02	2022-11-22	0.01
2021-11-23	0.02	2022-11-23	0.01
2021-11-24	0.02	2022-11-24	0.01
2021-11-25	0.02	2022-11-25	0.01
2021-11-26	0.02	2022-11-26	0.01
2021-11-27	0.02	2022-11-27	0.01
2021-11-28	0.02	2022-11-28	0.01
2021-11-29	0.02	2022-11-29	0.01
2021-11-30	0.02	2022-11-30	0.01
2021-12-01	0.02	2022-12-01	0.01
2021-12-02	0.03	2022-12-02	0.01
2021-12-03	0.11	2022-12-03	0.01
2021-12-04	0.11	2022-12-04	0.14
2021-12-05	0.11	2022-12-05	0.24
2021-12-06	0.12	2022-12-06	0.24
2021-12-07	0.11	2022-12-07	0.24
2021-12-08	0.11	2022-12-08	0.24
2021-12-09	0.11	2022-12-09	0.24
2021-12-10	0.11	2022-12-10	0.24
2021-12-11	0.11	2022-12-11	0.24
2021-12-12	0.12	2022-12-12	0.24
2021-12-13	0.11	2022-12-13	0.24
2021-12-14	0.11	2022-12-14	0.24
2021-12-15	0.11	2022-12-15	0.24
2021-12-16	0.12	2022-12-16	0.24
2021-12-17	0.11	2022-12-17	0.24
2021-12-18	0.11	2022-12-18	0.24

Date	PV Soiling Rate (%/day)	Date	PV Soiling Rate (%/day)
2021-12-19	0.11	2022-12-19	0.24
2021-12-20	0.12	2022-12-20	0.24
2021-12-21	0.11	2022-12-21	0.24
2021-12-22	0.11	2022-12-22	0.24
2021-12-23	0.11	2022-12-23	0.24
2021-12-24	0.11	2022-12-24	0.24
2021-12-25	0.11	2022-12-25	0.24
2021-12-26	0.11	2022-12-26	0.24
2021-12-27	0.11	2022-12-27	0.24
2021-12-28	0.11	2022-12-28	0.24
2021-12-29	0.12	2022-12-29	0.24
2021-12-30	0.11	2022-12-30	0.24
2021-12-31	0.11	2022-12-31	0.24
2022-01-01	0.11	2023-01-01	0.24
2022-01-02	0.11	2023-01-02	0.24
2022-01-03	0.13	2023-01-03	0.24
2022-01-04	0.2	2023-01-04	0.24
2022-01-05	0.2	2023-01-05	0.16
2022-01-06	0.2	2023-01-06	0.13
2022-01-07	0.2	2023-01-07	0.13
2022-01-08	0.2	2023-01-08	0.13
2022-01-09	0.2	2023-01-09	0.13
2022-01-10	0.2	2023-01-10	0.13
2022-01-11	0.2	2023-01-11	0.13
2022-01-12	0.2	2023-01-12	0.1
2022-01-13	0.2	2023-01-13	0.15
2022-01-14	0.2	2023-01-14	0.15
2022-01-15	0.2	2023-01-15	0.15
2022-01-16	0.2	2023-01-16	0.15
2022-01-17	0.2	2023-01-17	0.15
2022-01-18	0.2	2023-01-18	0.15
2022-01-19	0.2	2023-01-19	0.15
2022-01-20	0.2	2023-01-20	0.15
2022-01-21	0.2	2023-01-21	0.15
2022-01-22	0.2	2023-01-22	0.15
2022-01-23	0.2	2023-01-23	0.15
2022-01-24	0.2	2023-01-24	0.15
2022-01-25	0.2	2023-01-25	0.1
2022-01-26	0.2	2023-01-26	0.09
2022-01-27	0.2	2023-01-27	0.09
2022-01-28	0.2	2023-01-28	0.09
2022-01-29	0.2	2023-01-29	0.09
2022-01-30	0.2	2023-01-30	0.09
2022-01-31	0.2	2023-01-31	0.09
2022-02-01	0.2	2023-02-01	0.09
2022-02-02	0.2	2023-02-02	0.1
2022-02-03	0.19	2023-02-03	0.14
2022-02-04	0.31	2023-02-04	0.14
2022-02-05	0.31	2023-02-05	0.14
2022-02-06	0.31	2023-02-06	0.14
2022-02-07	0.31	2023-02-07	0.14
2022-02-08	0.31	2023-02-08	0.15
2022-02-09	0.31	2023-02-09	0.2
2022-02-10	0.31	2023-02-10	0.2
2022-02-11	0.31	2023-02-11	0.2
2022-02-12	0.31	2023-02-12	0.2
2022-02-13	0.31	2023-02-13	0.2
2022-02-14	0.31	2023-02-14	0.2
2022-02-15	0.31	2023-02-15	0.2
2022-02-16	0.31	2023-02-16	0.2
2022-02-17	0.31	2023-02-17	0.2
2022-02-18	0.15	2023-02-18	0.2
2022-02-19	0.19	2023-02-19	0.2
2022-02-20	0.19	2023-02-20	0.2

Date	PV Soiling Rate (%/day)	Date	PV Soiling Rate (%/day)
2022-02-21	0.08	2023-02-21	0.2
2022-02-22	0.09	2023-02-22	0.2
2022-02-23	0.09	2023-02-23	0.2
2022-02-24	0.09	2023-02-24	0.2
2022-02-25	0.09	2023-02-25	0.2
2022-02-26	0.09	2023-02-26	0.2
2022-02-27	0.09	2023-02-27	0.2
2022-02-28	0.09	2023-02-28	0.2
2022-03-01	0.09	2023-03-01	0.2
2022-03-02	0.09	2023-03-02	0.17
2022-03-03	0.08	2023-03-03	0.15
2022-03-04	0.18	2023-03-04	0.15
2022-03-05	0.18	2023-03-05	0.15
2022-03-06	0.18	2023-03-06	0.15
2022-03-07	0.18	2023-03-07	0.15
2022-03-08	0.18	2023-03-08	0.15
2022-03-09	0.18	2023-03-09	0.15
2022-03-10	0.18	2023-03-10	0.15
2022-03-11	0.18	2023-03-11	0.15
2022-03-12	0.18	2023-03-12	0.15
2022-03-13	0.15	2023-03-13	0.15
2022-03-14	0.24	2023-03-14	0.15
2022-03-15	0.24	2023-03-15	0.08
2022-03-16	0.24	2023-03-16	0.09
2022-03-17	0.24	2023-03-17	0.09
2022-03-18	0.24	2023-03-18	0.09
2022-03-19	0.13	2023-03-19	0.09
2022-03-20	0.13	2023-03-20	0.09
2022-03-21	0.13	2023-03-21	0.09
2022-03-22	0.13	2023-03-22	0.09
2022-03-23	0.13	2023-03-23	0.06
2022-03-24	0.13	2023-03-24	0.09
2022-03-25	0.13	2023-03-25	0.09
2022-03-26	0.13	2023-03-26	0.09
2022-03-27	0.14	2023-03-27	0.09
2022-03-28	0.19	2023-03-28	0.09
2022-03-29	0.19	2023-03-29	0.09
2022-03-30	0.19	2023-03-30	0.03
2022-03-31	0.19	2023-03-31	0.0
2022-04-01	0.19	2023-04-01	0.0
2022-04-02	0.06	2023-04-02	0.0
2022-04-03	0.07	2023-04-03	0.0
2022-04-04	0.05	2023-04-04	0.0
2022-04-05	0.05	2023-04-05	0.0
2022-04-06	0.05	2023-04-06	0.0
2022-04-07	0.05	2023-04-07	0.0
2022-04-08	0.05	2023-04-08	0.0
2022-04-09	0.05	2023-04-09	0.0
2022-04-10	0.05	2023-04-10	0.0
2022-04-11	0.05	2023-04-11	0.0
2022-04-12	0.05	2023-04-12	0.0
2022-04-13	0.05	2023-04-13	0.0
2022-04-14	0.05	2023-04-14	0.0
2022-04-15	0.05	2023-04-15	0.0
2022-04-16	0.05	2023-04-16	0.0
2022-04-17	0.05	2023-04-17	0.0
2022-04-18	0.05	2023-04-18	0.0
2022-04-19	0.05	2023-04-19	0.0
2022-04-20	0.05	2023-04-20	0.0
2022-04-21	0.03	2023-04-21	0.0
2022-04-22	0.03	2023-04-22	0.0
2022-04-23	0.03	2023-04-23	0.0
2022-04-24	0.03	2023-04-24	0.0
2022-04-25	0.03	2023-04-25	0.0

Date	PV Soiling Rate (%/day)	Date	PV Soiling Rate (%/day)
2022-04-26	0.03	2023-04-26	0.0
2022-04-27	0.03	2023-04-27	0.0
2022-04-28	0.03	2023-04-28	0.0
2022-04-29	0.03	2023-04-29	0.0
2022-04-30	0.03	2023-04-30	0.0
2022-05-01	0.03	2023-05-01	0.0
2022-05-02	0.02	2023-05-02	0.0
2022-05-03	0.05	2023-05-03	0.0
2022-05-04	0.05	2023-05-04	0.0
2022-05-05	0.05	2023-05-05	0.0
2022-05-06	0.05	2023-05-06	0.0
2022-05-07	0.05	2023-05-07	0.0
2022-05-08	0.05	2023-05-08	0.0
2022-05-09	0.03	2023-05-09	0.0
2022-05-10	0.0	2023-05-10	0.0
2022-05-11	0.0	2023-05-11	0.0
2022-05-12	0.0	2023-05-12	0.0
2022-05-13	0.0	2023-05-13	0.0
2022-05-14	0.0	2023-05-14	0.0
2022-05-15	0.0	2023-05-15	0.0
2022-05-16	0.0	2023-05-16	0.0
2022-05-17	0.0	2023-05-17	0.0
2022-05-18	0.0	2023-05-18	0.0
2022-05-19	0.0	2023-05-19	0.0
2022-05-20	0.01	2023-05-20	0.0
2022-05-21	0.04	2023-05-21	0.0
2022-05-22	0.04	2023-05-22	0.0
2022-05-23	0.04	2023-05-23	0.0
2022-05-24	0.04	2023-05-24	0.0
2022-05-25	0.04	2023-05-25	0.0
2022-05-26	0.04	2023-05-26	0.0
2022-05-27	0.03	2023-05-27	0.0
2022-05-28	0.04	2023-05-28	0.0
2022-05-29	0.04	2023-05-29	0.0
2022-05-30	0.04	2023-05-30	0.0
2022-05-31	0.04	2023-05-31	0.0
2022-06-01	0.04	2023-06-01	0.01
2022-06-02	0.03	2023-06-02	0.01
2022-06-03	0.0	2023-06-03	0.01
2022-06-04	0.0	2023-06-04	0.01
2022-06-05	0.0	2023-06-05	0.01
2022-06-06	0.0	2023-06-06	0.01
2022-06-07	0.0	2023-06-07	0.01
2022-06-08	0.0	2023-06-08	0.01
2022-06-09	0.0	2023-06-09	0.01
2022-06-10	0.0	2023-06-10	0.01
2022-06-11	0.0	2023-06-11	0.01

7.4 CORROSION SAMPLER (CORROSION RATE)

The corrosion sampler will be dismantled from the station during the maintenance visit after approximately 12 months of measurements. The metal samples will then be sent to the Fraunhofer lab for analysis and corrosion rate calculations. The results will be included in the final measurement report at the end of the current measurement campaign.



FRAUNHOFER-INSTITUT FÜR SOLARE ENERGIESYSTEME ISE

LIBERIA ATMOSPHERIC CORROSION ASSESSMENT 2020/2022

FINAL REPORT

Measurement of atmospheric corrosivity
by exposition of corrosion set-up

LIBERIA, MOUNT COFFEE ATMOSPHERIC CORROSION ASSESSMENT 2020/2022

FINAL REPORT

Measurement of atmospheric corrosivity by
exposition of corrosion set-up

Date: 21.03.2023

Mathias Drews
0761 4588 5907
Mathias.drews@ise.fraunhofer.de

Fraunhofer-Institut für Solare Energiesysteme ISE
Freiburg, Deutschland

For: CSP Service GmbH
Birk Kraas
Friedrich-Ebert-Ufer 30
51143 Köln

T: +49 2203 959 0036
E: birk.kraas@cspservice.de

Content

1	General Information	page 4
2	Corrosivity assessment	page 6
3	Results and Ranking	page 8

1 General Information

Location Information: Mount Coffee, Liberia

- Mount Coffee Measurements
- Latitude: 6.4978 ° N
- Longitude: -10.6517 ° E
- Elevation: 20 m
- Tropical monsoon climate
- Annual average temperature: 27.28 °C
- Annual average precipitation: 355,13 mm



Fig. 1 Location of Exposure

The corrosion set-up includes 12 standardized metal samples of aluminium, carbon steel, zinc and copper (three samples from each metal) mounted on aluminium frame with polyamide screws. The samples exposed in Mount Coffee are punched with the identification numbers:

- A240, A241, A242
- S240, S241, S242
- Z240, Z241, Z242
- C240, C241, C242

The corrosion set-up was exposed to the atmosphere under no shelter on a rack facing south (northern hemisphere). The standard exposure set-up is horizontal with an angle of 45°. The corrosion set-up must be exposed with a minimum height of 0.5 m above the ground to ensure that there is absolutely no contact with the floor or surrounding vegetation during the exposure periods. According to the standard ISO 9226:2012 to enable a full and exact comparison with other locations, the duration of exposure should be one full year (12 month / all seasons).

- Start of Exposure: 10. June 2021
- End of Exposure: 19. August 2022
- Total Duration of Exposure: 435 days

2 Corrosivity assessment

The measurements are taken by exposing standard specimens at the service location for one year according to international standard ISO 9226:2012. The standard specimens are flat plates of the four standard metals: aluminium (Al), copper (Cu), carbon steel (Fe) and zinc (Zn). The corrosivity of the exposure locations is deduced from the corrosion rate, calculated from the loss of mass per unit area of these standard specimens after exposure periods.









The removal of corrosion products is performed according to the international standard ISO 8407:2009. The values obtained from the measurements are used as classification criteria for the evaluation of atmospheric corrosivity according to the international standard ISO 9223:2012.

Table 1: Determined atmospheric corrosivity and corrosivity class, acc. to ISO 9226

Test site	Metal sample	Atmospheric corrosivity [g/m ²]	Corrosivity class
Mount Coffee, Liberia	Aluminium	0,22	C2
Mount Coffee, Liberia	Carbon steel	193,47	C2
Mount Coffee, Liberia	Zinc	8,80	C3
Mount Coffee, Liberia	Copper	14,88	C4

Table 2: Photo documentation of samples before exposure (reference, left) and after exposure (front side, right)

Corrosivity assessment

Copper	
	
Reference	Mount Coffee
Zinc	
	
Reference	Mount Coffee
Carbon Steel	
	
Reference	Mount Coffee
Aluminium	
	
Reference	Mount Coffee

3 Results and Ranking

The rate of corrosion of the metal samples is determined in accordance to the international standard ISO 8407:2009. The loss of weight after one year of exposure is determined. The corrosion rate r_{corr} derived from the mass loss measurement in grams per square meter and per year are calculated for each sample according to the international standard ISO 9226:2012. The atmosphere at the test site is classified from C1 to CX (low to extreme) according to its corrosivity. The results are used for the classification of the corrosivity of the atmosphere.

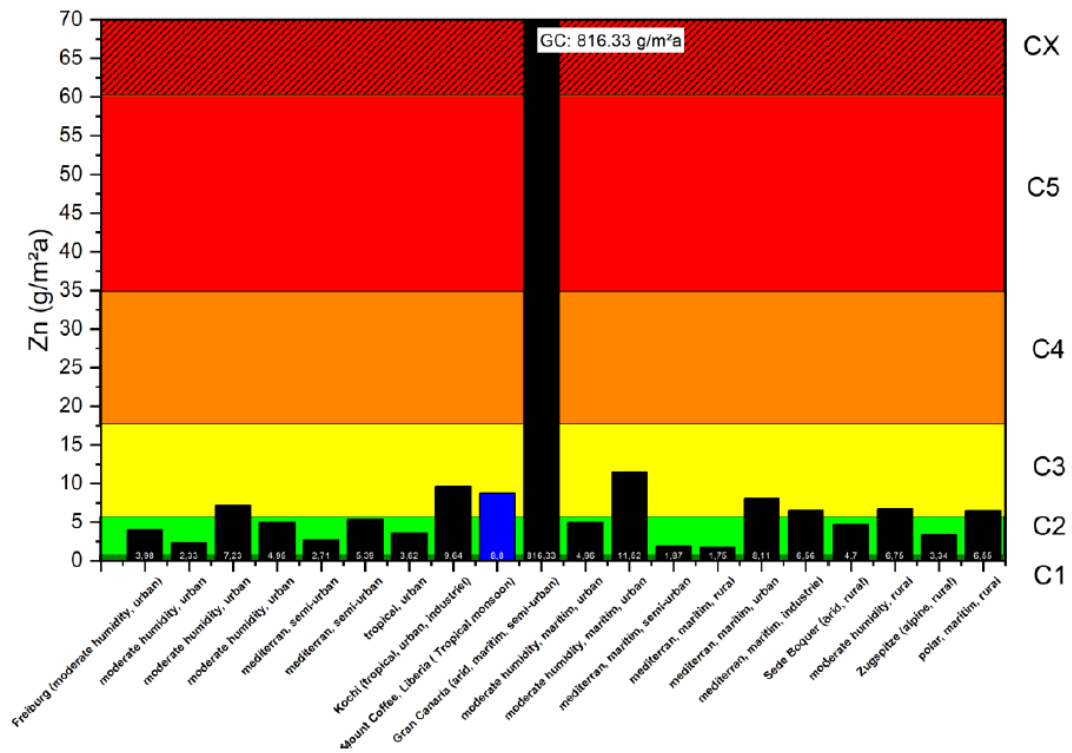


Fig. 4: Comparison of corrosivity classes of different locations (blue: Mount Coffee) for Zinc

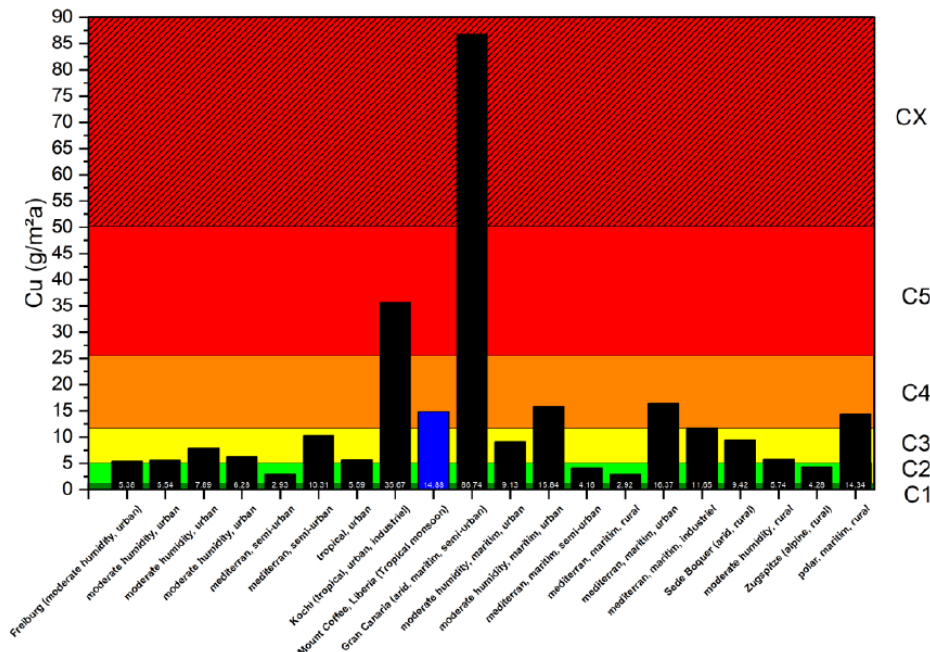


Fig. 5: Comparison of corrosivity classes of different locations (blue: Mount Coffee) for Copper

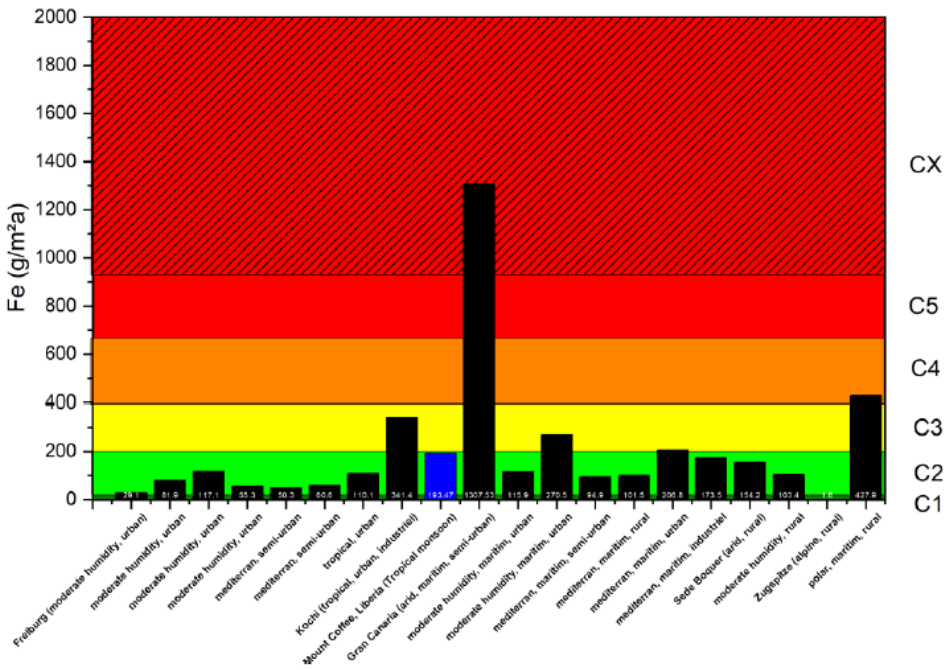


Fig. 6: Comparison of corrosivity classes of different locations (blue: Mount Coffee) for Carbon Steel

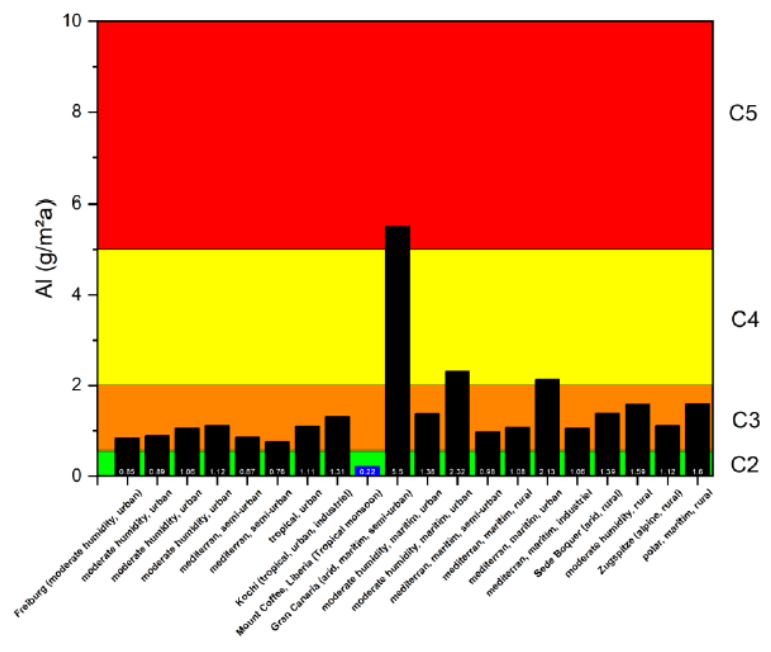


Fig. 7: Comparison of corrosivity classes of different locations (blue: Mount Coffee) for Aluminium

Results show a relatively low to moderate atmospheric corrosivity (C2) for carbon steel and aluminium, (C4) for copper, and (C3) for zinc.

8 DATA QUALITY CONTROL AND MEASUREMENT UNCERTAINTY

8.1 CLEAR SKY INDEX

When comparing the GHI measurement to the clear-sky GHI, which can be obtained from the CAMS McClear radiation service¹, one obtains the clear-sky index. It is the fraction of the measured GHI to the clear-sky GHI. For clear-sky days, the clear-sky index is expected to be close to 1 and for time stamps impaired by clouds, the clear-sky index deviates significantly from 1. On sites with frequent clear sky, a horizontal line of points should therefore form at the value of 1. An incorrect sensor calibration factor or another source of measurement bias would lead to a line of points forming above or below the horizontal line at a value of 1. As Figure 37 shows, the clear-sky index for this site is distributed around 1, indicating the valid calibration of the GHI sensor. The broad distribution around 1 indicates that there are few clear-sky days.

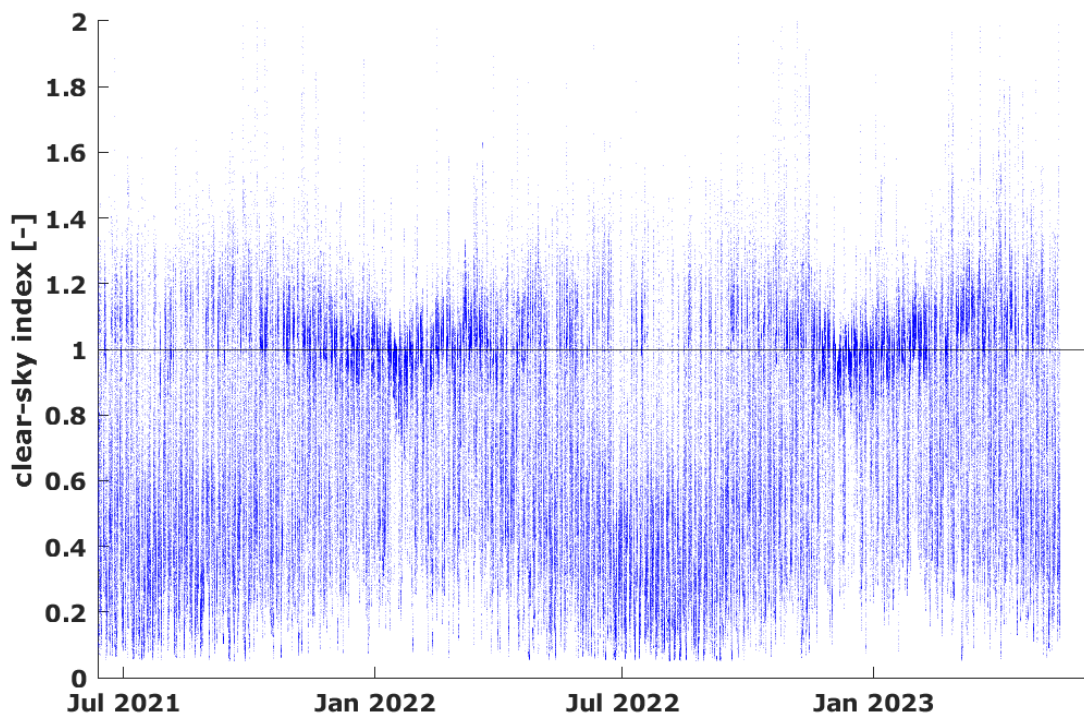


Figure 37: Clear-sky index for the GHI (1min resolution).

¹ <http://www.soda-pro.com/web-services/radiation/cams-mcclear>

8.2 DATA QUALITY ASSESSMENT

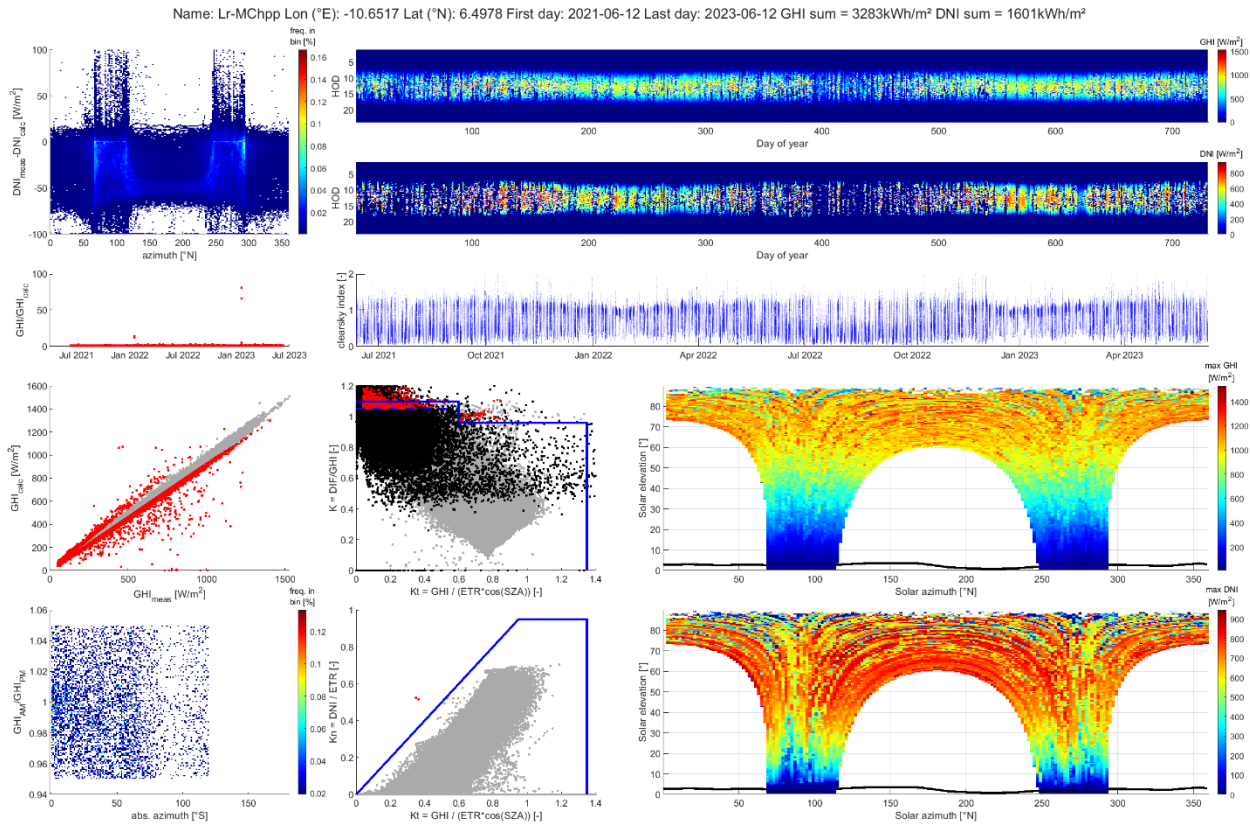


Figure 38: Multiplot overview of the data quality assessment (1min resolution).

Figure 38 shows the multiplot representation of the measurement data. The GHI comes from the CMP 10 pyranometer, while the DNI and DHI (named DIF in Figure 38) come from the RSI. Comparison between GHI measured (from the CMP 10) and GHI calculated (from the DNI and DIF coming from the RSI) is shown on the left side, in second and third row. All flags from the quality control are shown as red dots in both plots. The larger deviation between the calculated and measured GHI comes from the larger uncertainty in the DNI and DHI values from the RSI. It does not indicate a systematic problem of the GHI measurement by the CMP 10. The representations of the K-Tests are shown in the second column in the third and fourth row. The blue lines represent the limits of the K-Tests. Further information on the K-Tests can be found here² The black data points are points outside the limit of the test and outside of the minimal irradiation limit of the test. Flagged data points are shown in red. Additionally to the K-Tests, the BSRN's closure tests and extremely rare and physically possible limits test as well as the tracker-off test are applied³.

² <https://www.nrel.gov/grid/solar-resource/seri-qc.html>

³ <http://proceedings.ises.org/?doi=swc.2021.38.02>

8.3 IRRADIANCE DATA COMPARISON

As all three components of the solar irradiance are being measured, they can be compared to each other by calculating one component from the other two and then comparing the calculated DNI to the measured one. The DNI can be calculated according to the following formula:

$$DNI_{calc} = \frac{GHI - DHI}{\cos(SZA)}, \text{ with } SZA: \text{ Solar Zenith Angle}$$

Similarly, the GHI can be calculated from the DNI and the DHI.

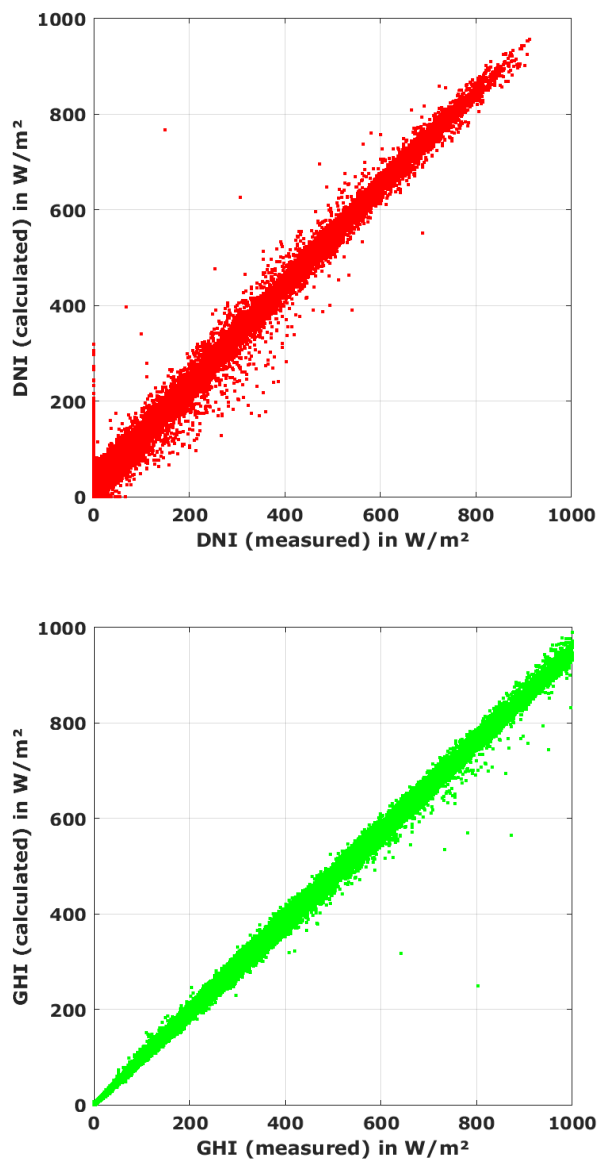


Figure 39: DNI calculated from GHI (CMP10) and DHI (RSI) in comparison with the DNI measured by the RSI (top), GHI calculated from DNI and DHI from the RSI sensor in comparison with the GHI measured by the CMP10 pyranometer (bottom)

8.4 MEASUREMENT UNCERTAINTY

In the literature, pyranometer calibration uncertainty is estimated with $\pm 3\%$ for solar zenith angles (SZA) from 30° to 60° . Field measurements in well-maintained measurement campaigns can be estimated with uncertainties of $\pm 3.0\%$ for SZA between 30° and 60° and up to $\pm 5.0\%$ depending on the maintenance. Due to the good adherence to the maintenance and cleaning schedule the uncertainty due to sensor soiling is estimated to be non-significant.

The calibration certificates for the installed CMP10 pyranometers state a value of $\pm 1.44\%$. Calibration in the laboratory is done at a fixed incidence angle, thus this value replaces the literature estimate of $\pm 3\%$. Since this is well justified and calibration verification did not give any reason of doubt, the value of $\pm 1.44\%$ is accepted.

For this measurement campaign, a measurement uncertainty (at 95% confidence interval) of $\pm 3.0\%$ for all GHI values at SZA between 30° and 60° is estimated.

This includes the calibration uncertainty from the manufacturer and the uncertainty due to

- Zenith response
- Azimuth response
- Spectral response
- Nonlinearity
- Temperature response
- Aging per year

according to literature values in the Best Practices Handbook, third Ed.⁴.

For the RSI measurements, the uncertainty is depended on the incident solar spectrum. In the literature, the overall expanded uncertainty is estimated to be 8% for photodiode pyranometers. For the RSI measurements used here with an outdoor field calibration before employment, the used correction functions and maintenance schedule, the uncertainty in DNI and GHI can be estimated to be $\pm 4\%$. This is in line with the specifications of a Tier 2 station by The Worldbank, which states that the uncertainty should be below 5% for daily values⁵.

⁴ <https://www.nrel.gov/docs/fy21osti/77635.pdf> chapter 7-7

⁵ <https://documents1.worldbank.org/curated/en/398831592957111931/pdf/ESMAP-Terms-of-Reference-for-Solar-and-Wind-Measurement-Campaign.pdf>

8.5 UNCERTAINTY OF LONG-TERM GHI AND DNI

The long-term uncertainty of GHI and DNI can only be estimated with long-term data from a satellite provider. Especially in regions where few stations so far existed, the uncertainty is higher than in other regions. The Global Solar Atlas states that for GHI an uncertainty of up to $\pm 8\%$ and $\pm 14\%$ for DNI can be expected for the region of the station (Countries in humid tropical climate (e.g. equatorial regions of Africa, America and Pacific, Philippines, Indonesia and Malaysia) and coastal zones (approx. up to 15 km from a body of water))⁶.

According to the contractor of World Bank for the Global Solar Atlas (Solargis) the uncertainty of the long-term values for a specific site can be reduced significantly according to the available period of ground measurements. The availability of a 12-month data series reduces the achievable uncertainty as shown in the diagram below.

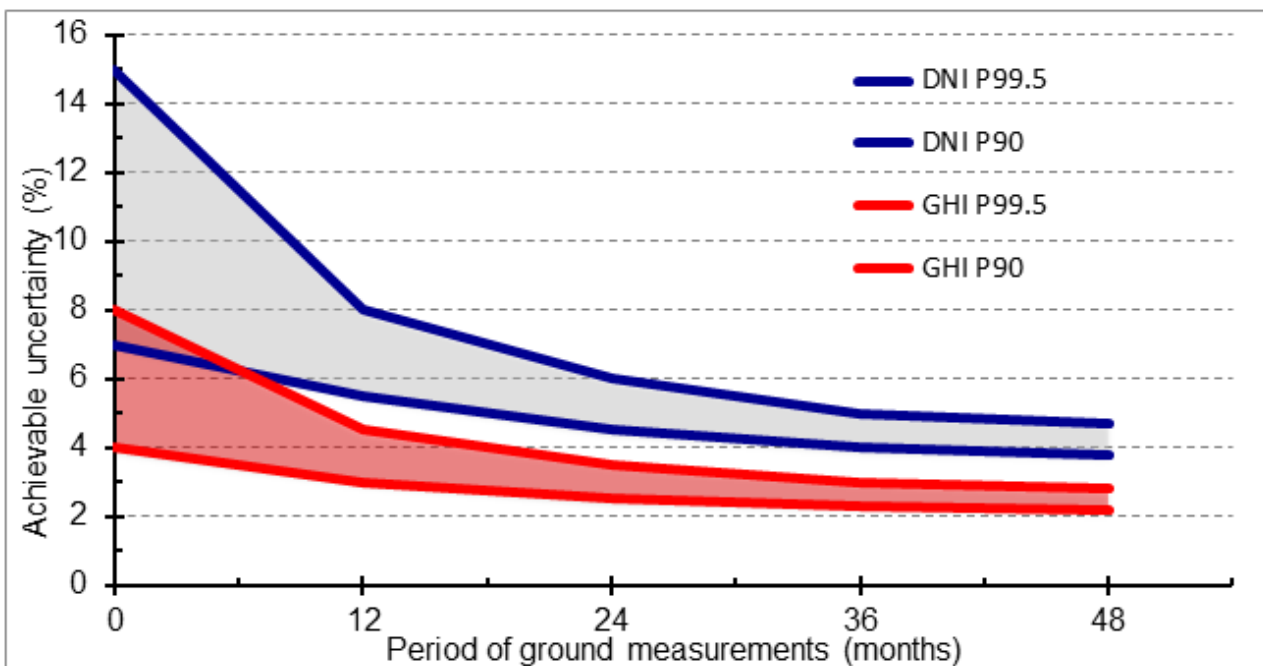


Figure 40 - Achievable uncertainty for long-term average GHI and DNI data in relation to the availability of ground measurement data for site-adaptation (source: <https://solargis.com/docs/methodology/site-adaptation>)

⁶ <https://globalsolaratlas.info/support/accuracy>

9 PHOTOGRAPHIC DOCUMENTATION

9.1 INSTALLATION (JUNE 2021)



Figure 41 - Fence and foundation



Figure 42 - Station and wind mast foundations



Figure 43 - Wind mast preparations



Figure 44 - Wind mast foundations, ground cable fixed to ground bolt, protective tube for wind mast cables.



Figure 45 - Water holes in foundations to prevent flooding (1).



Figure 46 - Water holes in foundations to prevent flooding (2).



Figure 47 - Wind direction sensor north mark aligned with mounting cantilever and north direction



Figure 48 - Wind sensors installed on wind mast



Figure 49 - Wind mast erected; wind direction sensor cantilever orientated to North



Figure 50 - Mounting of weather station structure



Figure 51 - CMP10 pyranometer serial number

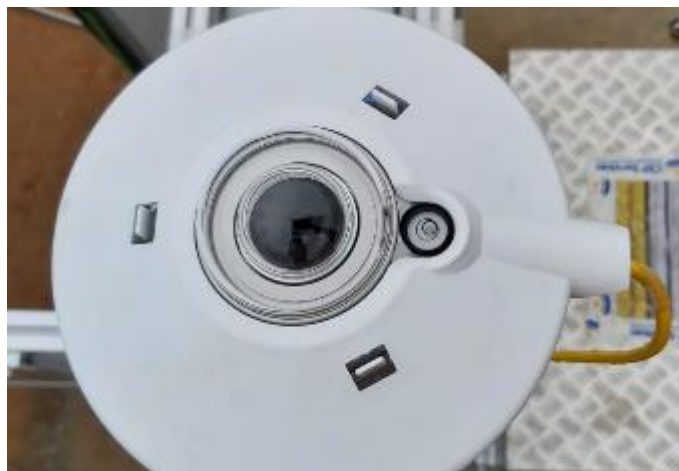


Figure 52 - CMP10 pyranometer levelling



Figure 53 - Sensor levelling of the RSI (1)



Figure 54 - Sensor levelling of the RSI (2)



Figure 55 - Serial number of RSI.



Figure 56 - Installed RSI.



Figure 57 - RSI motor serial number



Figure 58 - Rain sensor and corrosion sampler



Figure 59 - Rain sensor mounting bar levelling



Figure 60 - Rain sensor serial number



Figure 61 - T/RH sensor and modem antenna



Figure 62 - T/RH sensor serial number



Figure 63 - Control box interior; top: datalogger; bottom: fuses and 12V circuit distribution, relays, RSI motor controller



Figure 64 - Modem with SIM card



Figure 65 - Assembly of PV-S structure + modules



Figure 66 - PV-S support structure with 9° tilt angle towards South



Figure 67 - PV-S modules connections



Figure 68 - PV-S system reference panel A (clean panel)



Figure 69 - PV modules cleaning.



Figure 70 - 12V, 60Ah battery



Figure 71 - Wind mast with rain sensor and corrosion sampler



Figure 72 - Main mounting structure with solar sensors, T/RH sensor and PV panels for soiling measurement and power supply.



Figure 73 - Solar sensors and PV panels on mounting structure



Figure 74 - Site with completed station installation as seen from south-west. Picture taken from 6.49767°N, -10.65176°E

9.2 MAINTENANCE VISIT (JANUARY 2022)



Figure 75: Maintenance staff on site



Figure 76: Wind mast top section with sensors and camera



Figure 77: Wind mast with foundations and guying ropes



Figure 78: RSI sensor



Figure 79: RSI sensor levelling



Figure 80: CMP10 pyranometer



Figure 81: CMP10 pyranometer levelling



Figure 82: Rain sensor cleaning



Figure 83: Rain sensor levelling



Figure 84: Rain sensor top view after cleaning



Figure 85: Corrosion sampler



Figure 86: T/RH sensor and modem antenna on the station mounting structure

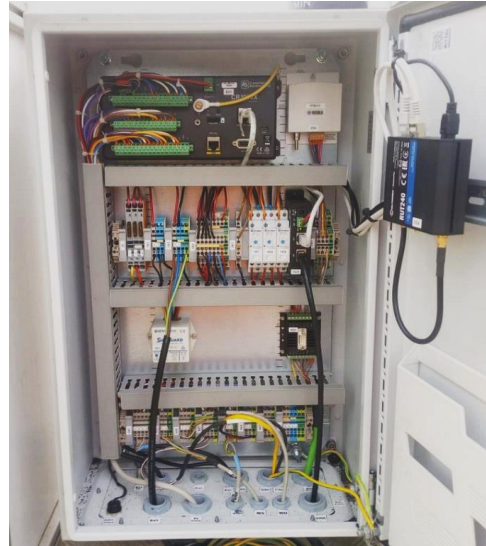


Figure 87: Control box interior; top: datalogger; bottom: fuses and 12V circuit distribution, relays, RSI motor controller and modem



Figure 88: Battery box interior



Figure 89: Station structure with PV modules



Figure 90: PV supply and soiling modules after cleaning



Figure 91: PV-S support structure with 9° tilt angle towards South



Figure 92: PV modules cleaning



Figure 93: Irradiation sensors cleaning



Figure 94: Site with complete station as seen from south



Figure 95: Site with complete station as seen from east

9.3 MAINTENANCE VISIT (AUGUST 2022)



Figure 96: Security camera view (the temporarily installed reference sensor can be seen right next to the permanently installed sensor on top of the weather station)



Figure 97: Wind mast top section with sensors and camera



Figure 98: Wind mast with foundations and guying ropes



Figure 99: RSI sensor



Figure 100: RSI sensor levelling



Figure 101: CMP10 pyranometer



Figure 102: CMP10 pyranometer levelling



Figure 103: Rain sensor cleaning



Figure 104: Rain sensor levelling



Figure 105: Rain sensor top view after cleaning

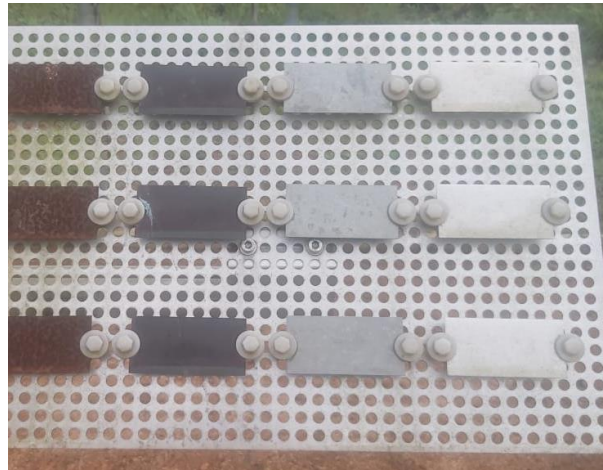


Figure 106: Corrosion sampler before dismantling the plates



Figure 107: T/RH sensor and modem antenna on the station mounting structure



Figure 108: Control box interior; top: datalogger; bottom: fuses and 12V circuit distribution, relays, RSI motor controller and modem



Figure 109: Battery box interior

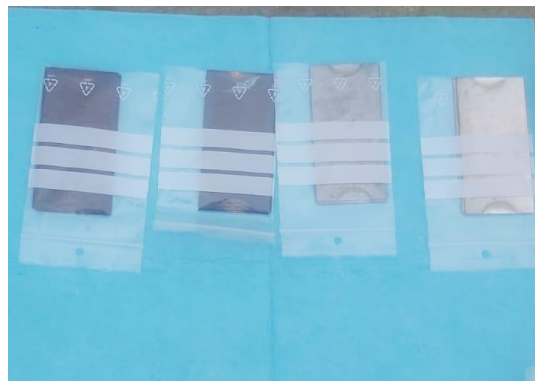


Figure 110: Corrosion samples dismantled and safely stored in individual plastic bags for shipping to the lab for analysis



Figure 111: Old RS1 PU, after change



Figure 112: PV-S support structure with 9° tilt angle towards south



Figure 113: Site with completed station as seen from south



Figure 114: Site with completed station as seen from east



Figure 115: Station as seen from north (after removal of the reference sensor on 2022-08-23)



Figure 116: Station as seen from north-east (after removal of the reference sensor on 2022-08-23)

9.4 MAINTENANCE VISIT (JANUARY 2023)



Figure 117: Maintenance staff on site



Figure 118: Wind mast with foundations and guying ropes



Figure 119: RSI sensor



Figure 120: RSI sensor levelling



Figure 121: CMP10 pyranometer



Figure 122: CMP10 pyranometer levelling



Figure 123: Rain sensor cleaning



Figure 124: Rain sensor levelling



Figure 125: Rain sensor top view after cleaning



Figure 126: Toolbox



Figure 127: T/RH sensor and modem antenna on the station mounting structure

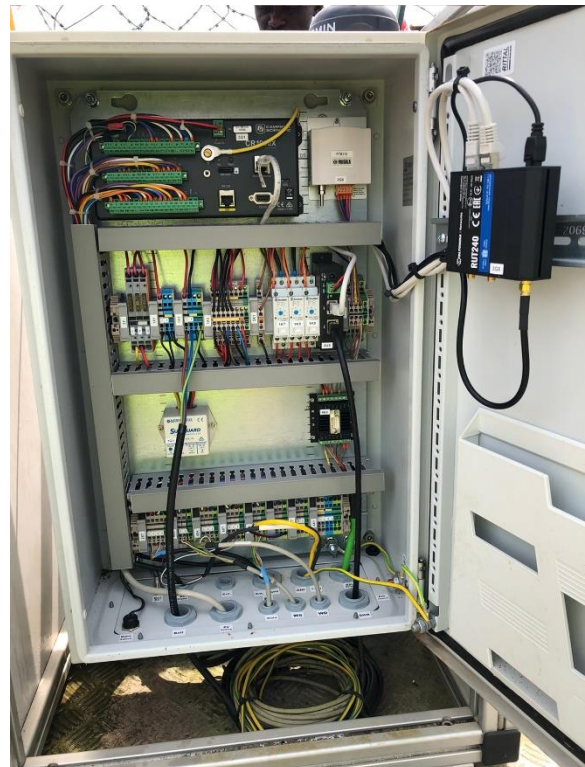


Figure 128: Control box interior; top: datalogger; bottom: fuses and 12V circuit distribution, relays, RSI motor controller and modem



Figure 129: Battery box interior



Figure 130: Station structure with PV modules



Figure 131: PV supply and soiling modules after cleaning



Figure 132: PV-S support structure with 9° tilt angle towards South



Figure 133: PV modules cleaning



Figure 134: Irradiation sensors cleaning



Figure 135: Site with completed station as seen from east



Figure 136: Site with completed station as seen from west

9.5 STATION HANDOVER (JUNE 2023)



Figure 137: Station handover visit – view from south



Figure 138: Station handover visit

10 CALIBRATION PROCEDURES AND CERTIFICATES

10.1 CALIBRATION OF SENSORS UPON STATION INSTALLATION

This section provides the calibration certificates for each sensor. All measurement equipment was new, unused and included factory calibrations upon installation of the station.

Table 13 – Sensor calibration upon installation of the station

Measured parameter	Sensor type	Serial number	Calibration date	Installation date
DHI, DNI	RSI solar sensor	CSPS.MS.19.201.0005	2020-03-03	2021-06-10 Dismounted: 2022-08-19
GHI	CMP10 pyranometer	210860	2021-02-12	2021-06-10
Wind speed (WS)	NRG 40C anemometer	17950-0334055	2020-04-12	2021-06-10
Wind direction (WD)	NRG #200M wind vane	10070-00009014	2020-12-13	2021-06-10
Barometric pressure (BP)	PTB110 (CS106)	S4750162	2020-11-20	2021-06-10
DHI, DNI	RSI solar sensor	CSPS.MS.21.203.0009	2022-06-07	2022-08-19

10.1.1 RSI Solar Sensor (CSPS.MS.19.201.0005)

Calibration Protocol

For Model: **Twin Rotating Shadowband Irradiometer**

Pyranometer Unit Serial Number: CSPS.MS.19.201.0005
 With pyranometer sensor: LI-COR LI200R PY108327 (primary)
 and LI-COR LI200R PY108328 (secondary)
 Original LI-COR Calibration Constant: 62.16 microamps per 1000 W/m²
 and 65.53 microamps per 1000 W/m²

Correction factors from (DLR2008)

	PY108327	PY108328
Constant Correction Factor	0.990	1.025
Diffuse Correction Factor	1.004	1.035
Root Mean Square Deviation (DNI)	14.4 W/m ²	13.5 W/m ²
Bias (DNI)	-0.5 W/m ²	-0.8 W/m ²
Root Mean Square Deviation (GHI)	6.3 W/m ²	6.7 W/m ²
Bias (GHI)	-0.2 W/m ²	0.9 W/m ²

Calibration period: 2019-10-08 to 2020-03-03
 Effective period: 653 h (GHI) 430 h (DNI) 653 h (DHI)
 Temporal resolution: 10 min

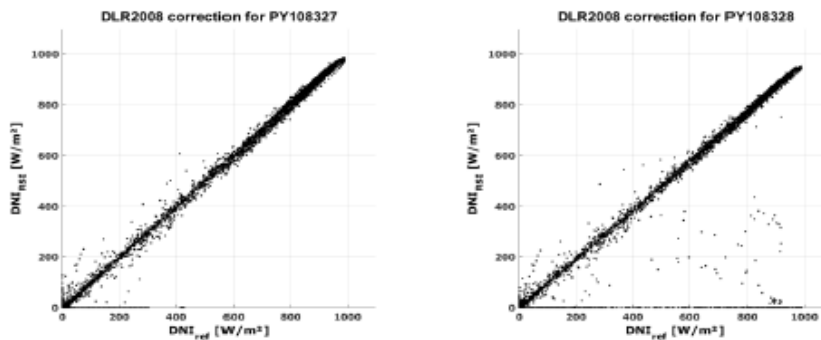


Figure 1: DNI after correction corresponding to chosen function set including calibration constant vs. reference DNI (10-min)

Please consult the detailed description for further information on the calibration process.
 Almeria, 12-Jun-2020

i. A. Dr.rer.nat. Natalie Hanrieder



DLR is statutorily represented by its Executive Board. The Executive Board may empower authorized persons to act as its representatives. DLR's head of Legal Department, D-51170 Cologne, provides information on the extent of this empowerment.

Plataforma Solar de Almeria
 Ctra. de Senes s/n
 04200 Tabernas, Spain
 Telephone +34 950 278802
 Telefax +34 950 365313
 Internet www.DLR.de

DETAILED DESCRIPTION OF THE RSI SENSOR CALIBRATION PROCEDURE

The RSI irradiation sensor is mounted and operated parallel to the reference DLR meteorological station during a specified period (recommended to be at least one month) at the Plataforma Solar de Almería in Spain for calibration under real sky conditions.

The Constant Calibration Factor and the Diffuse Correction are determined by comparing the reference direct normal and diffuse horizontal irradiance to corresponding RSI irradiance data as determined with the LI-COR (LI-200) Calibration Constant and including correction functions developed by DLR for RSIs with LI-COR LI200 pyranometers in 2008 (see publications: Geuder, N., Pulvermüller, B., Vorbrugg, O., "Corrections for Rotating Shadowband Pyranometers for Solar Resource Assessment", *Proc. of Solar Energy and Applications, part of SPIE Optics + Photonics, 10-14 August 2008, San Diego, USA*). The RMS deviation of the 10-minute means for DHI is minimized by variation of the thereby determined Diffuse Correction. Then the RMS deviation for the DNI is minimized using the Constant Calibration Factor.

Irradiance data from the RSI and the DLR station is logged as 60 second averages during the entire calibration process. For calibration, only the relevant operation range of solar thermal power plants was considered with DNI > 300 W/m², GHI > 10 W/m², DHI > 10 W/m² and at sun height angles > 5°. Outliers with deviations of more than 25% were not considered.

The following instruments were used during the calibration period:

Manufacturer	Model	Serial Number	Functionality/ Measurand	Calibration/Test remarks		
				constant	by	date
Kipp&Zonen	CMP21	110875	GHI	10.01 $\mu\text{V}/(\text{W}/\text{m}^2)$	DLR	Oct-2015
Kipp&Zonen	CV 2	070990	ventilation unit, GHI			
Kipp&Zonen	CMP21	110869	DHI	9.35 $\mu\text{V}/(\text{W}/\text{m}^2)$	DLR	Oct-2015
Kipp&Zonen	CV 2	070992	ventilation unit, DHI			
Hukseflux	DR03-05	10025	DNI	10.12 $\mu\text{V}/(\text{W}/\text{m}^2)$	DLR	Jun-2016
Campbell Scientific	CS215	E1839	air temp. and rel. humidity		Sensirion	
Campbell Scientific	CS100	3696476	air pressure		setra	Aug-2008
EKO	STR-22G		sun tracking		EKO	
Campbell Scientific	CR1000	7164	data logger for precise sensors			

10.1.2 RSI Solar Sensor (CSPS.MS.21.203.0009)

Calibration Protocol

For Model: Twin Rotating Shadowband Irradiometer

Pyranometer Unit Serial Number: CSPS.MS.21.203.0009
With pyranometer sensor: LI-COR LI200R PY110319 (primary)
and LI-COR LI200R PY110320 (secondary)
Original LI-COR Calibration Constant: 70.82 microamps per 1000 W/m²
and 72.23 microamps per 1000 W/m²

Correction factors from (DLR2008)

	PY110319	PY110320
Constant Correction Factor	1.050	1.037
Diffuse Correction Factor	1.035	1.033
Root Mean Square Deviation (DNI)	16.4 W/m ²	13.3 W/m ²
Bias (DNI)	-1.3 W/m ²	-0.5 W/m ²
Root Mean Square Deviation (GHI)	6.8 W/m ²	6.8 W/m ²
Bias (GHI)	3.0 W/m ²	1.6 W/m ²

Calibration period: 2021-11-26 to 2022-06-07
Effective period: 1926 h (GHI) 1230 h (DNI) 1926 h (DHI)
Temporal resolution: 10 min

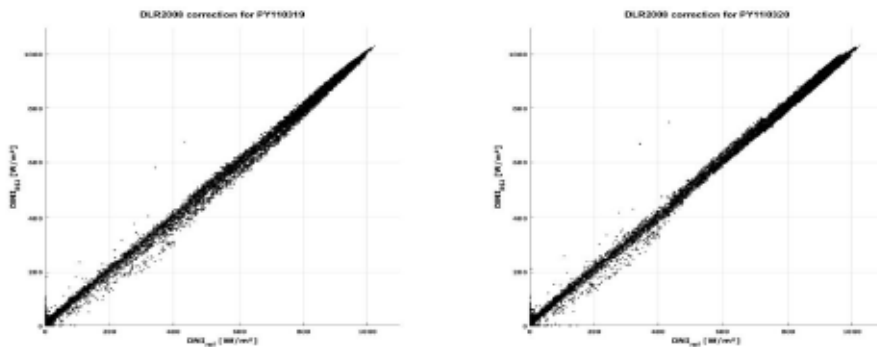


Figure 1: DNI after correction corresponding to chosen function set including calibration constant vs. reference DNI (10-min)

Please consult the detailed description for further information on the calibration process.
Almeria, 22-Jul-2022

i. A. Anne Forstinger, M.Sc.



DETAILED DESCRIPTION OF THE RSI SENSOR CALIBRATION PROCEDURE

The RSI irradiation sensor is mounted and operated parallel to the reference DLR meteorological station during a specified period (recommended to be at least one month) at the Plataforma Solar de Almería in Spain for calibration under real sky conditions.





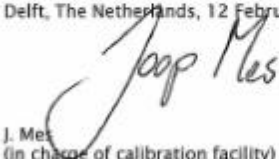
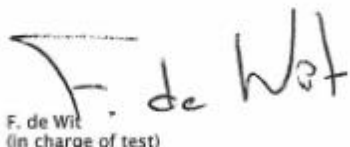
The Constant Calibration Factor and the Diffuse Correction are determined by comparing the reference direct normal and diffuse horizontal irradiance to corresponding RSI irradiance data as determined with the LI-COR (LI-200) Calibration Constant and including correction functions developed by DLR for RSIs with LI-COR LI200 pyranometers in 2008 (see publications: Geuder, N., Pulvermüller, B., Vorbrugg, O., "Corrections for Rotating Shadowband Pyranometers for Solar Resource Assessment", *Proc. of Solar Energy and Applications, part of SPIE Optics + Photonics, 10-14 August 2008, San Diego, USA*). The RMS deviation of the 10-minute means for DHI is minimized by variation of the thereby determined Diffuse Correction. Then the RMS deviation for the DNI is minimized using the Constant Calibration Factor.

Irradiance data from the RSI and the DLR station is logged as 60 second averages during the entire calibration process. For calibration, only the relevant operation range of solar thermal power plants was considered with $DNI > 300 \text{ W/m}^2$, $GHI > 10 \text{ W/m}^2$, $DHI > 10 \text{ W/m}^2$ and at sun height angles $> 5^\circ$. Outliers with deviations of more than 25% were not considered.

The following instruments were used during the calibration period:

Manufacturer	Model	Serial Number	Functionality/ Measurand	Calibration/Test remarks		
				constant	by	date
Kipp&Zonen	CMP21	110869	GHI	9.28 $\mu\text{V}/(\text{W/m}^2)$	OTT	Use: 2021-11-26
Kipp&Zonen	CV 2	070990	ventilation unit, GHI			
Kipp&Zonen	CMP21	110875	DHI	10.08 $\mu\text{V}/(\text{W/m}^2)$	OTT	Use: 2021-11-26
Kipp&Zonen	CV 2	070992	ventilation unit, DHI			
Kipp&Zonen	CHP1	090164	DNI	8.00 $\mu\text{V}/(\text{W/m}^2)$	OTT	Use: 2021-11-26
Campbell Scientific	CS215	E1839	air temp. and rel. humidity		Campbell Scientific	Use: 2021-11-26
Setra	Setra278	6814457	air pressure		setra	Use: 2021-11-26
EKO	STR-22G		sun tracking		EKO	
Campbell Scientific	CR1000	3868	data logger for precise sensors			

10.1.3 CMP10 pyranometer

			
Kipp & Zonen B.V. Delftechpark 35 2628 XH Delft The Netherlands +31 15 2755 210 info@kippzonen.com www.kippzonen.com			
ISO/IEC 17025 CALIBRATION CERTIFICATE			
CERTIFICATE NUMBER	022874210860		
PYRANOMETER MODEL	CMP 10		
SERIAL NUMBER	210860		
CALIBRATION DATE	12 February 2021		
INSTRUMENT CLASS	ISO 9060, Class A (Sec. Standard)*		
CALIBRATION PROCEDURE	ISO 9847 par5.3.2, A3		
REFERENCE PYRANOMETER	Kipp & Zonen CMP 21 sn 070114 active from 01 January 2021		
REFERENCE PYRANOMETER CALIBRATION PROCEDURE	ISO 9846 par5		
CALIBRATION LOCATION	Delft The Netherlands		
CUSTOMER			
REMARKS			
Delft, The Netherlands, 12 February 2021			
			
J. Mes (in charge of calibration facility)	F. de Wit (in charge of test)		
Page: 1 of 2			
Kipp & Zonen B.V. Trade name: OTT HydroMet Company registered in Delft	Trade register no.: 27239004 VAT no.: NL0055.74.857.B.01 Member of HMEI	EUR payments Deutsche Bank AG IBAN: NL70 DEUT 0265 2482 48 BIC: DEUTNL2A	USD payments only Deutsche Bank AG IBAN: DE00100701000162416200 BIC: DEUTDE33HAN33

ISO/IEC 17025 CALIBRATION CERTIFICATE

CERTIFICATE NUMBER 022874210860

Calibration procedure

The indoor calibration procedure is based on a side-by-side comparison with a reference pyranometer under an artificial sun fed by an AC voltage stabiliser. It embodies a 150 W Metal-Halide high-pressure gas discharge lamp and a reflector with a diameter of 16.2 cm. The lamp is positioned 1 m above the pyranometers producing a vertical beam. The reference- and test pyranometer are mounted horizontally on a table, which can rotate. The irradiance at the pyranometers is approximately 500 W/m². During the calibration procedure the reference and test pyranometer are interchanged to correct for any non-homogeneity of the beam. Temperature during calibration: 22 °C ± 2 °C.

Hierarchy of traceability

The measurements have been executed using standards for which the traceability to international standards has been demonstrated towards the RvA.

The reference pyranometer was compared with the sun and sky radiation as source under clear sky conditions using the "alternating sun-and-shade method" ISO 9846 paragraph 5. The measurements were performed in Delft, The Netherlands (latitude: 51.9969°, longitude: 4.3863°, altitude: 10m above sea level). Dates of measurements: 22-24 June 2020.

The receiver surface was pointed directly at the sun using a solar tracker. During the comparisons, the instrument received tilted global radiation intensities from 834 W/m² to 1124 W/m² with a mean of 992 W/m² and tilted diffuse radiation intensities from 83 W/m² to 250 W/m² with a mean of 148 W/m². The ambient temperature ranged from +19.0 °C to +29.9 °C with a mean of +23.9 °C.

The direct radiation on the reference pyranometer as obtained with the alternating-sun-and-shade method was compared to the DNI measured by the absolute cavity pyrheliometer PM06 SN 103. The PM06 is calibrated against the World Standard Group (WSG), maintained at the WRC, Davos every International Pyrheliometer Comparison (IPC). WRR factor of PM06: 0.99787 (from the last IPC-2015).

This calibration proved that the reference pyranometer has been stable and that the original sensitivity 8.37 µV/(W/m²) ± 0.11 µV/(W/m²) is valid and will be applied (see PM06 calibration details). Observed sensitivity differences between the consecutive years are well within the calibration uncertainty.

PM06 calibration details: The reference pyranometer was compared with the sun and sky radiation as source under mainly clear sky conditions using the "continuous sun-and-shade method". The pyranometer was installed horizontally. During the comparisons, the global radiation ranged from 638 W/m² to 1195 W/m² with a mean of 874 W/m². The solar zenith angle varied from 23.5° to 49.8° with a mean of 32.9°. The ambient temperature ranged from +12.5 °C to +26.2 °C with a mean of +23.7 °C. The sensitivity calculation is based on 435 individual measurements. The readings of the WSG are referred to the World Radiometric Reference (WRR). The estimated uncertainty of the WRR relative to SI is ±0.3%. The obtained sensitivity value and its expanded uncertainty (95% level of confidence) are valid for similar conditions and are 8.37 ± 0.11 µV/(W/m²). The measurements were performed in Davos (latitude: 46.8143°, longitude: -9.8458°, altitude: 1558 m above sea level). Dates of measurements: 24, 30 June 1, 2 July 2015. Global radiation data were calculated from the direct solar radiation as measured with the absolute cavity pyrheliometer PM02 (member of the WSG, WRR-factor: 0.998623 from the last International Pyrheliometer Comparison, IPC-2015) and from the diffuse radiation as measured with a continuous disk shaded pyranometer Kipp & Zonen CM2 2 SN 020059 (ventilated with heated air).

SENSITIVITY	9.59 µV/(W/m ²) at normal incidence on horizontal pyranometer
UNCERTAINTY	0.14 µV/(W/m ²) = 1.44 %
IMPEDANCE	23 ± 1.5 Ω

Justification of total instrument calibration uncertainty

The combined uncertainty of the result of the calibration is the positive "root sum square" of the following components.

1. The expanded uncertainty due to random effects and instrumental errors during the calibration of the reference CMP 21 is ±0.11/8.37 = ±1.31% (k=2). See traceability text.
 2. The expanded uncertainty of the transfer procedure (calibration by comparison) is estimated to be ±0.5% (k=2).
 3. The estimated uncertainty of the WRR relative to SI: ±0.3% (k=2).
- The expanded uncertainty is: $\sqrt{(1.31\%)^2 + 0.5\% + 0.3\%} = \pm 1.44\%$ (k=2).

The resistance measurement uncertainties are due to the PXI 4065 uncertainty in the 100 Ω range: 150ppm of range (=15mΩ) the cable resistance (estimated 0.1 Ω) and due to the electrothermal effect the measurement current in the thermal detector of the pyranometer. This was found to be a resistance error of 1.5 Ω, which results in a total resistance uncertainty of $\sqrt{(0.015\% + 0.1\% + 1.5\%)^2} = 1.5\%$ or 5%.

The PXI 4065 is calibrated by National Instruments Hungary, on 7 november 2018 at a temperature of 22.7 °C, under ISO 17025:2005 accreditation. This calibration is traceable to NIST and/or other National Measurement Institutes (NMI's).

The reported expanded uncertainty is based on the standard uncertainty of the measurement multiplied by a coverage factor k, such that the coverage probability corresponds to approximately 95%. The standard uncertainty has been determined in accordance with EA 04/2.

Notice

The calibration certificate supplied with the instrument is valid at the date of first use. Even though the calibration certificate is dated relative to manufacture, or recalibration, the instrument does not undergo any sensitivity changes when kept in the original packing.

* from October 2018 the classification conforms to ISO 9060:2018. Instruments issued before that date conform to ISO 9060:1990.

RvA is member of the European Co-operation for Accreditation (EA) and is one of the signatories to the EA Multilateral Agreement (MLA) and to the ILAC Mutual Recognition Arrangement (MRA) for the mutual recognition of calibration certificates.

Reproduction of the complete certificate is allowed. Parts of the certificate may only be produced with written approval of the calibration laboratory.

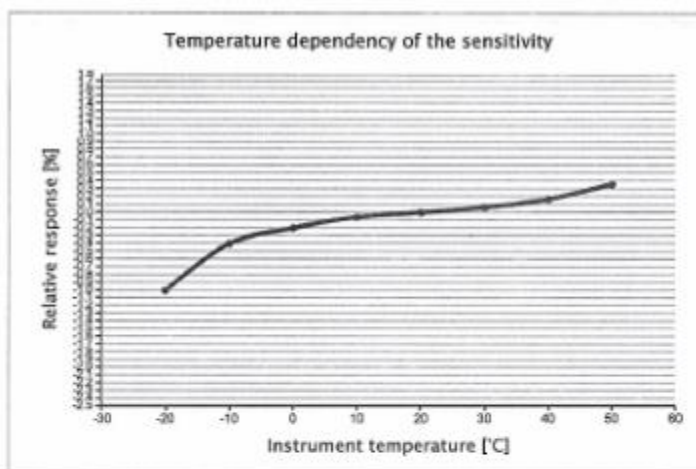
This certificate is issued provided that the Raad voor Accreditatie does not assume any liability.

Page: 2 of 2

MEASUREMENT REPORT PYRANOMETER

Routine measurement of temperature dependency during final inspection

PYRANOMETER TYPE	CMP 10
SERIAL NUMBER	210860
DATE OF MEASUREMENT	21 December 2020
PERFORMED BY	F. de Wit
PROCEDURE	<p>The pyranometer is mounted inside the climate chamber and illuminated with a white light source under normal incidence. A CMP22 pyranometer outside the chamber is used to monitor the lamp stability.</p> <p>The pyranometer is tested over a temperature range from 50 °C down to -20 °C in steps of 10 °C. The relative temperature dependency is plotted below.</p> <p>The measurement uncertainty of this characterisation is $\pm 0.1\%$ (k=2).</p>



Instrument temperature [°C]	Relative response [%]
-20	-1.00
-10	-0.40
0	-0.20
10	-0.06
20	0.00
30	0.07
40	0.17
50	0.36

MEASUREMENT REPORT PYRANOMETER

Routine measurement of directional error during final inspection

Mean cosine error of each new pyranometer type CMP 10 is measured by a simple routine.

Routine:

The pyranometerbase is placed against the vertical turntable of a goniometer in the parallel (0,5°) beam of a sunsimulator. Voltage output U(z) is measured for beam incidence (zenith) angles of 0°, 40°, 60°, 70° and 80° coming in over azimuth south (cable pointing to North). Next the pyranometer output U(-z) is measured for incidence angles of -80°, -70°, -60°, -40° and 0° consequently for azimuth south. The dark signal is measured at the beginning of the routine in the middle and at the end. For each beam incident angle the dark signal is interpolated.

During the CMP 10 measurement cycle, a check is done on the azimuth error at 40° and 70° by measuring voltages for azimuth-directions S, E, N and W. Also at -70° and -40° this azimuth error is measured and the mean of both azimuth measurements cancels out the eventual error in the 0° position.

With the extended procedure at both 40° and -40° and 70° and -70° the specific cosine error for 8 azimuth directions (40° S, W, N and E and 70° E, N, W, S) can be calculated according to formula 1 and verified whether it is within ± 10 W/m².

The applied formula for the relative cosine error is:

$$\frac{\left(\frac{U(z) + U(-z)}{2} - \text{zero}(z) \right)}{\left(\frac{U(0^\circ) + U(0^\circ)}{2} - \text{zero}(z) \right) \cos(z)} \cdot 100\% \quad \text{Formula 1.}$$

U(0°) Pyranometer output voltage for normal incidence
 U(z) Pyranometer output voltage for angles (z)
 Zero(z) Dark signal for angles

Relative cosine error at zenith angle in %

Zenith angle	South	East	North	West
40	-0.55	-0.43	-0.28	-0.41
60	-0.28			
70	-0.10	-0.56	-0.08	0.04
80	0.15			

Absolute cosine error for 1000 W/m² beam radiation in W/m²

Zenith angle	South	East	North	West
40	-4.20	-3.33	-2.14	-3.11
60	-1.38			
70	-0.35	-1.91	-0.28	0.13
80	0.26			

PYRANOMETER MODEL: CMP 10

SERIAL NUMBER: 210860

10.1.4 #40C anemometer



SOH Wind Engineering LLC

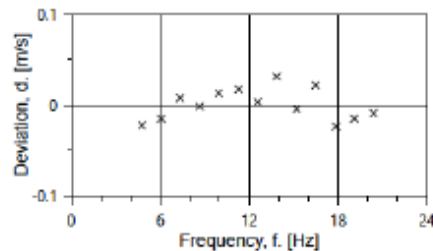
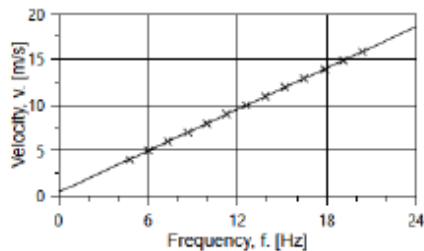
141 Leroy Road · Williston, VT 05495 · USA
 Tel 802.316.4368 · Fax 802.735.9106 · www.sohwind.com

CERTIFICATE FOR CALIBRATION OF CUP ANEMOMETER

Certificate number: 20.US1.01215 Date of issue: December 04, 2020
 Type: NRG 40C Anemometer Serial number: 179500334055
 Manufacturer: NRG Systems Inc, 110 Riggs Road, Hinesburg, VT 05461, USA
 Client: NRG Systems Inc, 110 Riggs Road, Hinesburg, VT 05461, USA
 Anemometer received: December 02, 2020 Anemometer calibrated: December 03, 2020
 Calibrated by: MEJ Procedure: MEASNET, IEC 61400-12-1:2017 Annex F
 Certificate prepared by: EJJ Approved by: Calibration engineer, EJJ

Calibration equation obtained: $v \text{ [m/s]} = 0.75816 \cdot f \text{ [Hz]} + 0.38739$
 Standard uncertainty, slope: 0.00135 Standard uncertainty, offset: 0.03575
 Covariance: -0.0000132 (m/s)²/Hz Coefficient of correlation: $\rho = 0.999990$
 Absolute maximum deviation: 0.031 m/s at 10.933 m/s
 Barometric pressure: 1003.1 hPa Relative humidity: 28.5%

Succession	Velocity pressure, q, [Pa]	Temperature in wind tunnel [°C]	Temperature in d.p. box [°C]	Wind velocity, v, [m/s]	Frequency, f, [Hz]	Deviation, d, [m/s]	Uncertainty u _c (k=2) [m/s]
1-first	9.35	21.5	26.0	3.976	4.7627	-0.022	0.023
13-last	14.55	21.8	26.1	4.962	6.0543	-0.015	0.026
2	21.00	21.5	26.0	5.959	7.3381	0.008	0.030
12	28.58	21.8	26.1	6.955	8.6646	-0.002	0.034
3	37.31	21.5	26.0	7.942	9.9477	0.013	0.038
11	47.44	21.8	26.1	8.962	11.2867	0.017	0.042
4	58.37	21.5	26.0	9.935	12.5884	0.003	0.046
10	70.60	21.9	26.1	10.933	13.8686	0.031	0.051
5	83.97	21.5	26.0	11.917	15.2134	-0.005	0.055
9	98.36	21.9	26.0	12.905	16.4829	0.021	0.059
6	114.28	21.6	26.0	13.905	17.8606	-0.024	0.063
8	130.48	21.8	26.0	14.863	19.1135	-0.015	0.067
7	148.35	21.7	26.0	15.846	20.4024	-0.009	0.071



AC-1746



Page 1 of 2

EQUIPMENT USED

Serial Number	Description
Njord1	Wind tunnel, blockage factor = 1.0017
2254	Control cup anemometer
-	Mounting tube, D = 12.7 mm
TT003	Summit Electronics, 1XPT100, 0-10V Output, wind tunnel temp.
TT001	Summit Electronics, 1XPT100, 0-10V Output, differential pressure box temp.
DP005	Setra Model 239, 0-1inWC, differential pressure transducer
HY002	Dwyer RHP-2D20, 0-10V Output, humidity transmitter
BP001	Setra Model 278, barometer
PL8	Pitot tube
XB002	Computer Board. 16 bit A/D data acquisition board
LAB2-PC	PC dedicated to data acquisition

The accuracies of all measurements were traceable to the SI through NIST or CIPM recognized NMI's. A real-time analysis module within the data acquisition software detects pulse frequency.



Photo of the wind tunnel setup. The cross-sectional area is 2.5m x 2.5m.

UNCERTAINTIES

The documented uncertainty is the total combined uncertainty at 95% confidence level ($k=2$) in accordance with EA-4/02. The uncertainty at 10 m/s comply with the requirements in the IEC 61400-12-1:2005 procedure. See Document US.12.01.004 for further details.

COMMENTS

(none)

Certificate number: 20.US1.01215

The results on this certificate relate only to the serial number listed.
All calibrations are done in the "As Found" condition unless otherwise noted.
This certificate must not be reproduced, except in full, without the approval of SOH Wind Engineering LLC

Page 2 of 2

10.1.5 #200M Wind vane



Factory Calibration

NRG Systems 200M Wind Direction Vane
Serial No. 10070 00009014

Product Description:

Manufacturer	Description	Cal. Date
NRG Systems	200M Wind Direction Vane	12/13/2020

NRG Systems, hereby certifies that the above instrumentation has been calibrated and tested to meet or exceed the published specifications. This calibration and testing was performed using instrumentation and standards that are traceable to the National Institute for Standards and Technology (NIST).

Standard Uncertainty of Degree Measurement = ±0.31°

The output (in Deg.) for this 200M sensor is defined by: $\theta = V * Scale\ Factor + Offset$

Criteria	Value	Units
200M Scale Factor	147.9896	Deg./Volt
200M Offset	-1.4056	Deg.

Linearity Results (R^2): 0.99999

Slope (Scale Factor) and Offset Conversion Chart for NRG Systems' Data Loggers.

To Scale to...	SymphoniePLUS3 and Older <i>[Symphonie Data Retriever (SDR) software]</i>		SymphoniePRO Data Logger <i>[SymphoniePRO Desktop Application]</i>	
	enter Scale Factor	and enter Offset	enter Scale Factor	and enter Offset
°	0.368	-5.3	147.9896	-1.4056

Procedure: WI-ELE-489

Calibration performed by: ms

Date: 12/13/2020

NRG Systems' management system has been certified to ISO 9001: 2015.

110 Riggs Road • Hinesburg, Vermont 05461 | a: +1 802.482.2255 f: +1 802.482.2272 | nrgsystems.com

10.1.6 CS106 (PTB100) barometer



1 (1)
Certificate report no. H47-20470021

CALIBRATION CERTIFICATE

Instrument PTB110 Barometer
Serial number S4750162
Manufacturer Vaisala Oyj, Finland
Calibration date 20th November 2020

This instrument has been calibrated against a Vaisala PTB220 factory working standard. The Vaisala PTB220 is traceable to the National Institute of Standards and Technology (NIST, USA) via Vaisala Measurement Standards Laboratory (MSL). Vaisala MSL has been accredited by FINAS according to ISO/IEC 17025 standard.

At the time of shipment, the instrument described above was within its operating specifications.

Calibration results

Reference pressure hPa	Calculated pressure hPa	Observed voltage Vdc	Correction* hPa	Uncertainty** hPa
510.3	510.3	0.043	0.0	± 0.15
610.0	610.0	0.458	0.0	± 0.15
700.0	700.1	0.834	-0.1	± 0.15
810.1	810.2	1.292	-0.1	± 0.15
900.0	900.0	1.667	0.0	± 0.15
1000.3	1000.3	2.085	0.0	± 0.15
1059.8	1059.8	2.333	0.0	± 0.15
1099.9	1099.9	2.500	0.0	± 0.15

*To obtain the true pressure, add the correction to the barometer reading. Interpolated corrections may be used at intermediate readings of the scale of the barometer.

**The calibration uncertainty given at 95 % confidence level, k = 2

Equipment used in calibration

Type	Serial number	Calibration date	Certificate number
HP34970A	EM 12997	2020-03-10	11-9485435-009
PTB220	PA 14018	2020-06-11	K008-D02088

Ambient conditions

Humidity: 32 ± 5 %RH Temperature: 23 ± 2 °C Pressure: 998 ± 20 hPa



Technician

This report shall not be reproduced except in full, without the written approval of Vaisala.

Doc214685-B

Vaisala Oyj | PO Box 26, FI-00421 Helsinki, Finland
Phone +358 9 894 91 | Fax +358 9 8949 2227
Email first.name.last.name@vaisala.com | www.vaisala.com
Domicile Vantaa, Finland | VAT FI01244162 | Business ID 0124416-2

10.2 SENSOR CALIBRATION FOR THE SECOND YEAR OF MEASUREMENTS

During the maintenance visit on 2022-08-19, a traveling standard reference pyranometer (CMP10, Kipp&Zonen, ISO 9060 Class A spectrally flat) was installed at the weather station to compare the readings of the reference pyranometer to the permanently installed pyranometer and confirm the validity of the sensor calibration. The reference pyranometer was sent to the World Radiation Center in Davos prior to the maintenance visit.

The sensor was installed during the maintenance on 2022-08-19 and dismantled on 2022-08-23.



Figure 139: Reference pyranometer installation

The comparison measurement was set up according to the measurement set-up procedures described in ISO 9847 (Calibration of field pyranometers by comparison to a reference pyranometer) as far as possible under field measurement conditions. Data was compared based on 1-minute averages of GHI, taken in 1s measurement resolution (same sampling and storage rate as the data from the permanently installed pyranometer).

The reference sensor was installed right next to the permanently installed pyranometer and connected to the station's data acquisition system. The data was stored and transmitted to the CSPS' server together with the measurement data from the other sensors. The data was analyzed by CSPS and the comparison between the two sensors performed

The deviation between the compared instruments should be within the combined calibration uncertainty ($\pm 1.9\%$) of both instruments.

Figure 140 shows the comparison of the CMP10 sensor with the CMP10 travelling standard sensor. The measurement values from the two pyranometers coincide well. The two devices have an average deviation of 0.4%, which is well within the combined calibration uncertainty. Therefore, the calibration of the previously installed CMP10 pyranometer is accepted as still valid and the measurements with the pyranometer were continued without any changes.

The calibration certificate of the permanently installed pyranometer was provided together with the installation report of the station in June 2021. For the calibration certificate of the reference sensor, please refer to Figure 141.

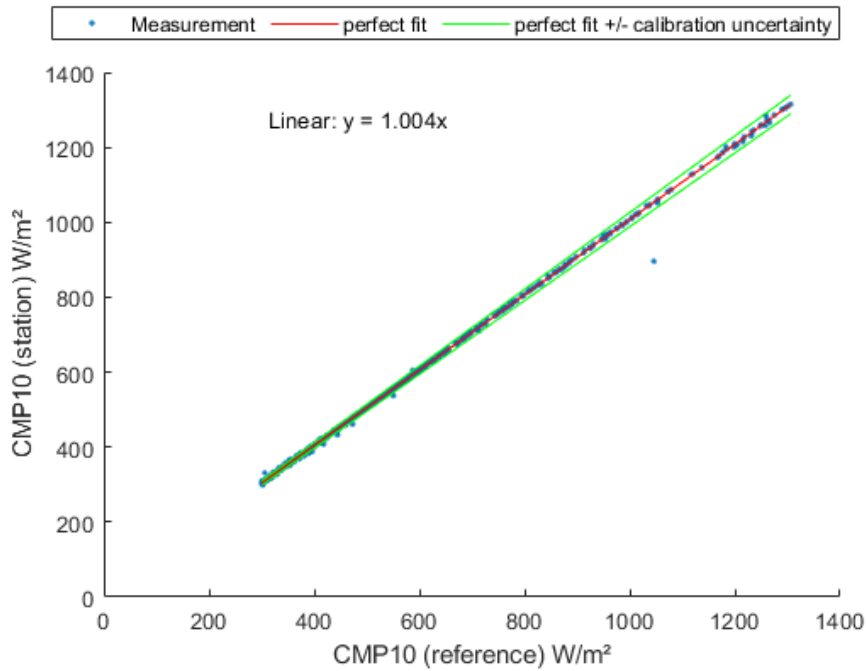


Figure 140: Comparison of GHI from permanently installed and reference pyranometers (CMP10)

Physikalisch-Meteorologisches Observatorium Davos World Radiation Center			
Calibration Certificate No. 2022-C-012			
Calibration Item	Pyranometer Manufacturer: Kipp & Zonen Type: CMP10 Serial Number: 211593		
Customer	CSP Services GmbH Friedrich-Ebert-Ufer 30 51143 Köln Germany		
Calibration Mark	2022-C-012		
Period of Calibration	2022 June 14, 20, 23, 30, July 2, 3		
Davos Dorf, 4 July 2022 R. Sober In charge of measurements		 Dr. W. Finsterle Head WRC Solar Radiometry Section	
<p>This certificate is consistent with the capabilities that are included in Appendix C of the CIPM MRA drawn up by the CIPM. Under the CIPM MRA, all participating institutes recognize the validity of each other's calibration and measurement certificates for the quantities, ranges and measurement uncertainties specified in Appendix C (for details see http://www.bipm.org).</p> <p>Calibration certificates without signature are not valid. This calibration certificate shall not be reproduced except in full, without the written approval of the Physikalisch-Meteorologisches Observatorium Davos and World Radiation Center.</p>			
Dorfstrasse 33, CH-7260 Davos Dorf Phone +41 81 417 51 11, Fax +41 81 417 51 90 www.pmodwrc.ch		Page 1 of 2	
Certificate No. 2022-C-012			
Calibration procedure This pyranometer was compared with the sun and sky radiation as source under mainly clear sky conditions using the "continuous sun-and-shade method". The calibration procedure follows QM-SOP-SRS-0025. The direct solar radiation is determined using the PMO2, member of the World Standard Group (WSG) and the diffuse radiation is measured using the shaded standard pyranometer of the World Radiation Center (WRC). The measurements were performed in Davos (latitude: 46.8143°, longitude: -9.8458°, altitude: 1588m). The readings are referred to the World Radiometric Reference (WRR) as stated in the WMO Technical Regulations. The ratio between the WRR and SI scales is 1.00336±0.00092 (k=1, Metrologia 49 (2012) S34-S38). The inclination of the receiver surfaces versus their horizontal position were set to 0 degrees, the instrument signal wire to the north. During the comparisons, the instrument received global radiation intensities ranging from 614 W/m² to 1128 W/m², with a mean of 873 W/m². The angle between the solar beam and the normal of the receiver surface varied from 23.5 degrees to 50.0 degrees, with a mean of 34.6 degrees. The ambient temperature ranged from 17.8 °C to 24.2 °C, with a mean of 20.8 °C. The sensitivity calculation and the single measurements deviation (σ) are based on 537 individual measurements. The obtained sensitivity value is valid for similar conditions.			
Calibration results Responsivity: $S = 9.82 \mu V / (Wm^2)$ Uncertainty: $U = \pm 0.12 \mu V / (Wm^2)$ The reported expanded uncertainty of measurements is stated as the standard uncertainty of measurement multiplied by the coverage factor k=1.96, which for a normal distribution corresponds to a coverage probability of approximately 95%.			
Calibrations Remarks Reference: WRR represented by the absolute pyrheliometer: PMO2 WRR-Factor of PMO2: 0.99477 (from the last International Pyrheliometer Comparison, IPC-2021 Diffuse radiation: Pyranometer CM22 S.N. 020059 with calibration factor: 8.92 (Ventilated with heated air, automatic shading disk, instrument-wire opposite sun) External calibration: Identifier DMM9, S.N. 0xEB19B0, last calibration 18.4.2013, last validation 31.3.2022; Identifier DMM15, S.N. 0xEB29B2, last calibration 18.4.2013, last validation 31.3.2022; Identifier DMM16, S.N. 0xEB18B3, last calibration 18.4.2013, last validation 31.3.2022; Identifier DMM17, S.N. 0xEAD395, last calibration 18.4.2013, last validation 31.3.2022			
Comments Instrument Condition: The calibration item was received fully functional and did not show any erratic behavior or irregularities during calibration. The dome was cleaned daily.			
Dorfstrasse 33, CH-7260 Davos Dorf Phone +41 81 417 51 11, Fax +41 81 417 51 90 www.pmodwrc.ch		Page 2 of 2	

Figure 141: Travelling standard reference pyranometer calibration certificate from World Radiation Center in Davos.